GENETIC AND DIETARY EFFECTS ON PHYSICAL PROPERTIES, ASSEMBLY AND SECRETION OF apoB-CONTAINING LIPOPROTEINS

A Dissertation

by

LIMIN WANG

Submitted to the Office of Graduate Studies of
Texas A&M University
in partial fulfillment of the requirements for the degree of

DOCTOR OF PHILOSOPHY

August 2003

Major Subject: Nutrition

GENETIC AND DIETARY EFFECTS ON PHYSICAL PROPERTIES, ASSEMBLY AND SECRETION OF apoB-CONTAINING LIPOPROTEINS

A Dissertation

by

LIMIN WANG

Submitted to Texas A&M University
in partial fulfillment of the requirements
for the degree of

DOCTOR OF PHILOSOPHY

Approved as to style and content by:

Rosemary L. Walzem (Chair of Committee)	John E. Bauer (Member)
Michael J. Davis (Member)	Stephen B. Smith (Member)
Robert S. Chapkin (Chair of Nutrition Faculty)	Alan R. Sams (Head of Department)

August 2003

Major Subject: Nutrition

ABSTRACT

Genetic and Dietary Effects on Physical Properties, Assembly and Secretion of apoB-containing Lipoproteins. (August 2003)

Limin Wang, M.D, Taishan Medical College;

M.S., Shanghai Medical University

Chair of Advisory Committee: Dr. Rosemary L. Walzem

The physical properties (i.e., mass, particle diameter and composition) of apolipoprotein B (apoB)-containing lipoproteins (apoB-LP) are a major determinant of atherosclerotic cardiovascular disease (ASCVD) risk. The objective of this research was to investigate how nascent apoB-LP physical properties affect circulating lipoprotein profiles and risk of disease. Relationships between apoB-LP physical properties and arterial plaque formation in four genotypes of mice with apoB isoform specific clearance defects were investigated. Multivariate statistical analysis found that arterial lesions were most closely related to genetic background and apoB concentration related to delayed clearance rate. For defining the dietary effects on circulating lipoprotein profiles, the physical properties of lipoproteins in hamsters fed high-carbohydrate diets containing either 60% fructose or 60% cornstarch for 2 wk were studied. Fructose increased very low-density lipoprotein (VLDL) particle diameter and decreased low-density lipoprotein (LDL) particle diameter. Elevations in all high-density lipoprotein (HDL) fractions were observed in the fructose-fed group. Further investigation was made of whether changes to the physical properties in

circulating lipoproteins resulted from changes to nascent particles in the assembly and secretion processes. Intermediate particles used for lipoprotein assembly were isolated from rough endoplasmic reticulum of hamster liver, and nascent VLDL were isolated from plasma after Triton WR-1339 injection of hamsters. A large, TG-rich apoB-deficient particle and a small, lipid-poor apoB-containing particle were isolated in each dietary setting. The diameter of first-step particles was larger in fructose feeding, which indicated that apoB degradation decreases and provides the basis for apoB oversecretion. Fructose feeding significantly increased the concentrations recovered from liver for these two particles and for nascent particles compared with chow or starch feeding. Collectively, these results demonstrate: 1) genetic factors can dictate metabolism, and metabolic conditions can critically affect the physical properties and further atherogenicity of apoB-LP; 2) changes in physical properties of circulating apoB-LP are derived from changes to the nascent particles; and 3) dietary factors can influence the assembly, secretion, and metabolism of apoB-LP. The findings of the research may provide a metabolic basis for the recognition of new targets that could regulate apoB-LP metabolism to prevent and treat ASCVD.

DEDICATION

To my parents, brother and sister.

ACKNOWLEDGMENTS

I would first to thank my advisor, Dr. Rosemary L. Walzem, for her guidance and strong encouragement. It would have been impossible for me to finish this dissertation without her invaluable help. It has been a great learning experience in her lab from conducting an experiment to writing a research paper during the past several years. I would also like to thank Dr. John Bauer, Dr. Michael Davis, and Dr. Stephen Smith for serving on my dissertation committee and for their help, advice and support. In addition, I would like to thank Kendall Hood for his excellent technical assistance and Jo Ann Pilkey, Robert Pottberg and Jo Ann Sanders for their excellent administrative support. Special thanks are extended to Dr. Stephen G. Young and Dr. Robert L. Hamilton from the Gladstone Institute of Cardiovascular Disease for generous provision of transgenic mouse plasma, technical support and invaluable advice. For brightening each day with laughter, I thank all the members from the Walzem family.

TABLE OF CONTENTS

LIST OF TABLES

TABLE Page

LIST OF FIGURES

FIGURE Page

FIGURE Page

CHAPTER I

INTRODUCTION

Pathogenesis of Atherosclerosis

Atherosclerotic cardiovascular disease (ASCVD) is a broad term for common, chronic pathological changes in blood vessels associated with the heart and brain. Atherosclerosis is an irregular thickening of the inner wall of the artery that reduces the size of the arterial lumen and compromises its functionality. The lesions of atherosclerosis occur principally in large- and medium-sized elastic and muscular arteries. Arteries are composed of three concentric layers termed the intima, the media and the adventitia. The innermost intimal layer consists of a sheet of endothelial cells that adhere tightly to the internal elastic lamia, a feltwork of collagens, glycoproteins and laminin. Internal elastic lamia functions as supporter of endothelial cells and separates endothelial cells from subendothelial space. The media consists exclusively of smooth muscle cells and extracellular matrix material. This layer provides the structure necessary for arterial wall to cope with the high pressure emulating from each contraction of the heart. The adventitia comprises a loosely woven connective tissue layer that contains nutrient arteries (Gordon, 1999). The main processes believed to be involved in the genesis of atherosclerotic lesions are: 1) formation of a fatty steak (Ross, 1999) (Fig. 1.1). The earliest visible lesion of atherosclerosis, the fatty streak, is a discrete marginated lesion comprised of lipid-laden monocytes, macrophages and T

This dissertation follows the style and format of the Journal of Nutrition.

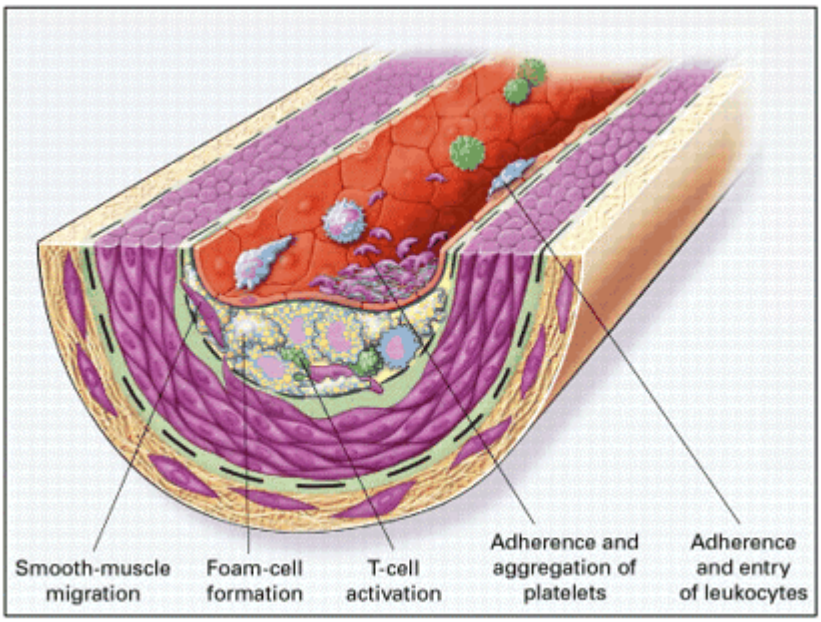

Figure 1.1 Fatty streak formation in atherosclerosis. Fatty streaks initially consist of lipid-laden monocytes and macrophages (foam cells) together with T lymphocytes. Later they are joined by various numbers of smooth muscle cells. The steps involved in this process include smooth muscle cell migration, foam cell formation, T cell activation, platelet adherence and aggregation, and the adherence and migration of leukocytes (Ross, 1999).

lymphocytes in the arterial wall. Expression of monocyte chemo-attractant and adhesion molecules on the endothelium is of central importance in recruiting circulatingmonocytes into the intima. The monocytes migrate into the subendothelial space where they differentiate into macrophages capable of engulfing large amounts of cholesterol and cholesteryl ester via the scavenger receptor pathway. The main source of foam cell lipid is chemically modified low-density lipoproteins (LDL), because unlike the LDL receptor, the scavenger receptor is not subject to feedback regulation by cellular cholesterol content. Macrophages may engulf large amounts of LDL-derived lipid. Lipid-laden macrophages appear to be filled with bubbles at low resolution magnification, hence the name foam cells. Collections of foam cells beneath an intact endothelium constitute a fatty streak; 2) formation of fibrous cap (Ross, 1999) (Fig. 1.2). As fatty streaks progress, proliferation of smooth muscle cells of the arterial wall leads to vessel thickening. In addition, the elaboration of connective tissue matrix by smooth muscle cells can produce a fibrous cap. The fibrous cap is characterized by the appearance of smooth muscle cells and extra-cellular lipid in the intima of the arterial wall; 3) Formation of fibrous plaque (Ross, 1999) (Fig. 1.3). With continued cell proliferation, necrosis, lipid accumulation, and connective tissue formation, the lesions increase in size until they become fibrous plaque with a dense fibrous cap. These plaques narrow arterial diameter and cause irregularities in the surface of the vessel thus altering blood flow. As lesions grow, the interior surfaces of the arteries become roughened. Eventually, some plaques rupture, breaking through the cell lining the interior surface of

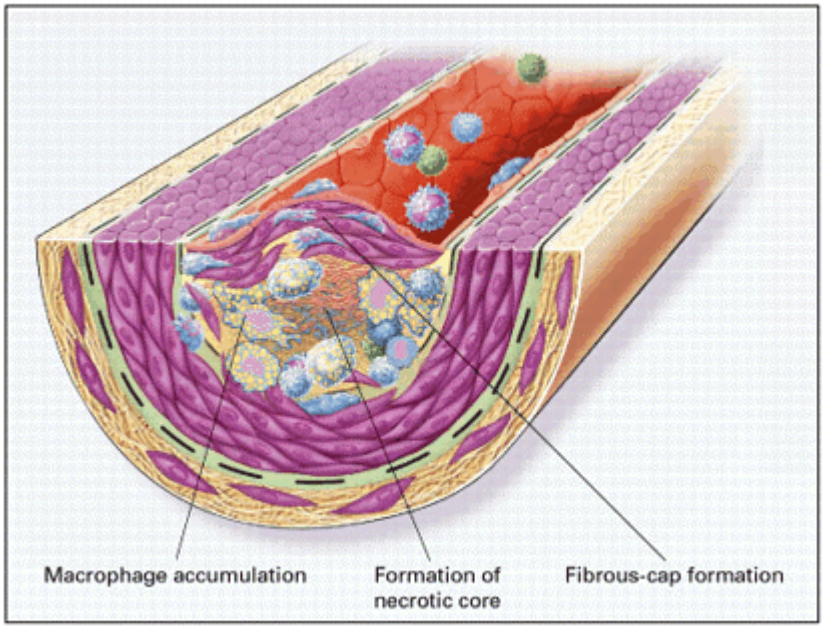

Figure 1.2 Formation of a fibrous cap of atherosclerosis. As fatty streaks progress to intermediate and advanced lesions, they tend to form a fibrous cap that walls off the lesion from the lumen. The fibrous cap covers a mixture of leukocytes, lipid and debris, which may form a necrotic core (Ross, 1999).

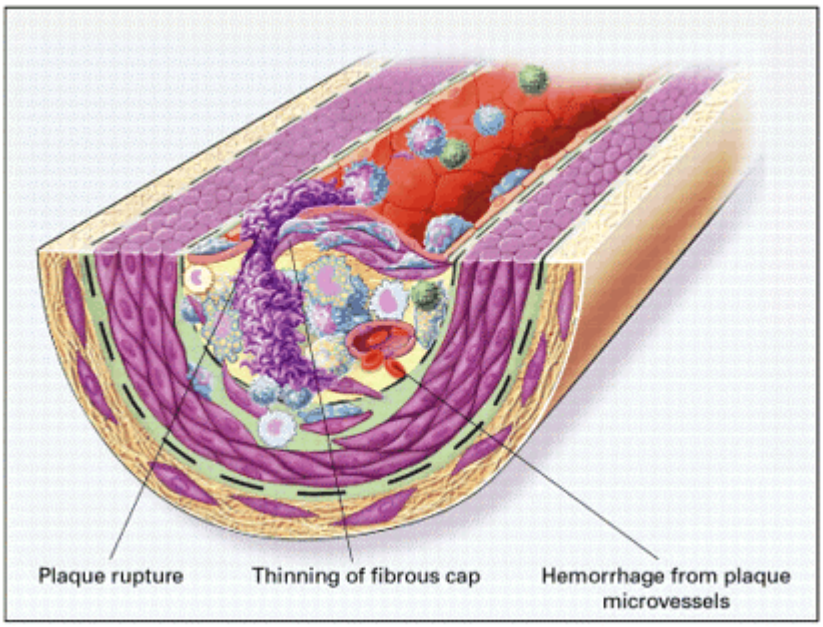

Figure 1.3 Fibrous plaques in atherosclerosis. Rupture of the fibrous cap or ulceration of the fibrous plaque can rapidly lead to thrombosis and usually occurs at sites of thinning of the fibrous cap that covers the advanced lesion (Ross, 1999).

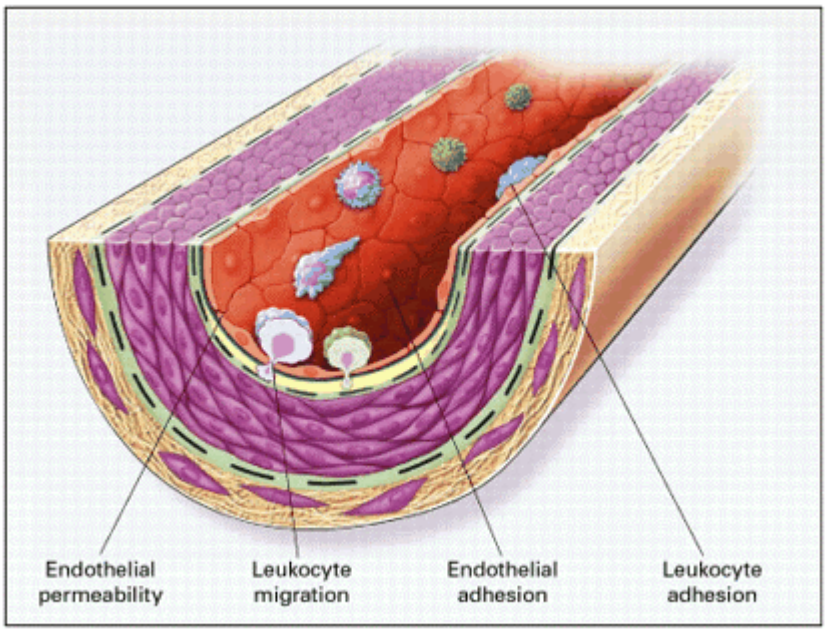

Figure 1.4 Endothelial dysfunction in atherosclerosis. The earliest changes that precede the formation of lesions of atherosclerosis take place in the endothelium. These changes include increased endothelial permeability to lipoproteins and other plasma constituents, leukocyte migration, endothelial adhesion and leukocytes adhesion (Ross, 1999).

the arteries. The rough surface attracts platelets to adhere and propagate to form platelet plaques (thrombus), which can cause sufficient stenosis or thrombosis, to impede blood supply and acutely obstruct arteries in the heart, brain or extremities, causing ischemia and tissue damage or death.

Although lesion progression is well documented and many of the processes of atherogenesis are known, the initial cellular and molecular mechanisms in atherosclerosis remain equivocal. Three hypotheses regarding the initial steps leading to the development of this complex, multifactorial, autoimmune inflammatory disease are currently being tested (Ross, 1999). The "response to injury" hypothesis, originally developed by Ross (1993), proposes that the initial event in atherosclerosis is injury to endothelial and smooth muscle cells of the arterial wall (Fig. 1.4). The earliest change that precedes the formation of visible atherosclerosis is endothelial dysfunction including increased endothelial permeability to lipoproteins and other plasma constituents. Enhanced arterial permeability is mediated by toxic chemicals and agents, which are released from macrophages and lymphocytes. (Ross, 1999; Newby, 2000; Newby and Zaltsman, 2000). The "oxidation" hypothesis states that oxidative modification of LDL could produce the relevant factors that are injurious to arterial endothelium and ultimately to smooth muscle cells (Henriksen et al., 1981a; Steinberg and Witztum, 1999). According to this hypothesis, LDL particles retained in the intima by proteoglycans undergo oxidative modification by pathways that require reactive intermediates such as superoxide (O_2^-) and hydrogen peroxide (H_2O_2). The oxidized

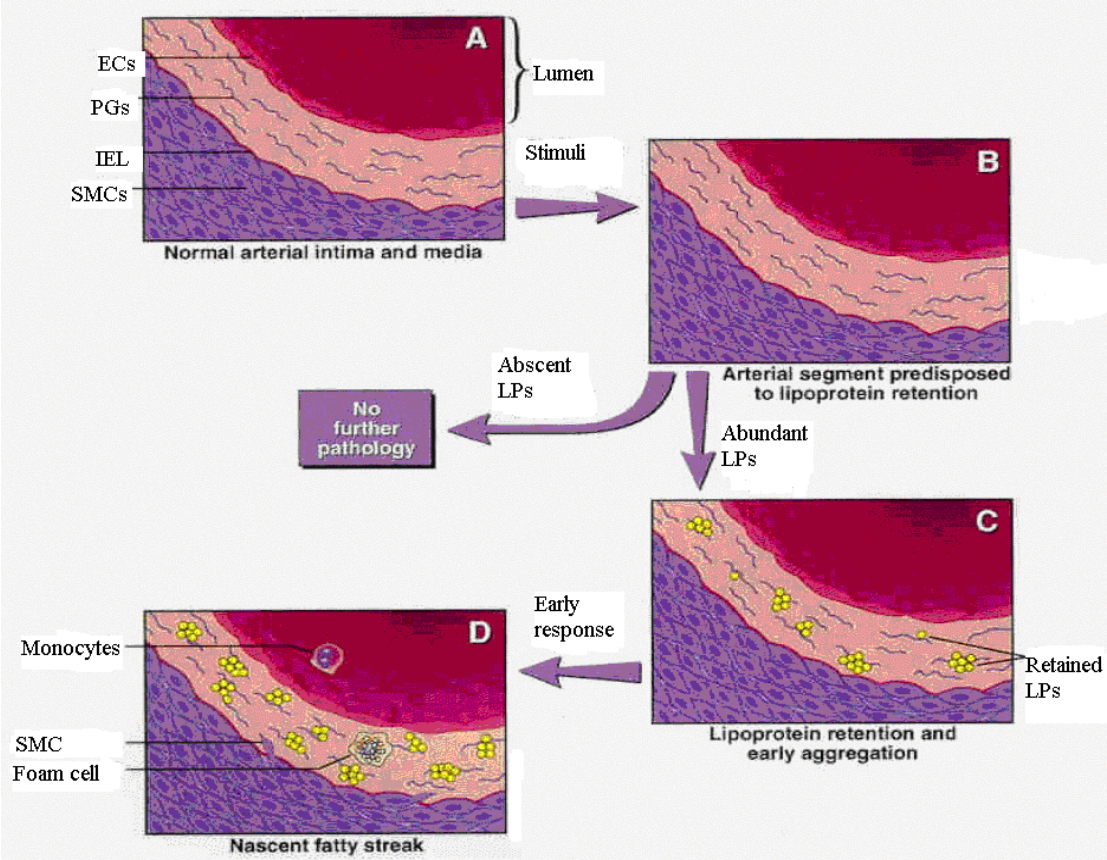

Figure 1.5 The response-to-retention model of early atherogenesis. (A) Mild to moderate hyperlipidemia causes lesion development only in specific sites, which are particularly lesion-prone by stimulating local synthesis of apoB-retentive molecules (B). Predisposing stimuli in the absence of abundant atherogenic lipoproteins are insufficient to cause atherogenesis. Predisposing stimuli in the presence of abundant atherogenic lipoproteins result in lipoprotein retention (C). Once significant retention has occurred, a cascade of early responses, including lipoprotein oxidation and cellular chemotaxis, leads to lesion development (D). ECs, endothelial cells; PGs, proteoglycans; IEL, internal elastic lamina; SMCs, smooth muscle cells; and LPs, lipoproteins (Williams and Tabas, 1995).

LDL particles can deliver various lipid oxides and hydroperoxides to target cells. These compounds variably act as cytotoxins, monocyte chemoattractants, stimulators of cholesteryl ester accumulation by macrophage, and inhibitors of macrophage movement (Steinberg et al., 1989b). The "response-to-retention" hypothesis, proposed by (Williams and Tabas, 1995) emphasizes that retention by and accumulation of apolipoprotein B (apoB)-containing lipoproteins (apoB-LP) within the subendothelial space of the artery wall provides the relevant oxidizing environment to create atherogenic species of lipoproteins (Williams and Tabas, 1998; Wood et al., 1998) (Fig. 1.5). According to the "response to retention" hypothesis, the atherogenicity of apoB-LP depends on four factors: 1) the plasma concentration of the atherogenic apoB-LP; 2) the difference between the arterial wall influx and efflux of apoB-LP; 3) modification of the retained apoB-LP and 4) inflammatory response to the modified retained apoB-LP. How are the atherogenic apoB-LP formed? Walzem et al. (1995) proposed that aged apoB-LP are more susceptible to oxidation and so more atherogenic. These hypotheses are not mutually exclusive, and the last hypothesis includes major components of the first two. There is ample recent evidence from epidemiological studies, as well as experiments *in vivo* and *in vitro,* to support the "response to retention" hypothesis as a very early step in the pathobiology of ASCVD. Convincing evidence indicates that specific changes in the physical properties of apoB-LP constitute a metabolic profile that is closely associated with the incidence of ASCVD (Walzem et al., 1995; Williams and Tabas, 1995; Wood et al., 1998).

apoB-containing Lipoprotein Heterogeneity and ASCVD

As early as 1950, Gofman et al. (1950) revealed the heterogeneous nature of the complexes in plasma that were responsible for lipid transport and also reported that many people who suffered from atherosclerosis had blood cholesterol concentrations in the normal range (< 240 mg/dL). This was the first time lipoprotein heterogeneity was reported to be as a major determinant of atherosclerotic risk. More recently, significant atherogenic potential was related to elevated concentrations of specific apoB-LP (Young, 1990; Walzem et al.; 1995; Packard and Shepherd, 1997). ApoB-containing lipoprotein heterogeneity is now believed to reflect dietary and genetic influences that affect lipoprotein metabolism and ASCVD risk. Lipoproteins can be heterogeneous with regards to composition, diameter, and atherogenicity (Krauss, 1994; Krauss, 1997, Millar et al., 1998, Demant and Packard, 1998; Kwiterovich, 2002).

Structure and function of plasma lipoproteins

Plasma lipoproteins are spheroidal particles that contain a hydrophobic nonpolar lipid core of triacylglycerol (TG) and cholesteryl ester (CE) that is surrounded by a more polar, amphipathic coat of apolipoprotein, phospholipid and unesterified (free) cholesterol (Mayes, 2000) (Fig. 1.6). The diameter and density of the lipoprotein particles are determined by the relative mass amounts of core-lipid: protein ratio. Plasma lipoproteins are typically classified into two major families based on apolipoprotein type: apoB-containing lipoproteins and apoAI-containing lipoproteins (Kwiterovich, 2002a). The apoBs are structural proteins and integral constituents of apoB-LP; a family

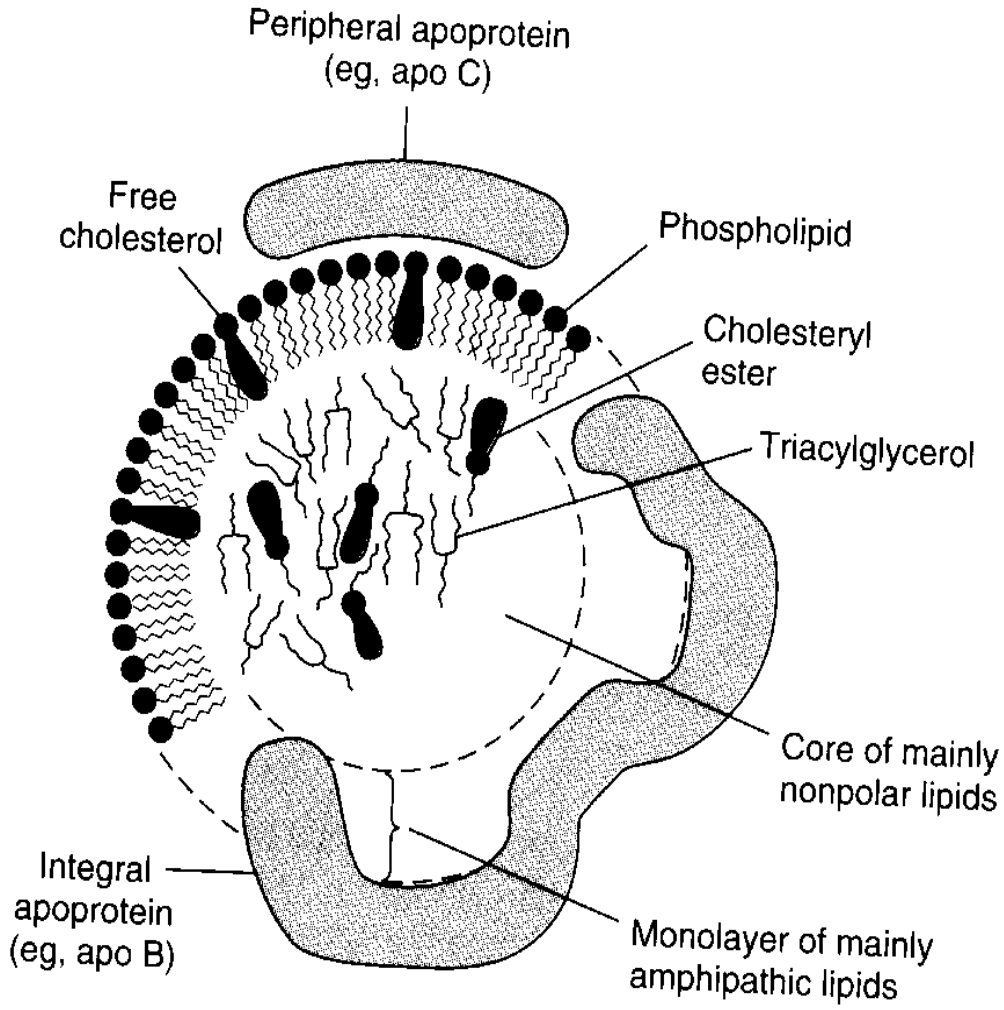

Figure 1.6 General structure of plasma lipoprotein (Mayes, 2000).

TABLE 1.1

Characterization of apoB-containing lipoproteins

Lipoprotein classes	Diameter (nm)	Hydrated Density (g/mL)	Major lipids	Major apoproteins	Subclasses
CM	90–1000	<0.95	TG	apoB48, apoCI, apoCII, apoCIII, apoE	
VLDL	30–90	095-1.006	TG	apoB100, apoCI, apoCII, apoCIII, apoE	$VLDL_1$ $VLDL_2$
IDL	28–35	1.006-1.019	TG Cholesterol	apoB100, apoCI, apoCII, apoCIII, apoE	IDL_1 IDL_2
LDL	20–26	1.019-1.063	Cholesterol	apoB100	LDL_{1-4}
Lp(a)	30	1.040-1.090	Cholesterol	apo(a), apoB100	$Lp(a)_5$ $Lp(a)_1$

(Kwiterovich, 2002b)

of lipoproteins that include the TG-rich chylomicrons (CM) and very low-density lipoproteins (VLDL) and their remnants, intermediate-density lipoproteins (IDL), LDL and lipoproteins (a) (Lp (a)) (Table 1.1). VLDL, LDL and IDL are transitional particle components of a continuous metabolic cascade in which TG is lost in a series of small lipolytic steps. There is only one apoB molecule per apoB-LP particle. Because of the nature of lipid/protein interactions between apoB and particle lipid, apoB is incapable of exchanging among lipoprotein particles. Mammals exhibit two isoforms of these high-molecular weight hydrophobic apolipoproteins: apolipoprotein B100 (apoB100) and apolipoprotein B48 (apoB48). ApoB100 represents the full length protein, which contains 4536 amino acids, and the apoB48 (2152 amino acids) isoform is a truncated version of apoB100, constituting 48% of the amino terminal residues of apoB100, hence the name "B48." In human and other mammals, CM are secreted from the intestine and particles that contain apoB48 as their structural base. CM serve as the transport vehicles for exogenous (dietary) lipid. Chylomicrons contain 88% of their weight as TG, and as a result are the least dense (0.98 g/mL < d < 1.006 g/mL) type of lipoprotein. Triacylglycerol is the major dietary fat that is transported from the intestine into the bloodstream.

Very low-density lipoproteins are primarily synthesized in the liver from which they transport fat of endogenous (hepatic) origin. VLDL particles contain about 56% of their weight as TG. VLDL also contain apoB100, the primary structural component, as well as apolipoproteins E and C (apoE, apoC). LDL particles are the metabolic end products of VLDL metabolism. Low-density lipoproteins are what remain after VLDL particles

have lost most of their TG and all of apoE and apoC. Thus, apoB100 is the major apolipoprotein in LDL and contains the domain required for interaction of this lipoprotein species with the LDL receptor (Betteridge et al., 1999). The major function of LDL is to deliver cholesterol to cells. Each LDL particle contains 58% of its weight being contributed by CE and unesterified cholesterol. Finally, apoB100 contains an unpaired cysteine residue at position 3426 that can participate in formation of lipoprotein(a) (Lp (a)) (Callow et al., 1994). Lp (a) is composed of two components: LDL and apolipoprotein(a) (apo(a)). Lp (a), unlike LDL, is not a metabolic product of a TG-rich, apoB-LP (Krempler et al., 1979).

apoB48 is essential for CM formation in the small intestine of all mammalians and VLDL formation in liver of some mammals. Functional differences in apoB isoform actions during metabolism arise from a lack of some domains in apoB48 that are contained in the carboxyl terminal of apoB100. Chylomicrons and CM remnants are cleared by LDL receptor-related proteins (LRP) and VLDL receptors by virtue of apoE, rather than apoB as is the case for LDL receptors (Spillane et al., 1995). apoB48 is the product of apoB mRNA editing, and as such represents a unique post-transcriptional modification (Davidson et al., 1995). A site-specific C-to-U editing reaction produces a UAA stop codon and translational termination of intestinal apoB mRNA at residue 2152. This C-to-U conversion, a site-specific hydrolytic deamination, is mediated by a multicomponent enzyme complex containing apobec-1 and other factors (Harris et al., 1993). apoB mRNA editing occurs in the small intestines of all mammals and in the

livers of mice and rats (Greeve et al., 1993). Unlike rats and mice, hamsters are similar to humans in that apoB editing occurs only in the intestine (Bravo et al., 1994).

The major apoAI-containing lipoproteins are high-density lipoproteins (HDL), the most dense of the plasma lipoproteins. The major function of HDL is responsible for redistributing cholesterol among peripheral tissues, as well as returning cholesterol to the liver for catabolism and excretion (Rader, 2002). HDL also have important anti-inflammatory properties (Cockerill et al., 1995; Calabresi et al., 1997). The predominant HDL core lipid is CE (30%), and the main HDL apolipoproteins are apoAI; apoAI is exchangeable.

apoB-containing lipoprotein metabolism and heterogeneity

Two major cascades for lipoprotein metabolism, the apoB-LP cascade and the HDL cascade, are interrelated (Fig. 1.7). The apoB-LP metabolic pathway is a lipolytic cascade that begins with lipoprotein lipase (LPL) mediated hydrolysis of TG from the TG-rich lipoproteins such as CM and VLDL. The lipolytic cascade arising from apoB48-LP is also known as the exogenous pathway, while that of apoB100-LP is termed the endogenous pathway.

The exogenous pathway is so called due to its role in transport of dietary lipids is known as the exogenous pathway (Fig. 1.7). As TG-rich apoB48-containing CM, are secreted from enterocytes, they pass first into lymph ducts and enter the bloodstream at the thoracic duct. In the blood, they bind to LPL, which hydrolyzes the core TG in the

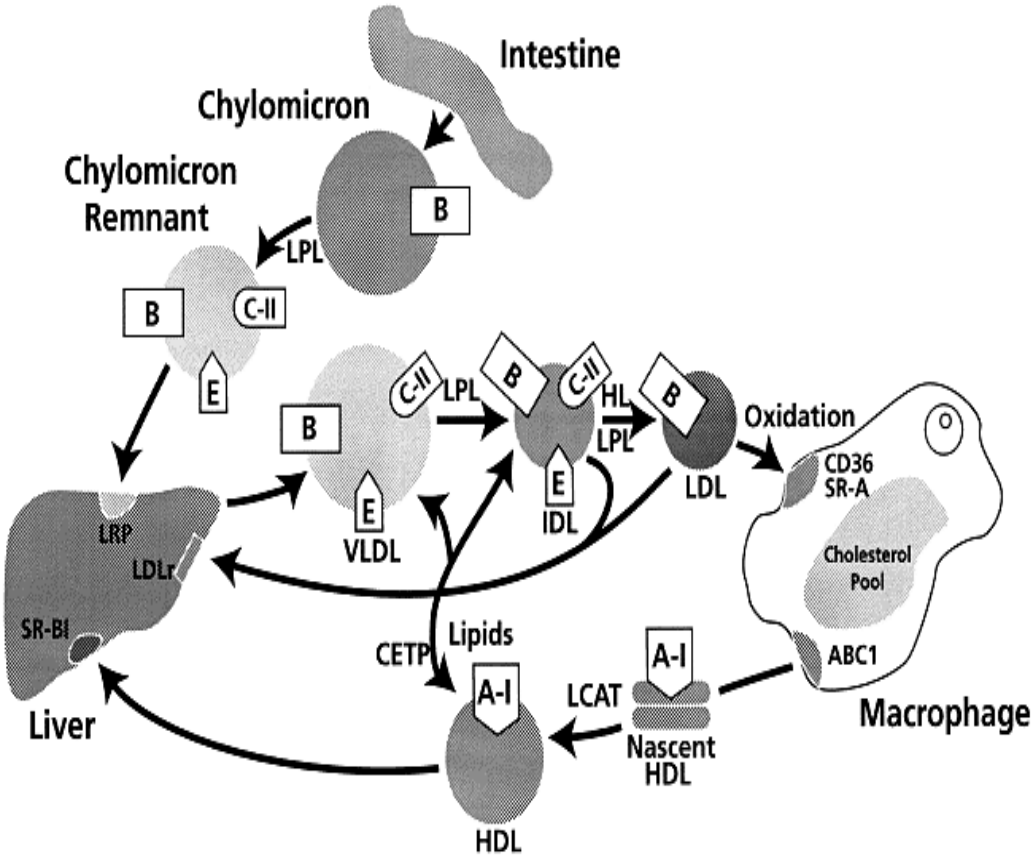

Figure 1.7 Lipoprotein metabolism. (Kwiterovich, 2000).

CM particles following activation by apolipoprotein CII (apoCII). Chylomicron hydrolysis yields CM remnants, which are quickly removed from the plasma (5-15 min), primarily by the interaction of apoE with LRP (Hussain et al., 1991). Thus, apoB48-containing CM are not usually present in plasma of fasted animals. The exogenous pathway is influenced mainly by the rate of entry and tissue disposition of dietary lipid, which is regulated by LPL (Braun and Severson, 1992). Lipoprotein lipase can in turn be regulated by hormones such as insulin (Appel and Fried, 1992).

The pathway for transport of hepatic lipid is described as the endogenous pathway (Fig. 1.7). As TG-rich apoB100-containing VLDL secreted from the liver enter the plasma, VLDL particles also interact with LPL in capillaries, and their core TG is hydrolyzed (Wang et al., 1992). VLDL hydrolysis yields VLDL remnants, which are hydrolyzed further by LPL to produce IDL. Intermediate-density lipoprotein particles have two fates. Some IDL are removed through the interaction of apoE or apoB with LDL receptor on the surface of liver and degraded, while others remaining in the plasma are converted through further hydrolysis by hepatic lipase (HL) to LDL (Nilsson-Ehle et al., 1980). LDL particles are normally removed from plasma by the interaction of apoB100 with the LDL receptor on the surface of hepatic and peripheral cells, whereas oxidized LDL are taken up by the scavenger receptors on the macrophages (Henriksen et al., 1981b).

The endogenous pathway is a means of delivering cholesterol as well as TG to tissues, and for this reason is also referred to as "forward cholesterol transport," while the HDL pathway for transport of cholesterol out of tissues is termed "reverse

cholesterol transport" (Fig. 1.7) (Barter and Rye, 1996). Lipid-poor apoAI particles (Pre-β HDL) secreted from the liver enter the plasma. In the circulation, the pre-β HDL acquire phospholipids and free cholesterol from peripheral tissues via the ATP-binding cassette protein-1 (ABC1) (McNeish et al., 2000) and form discoidal HDL. These particles become lipid-rich, mature HDL through transfer of redundant phospholipids from the surface of TG-rich lipoprotein particles undergoing lipolysis via phospholipid transfer protein (PLTP) and through esterification of cholesterol via the action of lecithin-cholesterol acyltransferase (LCAT) (Santamarina-Fojo et al., 2000). Mature HDL particles can return their cholesterol to the liver via the receptor SR-BI (Rigotti et al., 1997), or exchange cholesterol for TG from TG-rich lipoproteins via the action of cholesteryl ester transfer protein (CETP) (Tall, 1990). Interactions among apoB-LP and HDL serve to remodel particle composition. Intravascular remodeling is a fundamental driver for apoB-LP heterogeneity.

apoB-containing lipoproteins are heterogeneous in particle diameter, density, lipid and apolipoprotein content and composition. Differences in these physical properties are thought to affect atherogenic potential of individual apoB-LP (Chapman et al., 1998; Krauss, 1994). The apoB-LP metabolic pathway is critical to understanding how apoB-LP heterogeneity develops. Several lines of evidence have demonstrated that the physical properties of apoB-LP influence their subsequent metabolism and heterogeneity. Particle size and TG content of VLDL affect lipoprotein metabolic fate (Kasim-Karakas et al., 1997). The trace-labeled VLDL studies by Packard et al. (1984) showed that in humans most of large VLDL ($VLDL_1$) particles were cleared rapidly, and

less than 10% were converted to LDL, while smaller, less TG-rich $VLDL_2$ particles released by the liver were the major precursor to LDL. The same group (Gaw et al., 1995) also found that the production of IDL and LDL was variable over the range of VLDL and was inversely related to the plasma TG level. Low-density lipoprotein heterogeneity, first reported by Fisher (1983), is strongly associated with the atherogeneity of lipoprotein class.

Atherogenicity of apoB-containing lipoproteins

Elevated circulating apoB-LP has long been linked to the premature development of ASCVD (Young, 1990). Although the National Cholesterol Education Program (NCEP) Adult Treatment Panel (ATP) III singled out LDL cholesterol as the principal target of therapy (NCEP, 2001), several points must be made about LDL. First, LDL-apoB concentration, rather than LDL cholesterol concentration, defines the molar concentration of LDL particles in blood. Second, the clinical measurement of LDL cholesterol includes the cholesterol content of IDL as well as that of LDL, thus IDL probably rivals LDL in atherogenic potential (Tribble et al., 2001). Third, LDL and IDL are not all encompassing of atherogenic lipoproteins; some VLDL probably are also atherogenic (Grundy, 1997). Importantly, not all apoB-LP possess similar atherogenic potential. Some lipoprotein subclasses may be quite atherogenic, whereas others may carry little risk or even protect against ASCVD (Krauss, 1994; Krauss, 1998; Hodis et al., 1999). Currently, apoB-LP physical heterogeneity is believed to reflect atherogenic potential and so influence ASCVD risk (Steinberg et al., 1989a; Nigon et al., 1991;Galeano et al., 1994; Gaw et al., 1995; Nielsen et al., 1996; Packard and Shepherd,

1997). For example, small VLDL remnant particles filter into the arterial wall more readily than larger particles (Nordestgaard and Nielsen, 1994). VLDL, CM and their remnants from patients with hypertriacylglycerolemia have the decreased ability to bind LDL receptor via apoE (Zannis and Breslow, 1982). Two distinct LDL phenotypes, pattern A and pattern B, were identified in humans (Krauss and Burke, 1982; Austin et al., 1988; Austin et al., 1990). Pattern A is characterized by large (diameter > 25.5nm), buoyant, CE-rich, monodisperse particles, and pattern B is characterized by predominately smaller (diameter < 25.5nm), denser, relatively CE-poor, polydisperse LDL particles. Genetic background is known to contribute to the determination of LDL phenotypes (Feingold et al., 1992), in part through diet responsive changes in TG-rich lipoprotein metabolism (Dreon et al., 1994). Despite these associations, the basis for apoB-LP atherogenicity has not been fully explained.

The relation between the heterogeneity of apoB-LP particles and ASCVD has attracted considerable interest with numerous investigators working to determine the bases for differences in atherogenicity (Austin et al., 1988; Chapman et al., 1998). This interest has culminated in the definition of atherogenic lipoprotein phenotype (ALP) as a risk factor that is predictive of the development of ASCVD (Krauss, 1994; Lamarche et al., 1997) The ALP consists of elevated plasma TG concentrations, low HDL-cholesterol concentrations and small, dense LDL particles. Plasma TG is the major determinant of the appearance of ALP (Griffin et al., 1994).

Ginsberg (2000) proposed a metabolic mechanism for the production of small, dense LDL (Fig. 1.8). Due to some abnormal metabolic event, adipose tissue produces an increased flux of free fatty acid to the liver. Normally, over half of the fatty acids that derive from hydrolysis of apoB-LP by LPL can enter the adipose tissue; the remaining fatty acids are used by muscle or transported back to the liver (Betteridge et al., 1999). If there is a deficiency in fatty acid uptake by adipose tissue, such as occurs during insulin resistance, fatty acids will accumulate in plasma. Elevated plasma fatty acids increase liver fatty acids and in so doing increase liver TG. Increased liver TG will lead to VLDL overproduction. During circulation, the TG in VLDL is exchanged for CE on large LDL particles by CETP. In situations where VLDL-TG becomes very high, the more concentrations of VLDL and LDL particles shift towards VLDL causing the equilibrium driven CETP reaction to produce a TG-rich LDL. The TG in LDL can be hydrolyzed by LPL or HL, producing LDL particles that are depleted of CE and that are smaller and denser. Accumulation of fatty acids in plasma disrupts binding to lipases as well as lipase binding to the endothelium. These actions cause the VLDL to detach from the surface of the endothelial cell (Sniderman, 2000), and delay the clearance of apoB-LP and their remnants.

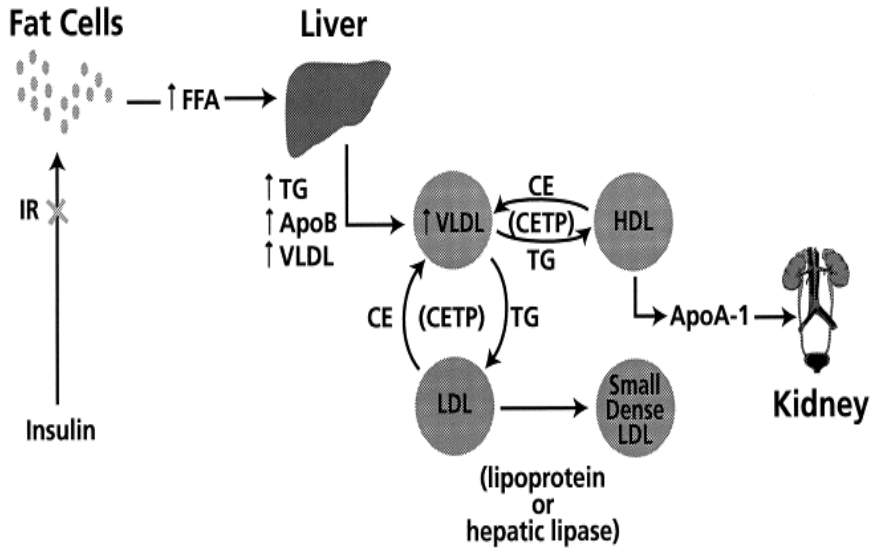

Figure 1.8 Mechanism of the production of small, dense low-density lipoprotein (Kwiterovich, 2000).

The above metabolic scenario appears to be relevant to three different clinical conditions and to be driven by apoB-LP overproduction. Indeed, subjects with familial combined hyperlipidemia exhibit a pattern B phenotype for LDL in association with other symptoms of familial combined hyperlipidemia. Subjects with familial combined hyperlipidemia overproduce VLDL, increasing secretion of large TG-rich $VLDL_1$ particles and small CE-rich $VLDL_2$ (Demant and Packard, 1998). Following exchange of CE in LDL for TG in large $VLDL_1$ by CETP, the TG in LDL can be hydrolyzed by hepatic lipase, producing small, dense LDL (Fig. 1.8).

Impaired fatty acid uptake often occurs in patients with insulin resistance or "Syndrome X" (Sniderman et al., 2001). Patients with these conditions exhibit impaired insulin mediated suppression of TG lipolysis by hormone-sensitive lipase present in adipocytes. Failure to suppress hormone sensitive lipase activity promotes the hydrolysis and release of fatty acids from adipose tissue and elevated free fatty acid production (Ginsberg, 2000). The CE in HDL can also exchange, via CETP with the TG on VLDL, producing a TG-rich HDL. The delipidated apoAI is likely to be catabolized rapidly by the kidney, and hence small, dense LDL particles are often accompanied by decreased HDL cholesterol level.

Small dense LDL are often observed in a shift from high-fat to high-carbohydrate diet. Dreon et al. (1994) analyzed changes in LDL pattern in 105 healthy men consuming high-fat diets for 6 wk followed by high-carbohydrate diets for another 6 wk and found that: one-third of men exhibiting a pattern A profile while consuming high-fat diet transformed to a pattern B profile while consuming the high-carbohydrate diet. In

other words, there was a shift in LDL particle from larger, less dense LDL to smaller, denser LDL.

Altered VLDL and CM metabolism cause abnormal apoB-LP clearance and can also affect the apoB-LP physical properties. Indeed changes in apoB-LP physical properties appear to provide a ready index to particle clearance in some settings. Both VLDL and CM require LPL to hydrolyze TG. Overproduction of VLDL increases the number of VLDL particles available to compete with CM for LPL (Betteridge et al., 1999). As a result, degradation of TG-rich apoB-LP is retarded and removal of both VLDL and CM from plasma is delayed. Walzem et al. (1995) reported the delayed apoB-LP clearance increases the susceptibility of particles to oxidation.

ALP appears to stem from a disturbance of the metabolism of TG-rich apoB-LP, with overproduction of VLDL from the liver or increased delivery of free fatty acids to the liver. As described above, the appearance of small dense LDL in plasma is believed to provide the key clinical marker of this type of metabolic dysfunction. The Quebec Cardiovascular Study disclosed that high levels of LDL pattern B (small dense LDL) were significantly more prevalent in patients with ASCVD, and were associated with a three-fold increased risk of coronary artery events (Lamarche et al., 1997).

Several mechanisms are thought to render small dense LDL potentially more atherogenic than their larger and lighter counterparts. Cell culture studies (Nigon et al., 1991) showed small dense LDL bound with lower affinity to the LDL receptor. Galeano et al. (1994) demonstrated that the modification of apoB structural conformation in the binding region of the polypeptide increased the residence time of small dense LDL in

serum, thereby allowing more time for infiltration across the endothelial barrier and interaction with components of the subendothelia. The influx rate of plasma lipoproteins across the endothelium and into the subendothelial space is a function of particle diameter (Nordestgaard and Nielsen, 1994). Thus, small dense LDL could infiltrate at a faster rate than either large LDL, IDL or VLDL, and would also pass out at a faster rate if not for their selective binding to components of the extracellular tissue matrix such as proteoglycans. However, a preferential binding of small dense LDL to proteoglycans causes them to be sequestered in the arterial wall (Anber et al., 1996), where they can undergo chemical and physical modifications that confer a number of pro-atherogenic properties (Heinecke et al., 1993). In this respect, small dense LDL seem to be the physical manifestation of increased particle age, a feature known to lead to increased susceptibility to oxidation (Walzem et al., 1995). Indeed, Tribble and Krauss showed that oxidative susceptibility in LDL particles was inversely related to particle diameter (Tribble et al., 1992). These findings have now been extended to documentation of a progressive increase in particle susceptibility to oxidation with progression through the lipolytic cascade leading to either LDL pattern A or pattern B (Tribble et al., 2001). Importantly IDL and LDL intermediates from pattern B subjects were always more susceptible to oxidation than comparable particles isolated from pattern A subjects.

Oxidized LDL are more readily scavenged by vascular scavenger LDL receptors and have a longer residence time in the vascular matrix. This leads to enhanced lipid deposition in the arterial wall (Reusch, 2002). Small dense LDL often coexist with other lipoprotein abnormalities such as elevation in plasma TG and low HDL cholesterol

(Austin et al., 1990). Plasma TG concentrations have been recognized as an independent risk factor for ASCVD (Hokanson and Austin, 1996). Zilversmit (1979) proposed that elevated post-prandial TG concentrations exert their adverse effect by promoting the production of atherogenic CM remnants. CM remnants have the ability to mediate cholesterol influx into the arterial wall intima in human subjects, thereby promoting atherogenesis (Shaikh et al., 1991).

The post-prandial lipemic response not only represents the influx of dietary TG to the circulation, but it is also a very significant period during which composition and metabolic fate of the cholesterol-rich lipoproteins, such as LDL and HDL, are determined. Elevated post-prandial lipemia promotes the catabolism of HDL, and low concentrations of HDL cholesterol are associated with an increased risk of ASCVD (Assmann et al., 1996). A strong inverse relationship between the concentration of HDL cholesterol and the incidence of ASCVD has been consistently observed in prospective epidemiological studies (Gordon et al., 1977; Robertson et al., 1977; Assmann et al., 1996) and clinical intervention studies (Gordon et al., 1986; Mackness et al., 1993). The ability of HDL cholesterol to predict ASCVD independently of any other known risk factors is exemplified by data from a 6-year follow-up in the Prospective Cardiovascular Munster (PROCAM) study (Assmann et al., 1996). The results from the prospective studies by Gordon's group (Gordon et al., 1989; Gordon and Rifkind, 1989) demonstrate ASCVD risk is increased by 2% in men and 3% in women for every 1 mg/dL (0.026 mmol/L) reduction in HDL cholesterol. The correlation remains statistically significant after adjustment for other risk factors such as LDL cholesterol and TG concentrations.

Low concentrations of HDL cholesterol are frequently observed in patients with ASCVD, and attention has focused on low HDL cholesterol as a potential target for therapeutic intervention. Moreover, abnormalities in apoB-LP metabolism and HDL concentration are often metabolically interrelated. At present, it is unknown whether these interrelated lipoprotein pathways can be affected independently of one another.

From the above, several points can be made about the atherogenicity of apoB-LP. First, an increased molar concentration of apoB-LP particles is not adequately represented by plasma cholesterol concentration due to the variability in size and cholesterol content of individual lipoprotein particles. Second, small dense LDL penetrate the vascular wall more readily and bind to proteoglycans more avidly, tendencies that put this LDL subclass "in harms way" more often than other larger particles. Third, the metabolic scenario that underlies the formation of small dense LDL by definition imposes some structural features on the LDL particles. In other words, the atherogenicity of apoB-LP in the majority of individuals arises from increased age and oxidization as suggested by the surrogate markers of small diameter and increased density, and not from its cholesterol content *per se*.

Genetic Effect on apoB-containing Lipoprotein Metabolism in Transgenic Mice

In human populations, complex lipid profiles comprised of lipoprotein particles of differing atherogenic potentials arise from genetic and environmental factors, including diet. As a multifactorial disease, ASCVD demands an *in vivo* system to complement *in vitro* work and to address those issues that are unanswerable in simplified systems. Transgenic and knockout mouse models constitute simplified *in vivo* model systems and

are providing surprising insight into lipoprotein metabolism and atherogenesis. In humans, mutations in one or both of the LDL receptor genes result in familial hypercholesterolemia (Goldstein et al., 1977). Ishibashi et al. (1993) generated LDL receptor-deficient mice by gene targeting embryonic stem cells. Both heterozygous and homozygous deficient mice developed elevated total plasma cholesterol levels. Kinetic studies demonstrated a significant delay in both VLDL and LDL clearance from the plasma of the LDL receptor knockout mice compared with control mice (Ishibashi et al., 1993) Using homologous recombination in embryonic stem cells, Plump et al. (1992) disrupted specifically the apoE gene and generateD apoE-deficient mice, which showed delayed clearance of VLDL and led to accumulation of apoB-containing particles in the plasma as well as consequent premature atherosclerosis. Transgenic mice expressing the human apoB gene were developed via microinjection of a genomic apoB clone contained on a phagemid vector (Callow et al., 1995). The resultant mice showed high-level expression of the human apoB transgene and human-like LDL and HDL concentrations in animal fed a low-fat, low-cholesterol diet. Interestingly, the human apoB transgene was expressed in the liver and heart, but transgene expression was completely absent in the intestine (McCormick and Nielsen, 1998). In addition, Young and his associates (Kim et al., 1998) used gene targeting to insert an apoB83 mutation in the mouse apoB gene to create a mouse model of familial hypo-beta-lipoproteinemia. This group (Raabe et al., 1998) again used gene targeting to knock out mouse microsomal triglyceride transfer protein (MTP) gene to create a mouse model for abeta-lipoproteinemia, which is an inherited human disease characterized clinically by an

absence of apoB-LP in the plasma due to mutations in the gene for MTP. Inactivation of the murine MTP gene in liver caused a striking reduction in VLDL-TG and large decreases in both VLDL/LDL and HDL cholesterol concentrations (Raabe et al., 1999). In a separate study, this group (Farese et al., 1996) used gene targeting to introduce stop and nonstop mutations into the apoB48 editing codon in the mouse apoB to produce apoB100-only (*Apob*$^{100/100}$) and apoB48-only (*Apob*$^{48/48}$) mice. Veniant et al. (1997) used these mice to investigate the effect of apoB isoform on the susceptibility of these mice to atherosclerosis. Animals with similar cholesterol levels had similar amounts of atherosclerosis regardless of apoB isoform. The authors concluded that there was no intrinsic difference in the atherogenicity of apoB100 and apoB48 proteins. Differences in the atherogenicity of apoB100- and apoB48-containing lipoproteins in free-living humans must therefore arise from selective changes in particle metabolism. Veniant et al. (2000) next characterized *Apob*$^{100/100}$ mice that were LDL receptor-deficient homozygous (*Ldlr*$^{-/-}$*Apob*$^{100/100}$), and compared them to *Apob*$^{100/100}$ mice that were apoE-deficient homozygous (*Apoe*$^{-/-}$*Apob*$^{100/100}$). Both mouse strains developed plaque when fed a low-fat chow diet. Although the total plasma cholesterol concentrations were approximately the same in the two types of mice, the *Ldlr*$^{-/-}$*Apob*$^{100/100}$ mice developed lesions that covered 14% of the arterial surface, while lesions in the *Apoe*$^{-/-}$*Apob*$^{100/100}$ mice covered only 4.5% of the arterial surface. The observation that one set of mice had more plaque than the other at equal cholesterol concentrations does not expressly suggest increased numbers of small diameter particles. However when measured, almost all of the cholesterol in *Apoe*$^{-/-}$*Apob*$^{100/100}$ mice was in VLDL-sized particles, whereas

nearly all of the cholesterol in *Ldlr*$^{-/-}$*Apob*$^{100/100}$ mice was in LDL-sized particles. In separate studies, ablation of apoE from *Apob*$^{48/48}$ mice reduced particle diameter but actually increased particle diameter in *Apoe*$^{-/-}$*Apob*$^{100/100}$ mice (Veniant et al., 1998). From these studies, it is apparent that: 1) in isolation, either apoB48 or apoB100 can give rise to atherogenic lipoproteins; 2) that the metabolic basis for their atherogenicity arises from delayed particle clearance; and 3) the metabolic defect of delayed particle clearance is physically manifested by a decrease in particle diameter. Thus in free-living humans, small dense lipoproteins are likely to provide a surrogate marker for delayed apoB-LP clearance. However, to date complex mixtures of apoB-LP types that occur in humans have not been investigated in a systemic way in these same mouse models. The issue is an important one in as much as dietary changes influence apoB48 and apoB100 metabolism differently.

a**poB-containing Lipoprotein Assembly**

apoB-containing lipoproteins are assembled in a complex, multistep process that involves interplay among protein and lipid biosynthetic, trafficking and maturation factors. A two-step model for lipoprotein assembly was initially suggested by the electron microscopy studies of Alexander et al. (1976). In the first step, two apoB-LP precursors, an apoB-containing apoB-LP precursor (first-step particle) and an apoB-deficient, lipid-rich apoB-LP precursor (second-step particle) were proposed to produce independently (Alexander et al., 1976). In the second step, two apoB-LP precursors combined to form a mature VLDL particle.

Translating the immuno-electron microscopic images into measurable biochemical events proved challenging. Difficulties arose both from the membranous nature of the endoplasmic reticulum (ER) where apoB-LP assembly occurred and the models used to study the process. *In vitro* culture of transformed cell lines that retain metabolic features of their differentiated counterparts are attractive model systems. Spring et al. (1992) found that expression of various truncated versions of apoB100 in the human hepatoma cell line- HepG2 cells did result in the assembly of lipoprotein particles. However, they were unable to produce particles of VLDL-density leading them to observe that the second step of apoB-LP assembly was missing in this cell line. The now classic example of the two-step assembly of apoB-LP is found in apoB48 VLDL assembly in the McA-RH7777 cell line (Boren et al., 1994). McA-RH7777 cells, rat liver derived cells, are the only hepatoma available that produces apoB-LP of VLDL-density that are also suitable for stable transfection with recombinant apoBs. McA-RH7777 cells cultured in the absence of oleic acid incorporate apoB48 into particles with a density similar to HDL, but when cultured in the presence of oleic acid, secrete apoB48 as particles of VLDL-density.

In order to demonstrate the two-step of lipoprotein assembly, the investigators employed pulse-chase methodology in which a "pulse" of radioactive amino acid labels proteins of interest, while the "chase" period allows investigators to track protein movement through the cell after replacement of the labeling media with "chase" media that contains no radioactive amino acids. S^{35}-methionine is commonly used as a marker in such studies, and in general cultures are exposed to the label for 10 min and then

chased with surplus of cold methionine for periods between 0 and 180 min. Various other treatments such as the absence or presence of cycloheximide, to stop protein synthesis are also used to form certain experimental endpoints. When cultured in the absence of oleic acid, McA-RH7777 labeled apoB was recovered only in particles of HDL density. When cultures were supplemented with oleic acid, labeled apoB-VLDL were secreted (Boren et al., 1994). Such results clearly demonstrate that the small particles of HDL-density were converted to large particles of VLDL-density with increased availability of core lipid precursors. Further evidence for a two-step mechanism in this model came from the observation that Brefeldin A at low concentration inhibited only the secretion of apoB48-VLDL but not apoB48-HDL (Rustaeus et al., 1995; Rustaeus et al., 1998). Brefeldin A is known to inhibit guanine nucleotide exchange proteins which acts as on adenosine diphosphate ribosylation factor 1 (Donaldson et al., 1992) This finding suggested that the first step of assembly occurred but not the second as addition of bulk TG during the second step would be expected to transform apoB48-HDL into less dense apoB48-VLDL. Furthermore, based on the results of elegant morphological studies, Hamilton et al. (1998) confirmed that VLDL-sized lipid droplets exist in the secretory pathway when no apoB is produced in the cell. The observation also suggests that formation of the second-step particle is an independent process. Recently, by combining an extraction procedure with pulse-chase experiments, Stillemark et al. (2000) showed efficient VLDL assembly requires apoB chains of at least apoB48 size. Nascent polypeptides as small as apoB20 were associated

with particles in the HDL density range. Thus, the structural requirements of apoB to form HDL-like first-step particles differ from those to form second-step VLDL.

In general, apoB100 and apoB48 appear to assemble into apoB-LP through similar two-step mechanisms (Glickman et al., 1986). This process was illustrated in cartoon form by (Rustaeus et al., 1995) (Fig. 1.9). Henceforth this review will focus on the assembly and secretion of apoB100-containing lipoproteins.

Formation of apoB-containing apoB-LP precursor

apoB-containing apoB-LP precursor is formed in rough ER during the translation and translocation of apoB to the lumen of the rough ER through a short post-translation period (Boren et al., 1992; Rustaeus et al., 1998). apoB is synthesized by the ribosomes on the rough ER, translocated into the lumen of the ER by a process in which apoB is only loosely associated with the translocon (Rustaeus et al., 1998). The lipid components of the first-step particle are added co- and post-apoB translation by MTP, which can bind and transfer several classes of lipid molecules (TG, CE and phospholipids) between

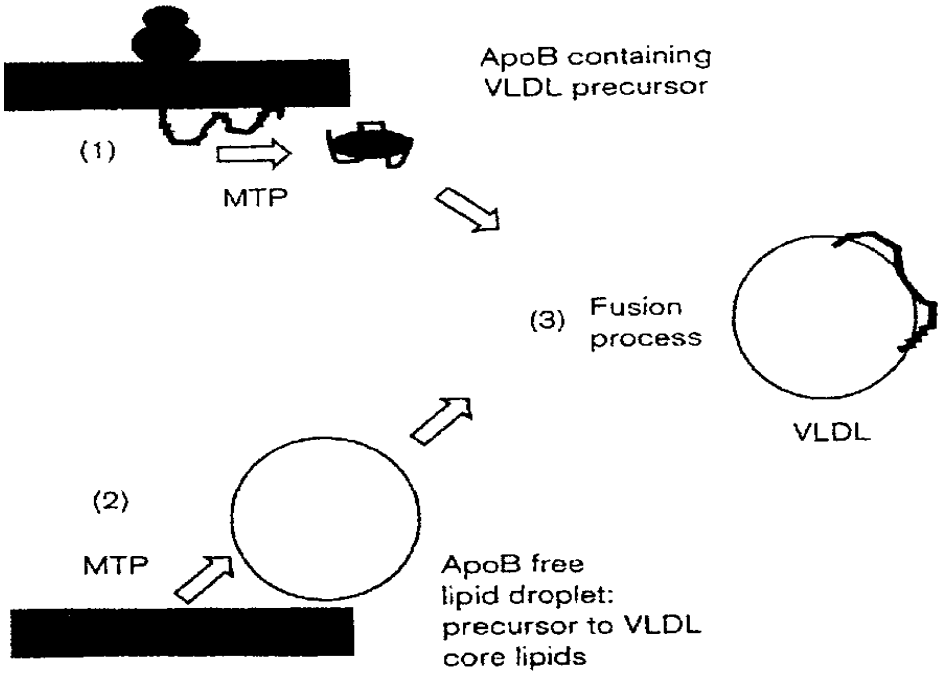

Figure 1.9 Assembly of very low-density lipoprotein. Two precursors are formed independently. apoB-containing VLDL precursor is produced during the translation and concomitant translocation of apoB to the lumen of ER and during a short period after the protein has been completely synthesized. The process is dependent on MTP. apoB-free lipid-rich precursor is formed in a process that is catalyzed by MTP. Two precursors are fused to form a mature VLDL particle (Olofsson et al., 1999).

membranes (Atzel and Wetterau, 1993). The MTP-mediated lipid transfer process produces a partially lipidated apoB-containing apoB-LP precursor, i.e. the first-step particle. MTP is essential for apoB lipidation, and it is the lack of functional MTP that leads to abeta-lipoproteinemia (Wetterau et al., 1992). The partially lipidated apoB-containing apoB-LP precursor is loosely associated with the ER membrane, and may form a mature lipoprotein particle that is eventually secreted from the cell.

Formation of lipid-rich apoB-deficient apoB-LP precursor

Using immunology with electron microscopy, Alexander et al. (1976) showed VLDL-sized particles without immuno-detectable apoB being present in the smooth ER. This observation indicated that lipid-rich apoB-deficient precursor was formed in the lumen of smooth ER. To date, the mechanism for the formation of the lipid-rich precursor is not clear. Raabe et al. (1999), using a liver-specific knockout of MTP, showed that VLDL-sized particles disappeared when the MTP gene was ablated. In addition, Wang et al. (1999) reported that an inhibition of MTP inhibited the transfer of TG from the cytosol to the lumen of the apoB-LP secretory pathway. These results suggest that MTP is also needed for the formation of lipid-rich apoB-deficient apoB-LP precursor, (i.e. second-step assembly intermediate).

Assembly and secretion of the apoB-LP particle

Alexander et al. (1976) showed that immuno-detectible apoB appeared in association with VLDL-sized LP particles both in the smooth termini of the rough ER and in the distal portion of the secretory pathway. Thus, in a two-step model, it is proposed that apoB-containing LP precursor and lipid-rich apoB-deficient LP precursor form separately and are then assembled within the lumen of the ER (Fig. 1.10) by an as yet poorly described process. The process that joins the two assembly intermediates appears to be independent of MTP (Stillemark et al., 2000), but requires chaperone proteins and energy (Olofsson et al., 2000). The nascent apoB-LP particles then move to the Golgi complex where their structure and composition can be modified (e.g., by glycosylation) (Voet et al., 1999). The Golgi vesicles filled with nascent apoB-LP migrate to the cell surface where apoB-LP are exported by exocytosis into the subendothelial space (Fig. 1.11).

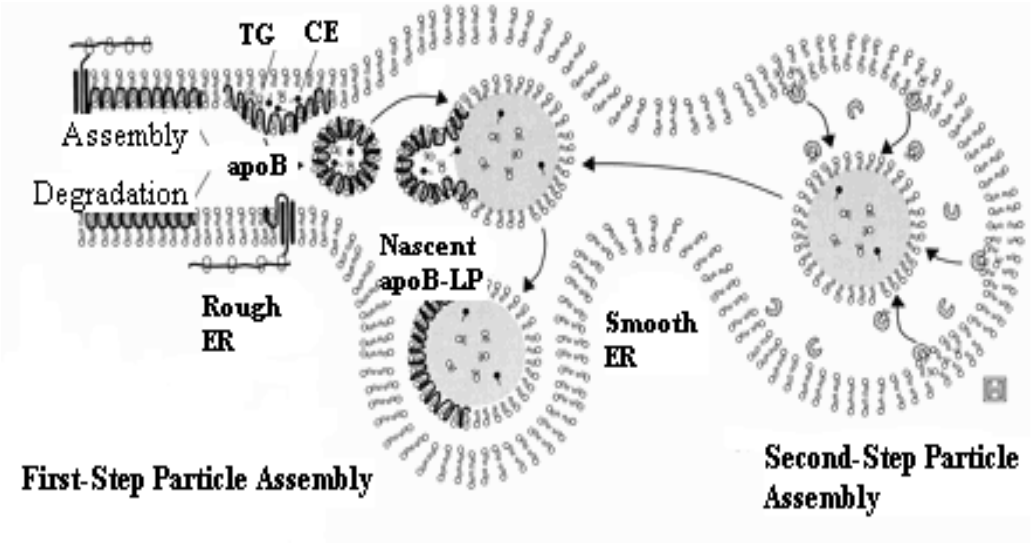

Figure 1.10 A two-step model for the assembly of apoB-containing lipoproteins. The two-step hypothesis predicts that two assembly precursors are assembled within the lumen of the ER. In step 1, small, dense, partially lipidated apoB-containing particles (first-step particles) are released from the rough ER membrane. In step 2, lipid-rich apoB-free particles (second-step particles) are formed in the lumen of smooth ER. The two precursors join together, producing a completed nascent apoB-LP. (Hamilton et al., 1998).

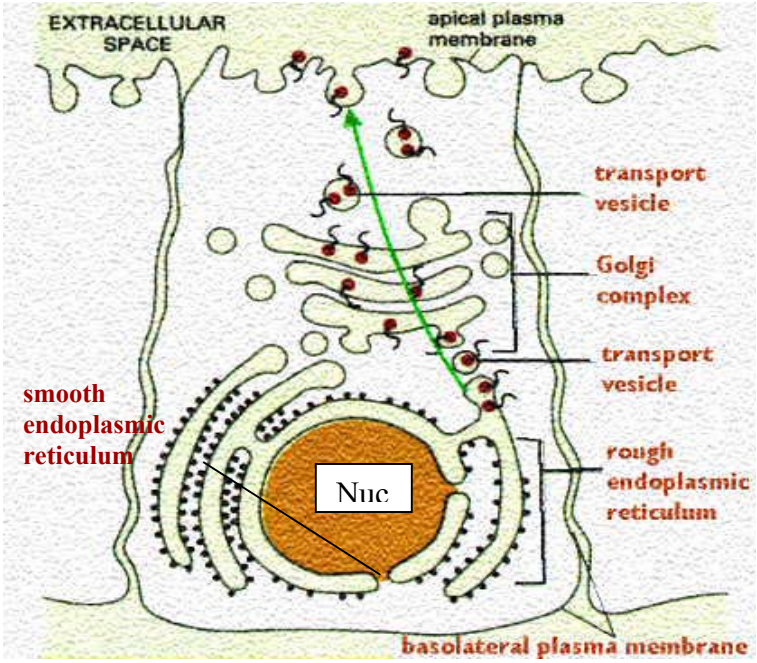

Figure 1.11 Nascent lipoprotein secretion pathway. The nascent apoB-containing lipoprotein (apoB-LP) particles move to Golgi complex where nascent particles can be modified (glycosylation). The Golgi vesicles then migrate to the cell surface where apoB-LP are exported by exocytosis into the subendothelial space. Nuc , nucleus (Bannykh and Balch, 1997).

Regulation of the assembly and secretion of apoB-LP

Studies from cultured cells and animal models show that the availability of lipid, and apoB and MTP activity all influence the assembly and secretion of apoB-LP. Lipid availability greatly influences translocation and post-translational regulation of apoB for assembly into lipoprotein particles and secretion (Dixon and Ginsberg, 1993). The translocation of apoB is atypical for secretory proteins in that it slows or even stops, depending on the availability of lipid. If lipid is inadequate, inefficient translocation results in exposure of apoB to the cytosol where it complexes with heat shock protein 70 (HSP 70) (Zhou et al., 1995), and this, in turn, leads to ubiquitination and proteasomal degradation of nascent apoB (Fisher et al., 1997). In contrast, if lipid is available, apoB translocation is efficient, and apoB is targeted for assembly and secretion. Many studies demonstrate that TG availability is the major factor in the post-translational regulation of apoB-LP assembly and secretion, and the mechanism of apoB secretion stimulated by fatty acid appears to stimulate TG synthesis and secretion. Arbeeny et al. (1992) reported that fatty acid synthesis, TG synthesis and apoB secretion were inhibited when primary hamster hepatocytes were treated with an inhibitor of acetyl coenzyme A carboxylase, a key regulatory enzyme of *de novo* fatty acid synthesis, but when oleic acid, an end product of fatty acid synthesis, was added to the medium, the inhibition of fatty acid synthesis was reversed. Similar effects were observed when HepG2 cells were treated with an inhibitor of fatty acid synthetase (Wu et al., 1994). However, the type of fatty acid supplied to hepatocytes has a marked influence on the assembly and secretion of apoB-LP. For example, while oleic acid promotes apoB secretion by stimulating TG

synthesis and availability, while n-3 fatty acids inhibit apoB secretion, presumably by reducing the ability of hepatocytes to synthesize or mobilize TG for secretion (Lang and Davis, 1990; Wang et al., 1994). The availability of intracellular cholesterol and cholesteryl ester also regulates the assembly and secretion of apoB-LP. Some investigators (Cianflone et al., 1990; Spector et al., 1979) reported a major regulatory role for the intracellular cholesterol esterifying enzyme ACAT, which is located in the rough ER of rat liver. Cianflone et al., (1990) reported that lovastatin or inhibitor of ACAT (58-035) decreased CE synthesis as well as apoB secretion.

Phospholipids are also required for the assembly and secretion of apoB-LP. Phosphatidylcholine is the predominant phospholipid in plasma lipoproteins, and secretion of apoB-LP was impaired in choline-decificent rats (Verkade et al., 1993). Phospholipids are made in both smooth ER and rough ER (Van Golde et al., 1971), and have a long half life in liver (several hours in PL versus < 1 hour in TG) (Glaumann et al., 1975). Therefore, under most metabolic conditions phospholipids would be available for assembly into lipoproteins.

Availability of lipid is important not only in the regulation of apoB turnover and availability for apoB-LP assembly and secretion, but also influences the heterogeneity of secreted apoB-LP. For example, Ellsworth et al. (1986) observed that when HepG2 cells were incubated with oleic acid, secreted apoB and TG were both redistributed from the LDL to the VLDL density range. Wang et al. (1988) reported that 47% of the TG secreted by HepG2 cells was present in the IDL density range. Therefore, the supply of

nutrients to the liver cell may play an important role in determining the heterogeneity of lipoprotein that is secreted.

As described above, under most metabolic conditions, the requirement for lipid to drive apoB-LP assembly is greater than the requirement for apoB. However, the availability of lipid is determined by nutritional status. Studies in rat hepatocytes provided evidence that hepatocytes from fasted rats displayed a marked decrease in the secretion of apoB-LP, in contrast hepatocytes from rats fed carbohydrate-rich diets displayed increased secretion of apoB-LP (Ford et al., 1968; Bell-Quint and Forte, 1981). Recently, evidence from animal studies (Taghibiglou et al., 2000) and clinical trials (Parks et al., 1999) showed that a diet high in carbohydrate induced TG synthesis and elevated TG concentration. Increased availability of TG increases VLDL assembly and secretion, and can result in the overproduction of VLDL. In summary, the assembly and secretion of apoB-LP can be significantly influenced by the availability of lipid, which could be mainly determined by diet supply.

apoB is another important factor that regulates the assembly and secretion of apoB-LP. apoB gene knockout mice demonstrated reduced plasma apoB levels (Farese et al., 1995). Furthermore, Linton et al. (1993a) reported that plasma concentrations of LDL and human apoB were increased in transgenic mice expressing human apoB100. However, a controversy regarding the regulation at the apoB mRNA level exists. Some studies (Pullinger et al., 1989; Leighton et al., 1990; Moberly et al., 1990) showed that apoB mRNA level does not change when apoB secretion is altered over a wide range, indicating that apoB mRNA level does not regulate apoB secretion. Dashti et al. (1989)

also demonstrated that apoB mRNA concentrations were increased by insulin or oleic acid, whereas other studies suggested that it is possible that apoB secretion is partially regulated at the mRNA level. For example, Hennessy et al. (1992) reported that the hepatic apoB mRNA level was 87% higher in Cebus monkeys fed coconut oil and cholesterol than in animals fed corn oil without cholesterol. Dashti (1992) and Theriault et al. (1992) demonstrated that 25-hydroxycholesterol and thyroid hormone increased apoB mRNA levels and regulated apoB secretion at the transcriptional level. The apoB mRNA level and translational rate in hepatic cells are largely constitutive (Yao et al., 1997). Thus the assembly and secretion of apoB-LP are regulated primarily at the levels of co- and post-translational degradation of apoB, with degradative sorting being linked to apoB failure to acquire sufficient lipid to attain proper conformation for subsequent assembly processes (Fisher et al., 2001)

Normally, apoB are produced in excess, and the availability of cellular lipid and other factors regulate apoB secretion (Davis, 1999). Thus, translated apoB may enter either the degradation pathway or be assembled into lipoproteins that are subsequently secreted. There are three pathways leading to apoB degradation. The first pathway is ER-associated degradation. Newly synthesized apoB in ER are initially complexed with small amounts of lipid shuttled by MTP (Berriot-Varoqueaux et al., 2000). During lipid deprivation (Dixon and Ginsberg, 1993) or MTP deficiency (Wetterau et al., 1992), this initial lipidation step fails, and the lipid-poor apoB becomes misfolded leading to its ubiquitinylation and targeting to proteasomal degradation (Fisher et al., 1997). The second mechanism is a post-ER, pre-secretory, proteolytic degradative pathway, which

was recently proposed by Fisher group (Fisher et al., 2001; Williams and Fisher, 2001). The process occurs between particle lipidation and assembly in the ER and export across the plasma membrane (Fisher et al., 2001). Post-ER, pre-secretory proteolysis can be triggered by n-3 fatty acids through a signal responsible for targeting apoB-LP to degradation in cells before the particles exit from the ER. This signal serves to trigger the appropriate trafficking of the doomed substrate to post-ER degradation. It has been suggested that insulin-stimulated apoB degradation involves phosphoinositide 3-kinase (PI3K) translocation to the ER membrane and the sorting of apoB to a post-ER degradative pathway (Phung et al., 1997).

The third mechanism for degradation of newly synthesized apoB is the re-uptake pathway. Re-uptake can occur after fully assembled apoB-containing particles have been exported across the plasma membrane but before they have diffused from the vicinity of the cell (Williams et al., 1990; Williams et al., 1992). Nascent particles have a chance of encountering cell surface receptors, including LDL receptors (Williams et al., 1990) and heparan sulfate proteoglycans (Williams et al., 1992), and being taken back into the cell for destruction in the lysosomes. The nature of LDL receptor ligand affinity would select against smaller diameter particles. Thus, the availability of lipid modulates apoB degradation as well as the level of apoB mRNA. However, between these two factors, it appears that the availability of lipid is more important in the regulation of apoB-LP assembly and secretion.

Research has established that MTP is required for apoB-LP assembly. The first direct evidence that linked MTP and a defect in apoB-LP production came from studies

(Wetterau et al., 1992) of abeta-lipoproteinemia. This genetic disorder is characterized by a defect in the production of CM and VLDL, due to defects in the MTP. Jamil et al. (1998) used an MTP inhibitor to inactivate MTP in HepG2 cells, and found that resultant decrease in MTP activity produced a proportional decrease in apoB secretion.

Several studies indicated that MTP plays an important role in the early stages of lipoprotein assembly. Cell culture studies (Gordon et al., 1994) showed that the products of the first-step of lipoprotein assembly, small, dense apoB-LP, were not observed in the absence of MTP. Raabe et al. (1999) reported that in MTP knockout mice, VLDL-sized, lipid–rich particles (putative second-step particles) within the ER were not detected. However, the role of MTP in the second-step of apoB-LP assembly remains controversial. Some studies (Gordon et al., 1996; Rustaeus et al., 1998) showed that TG addition to the nascent VLDL was MTP independent, whereas others (Wang et al., 1999) found that it was MTP dependent. In animal models, MTP large subunit gene expression is regulated in response to diet (Bennett et al., 1996; Lin et al., 1994). A high-fat diet increases MTP gene expression by 50% in liver and 200% in the intestines of hamsters (Bennett et al., 1996).

As mentioned above, lipoprotein particles are complex and include at least four different kinds of lipid, and the relative availability of each class of lipids found in apoB-LP influence their assembly and secretion. The synthesis of all VLDL lipid classes is coordinately changed in response to nutritional and hormonal state (Davis, 1999). Fasting decreased, whereas carbohydrate feeding increased, the synthesis of all VLDL lipids (Boogaerts et al., 1984), suggesting a co-ordinated regulation of metabolic

pathways related to the regulation of the assembly and secretion of apoB-LP. There are several interrelated systems that regulate gene expression to control the flux through various lipid metabolic pathways. Recently, sterol regulatory element binding proteins (SREBP) were linked to control of several pathways related to cholesterol and fatty acid metabolism (Brown and Goldstein, 1997). The SREBP are a superfamily of nuclear transcription factors (proteins) that bind to sterol regulatory element-1 (SRE-1). The SRE-1 is an upstream promoter sequence binding of SREBP present on some genes involved in the biosynthesis and metabolism of different classes of lipid. SRE-1 activates expression of these genes. The SREBP regulate transcription of a number of genes (Table 1.2) including 3-hydroxy-3-methylglutaryl coenzyme A (HMG-CoA) reductase, HMG-CoA synthase, farnesyldiphosphate synthase and squalene synthase. The SREBP also modulate expression of LDL receptor, fatty acid synthase, glycerol-3-phosphate acyltransferase and other enzymes involved in lipid metabolism (Gurr et al., 2002).

Dietary Effect of High-carbohydrate Diet on apoB-containing Lipoproteins

As discussed above, the assembly and secretion of apoB-LP is a complex, process modulated by a variety of factors. Lipid, apoB and MTP are all required for the assembly and secretion of apoB-LP. In particular, the availability of all lipids, and most particularly TG can be significantly modulated by diet. Thus, diet has the potential to play a major role in both targeting apoB for secretion and determining the heterogeneity

TABLE 1.2

Genes whose expression is regulated by the sterol regulatory element binding protein (SREBP) system

Gene	Function in cell
LDL-receptor	Import of LDL particles
HMG-CoA systhase	*de novo* cholesterol synthesis
Squalene synthase	*de novo* cholesterol synthesis
Farnesyl diphosphate synthasr	*de novo* cholesterol synthesis
Lanosterol synthase	*de novo* cholesterol synthesis
Acetyl-CoA carboxylase	*de novo* fatty acid synthesis
Fatty acid synthase	*de novo* fatty acid synthesis
Stearoyl-CoA desaturase	Synthesis of oleate
Glycerol 3-phosphate acyltransferase	Triacylglycerol and phospholipid synthesis
Lipoprotein lipase	Import of lipoprotein-triacylglycerol
PPAR-γ	Induction of adipocyte differentiation
Leptin	Signal fat store size

Stimulation occurs in response to low cellular cholesterol content (Gurr et al., 2002).

of the secreted apoB-LP. Both of these processes may significantly affect the metabolism and the potential atherogenicity of the plasma apoB-LP.

High-carbohydrate diet is known to decrease plasma LDL cholesterol, a positive effect with regards to spontaneous risk for ASCVD (Grundy, 1986; Grundy et al., 1986; Krauss et al., 2000). Current dietary guidelines for reducing the risk for ASCVD emphasize the replacement of saturated fat with complex carbohydrates so that total fat intake does not exceed 30% of energy intake (Krauss et al., 2000). However, as early as 1950, Watkin et al. (1950) observed that the carbohydrate-induced decreases in plasma LDL cholesterol concentration was frequently accompanied by elevation of plasma TG, an independent risk factor for ASCVD (Criqui et al., 1993). Over the past five decades many studies by numerous investigators have examined the effects of high-carbohydrate diet on risk factors for ASCVD. The debate as to whether a net benefit to ASCVD risk is provided by consumption of low-fat, high-carbohydrate diet has continued (Connor and Connor, 1997; Katan et al., 1997; Ornish, 1998; Rudel, 1998). This section focuses on the effect of high-carbohydrate diets on apoB-LP biology.

The increase in plasma TG concentration is a major, consistent and reproducible effect of increasing dietary carbohydrate (> 55% Kcals from carbohydrate). This effect has been observed from clinical trials (Bantle et al., 2000; Melish et al., 1980; Reaven et al., 1965) and animal experiments, including different animal species (Kasim-Karakas et al., 1996; Kazumi et al., 1985; Kazumi et al., 1986; Remillard et al., 2001; Taghibiglou et al., 2000). The hypertriacylglycerolmia produced by high-fat diet (> 30% Kcals from fat) is believed to increase atherosclerotic risk (Austin et al., 1998). High-fat diet

increases the influx of dietary TG within circulation, resulting in elevated plasma TG concentrations, which is risk factor for atherosclerosis. Whether carbohydrate-induced hypertriaclyglycerolmia shares metabolic mechanisms with lipid–induced hypertriacylglycerolemia, and creates a similar atherogenic risk has been the subject of intense study. Studies demonstrated that consumption of high-carbohydrate diet is associated with elevation in both the amount of TG per apoB-LP particle (Schonfeld, 1970) and the number of apoB-LP particles in the plasma (Ginsberg et al., 1981). Reaven et al. (1965) proposed that carbohydrate-induced hypertriacylglycerolemia resulted primarily from overproduction of TG. In addition, carbohydrate-induced hypertriacylglycerolemia reflected a defect in peripheral clearance mechanisms in as much as clearance rate did not match production rates (relative overproduction of VLDL) (Huff and Nestel, 1982). The most obvious metabolic explanation for carbohydrate-induced hypertriacylglycerolemia would be increased conversion of carbohydrate to fat in the liver via the *de novo* lipogenesis pathway, resulting in VLDL-TG overproduction. However, evidence has shown the fractional contribution from hepatic *de novo* lipogenesis to total VLDL-TG fatty acids is less than 5% (Hellerstein et al., 1991) in healthy subjects consuming high-fat diet. Obese, hyperinsulinmic human exhibit a *de novo* lipogenesis contribution of < 3-fold higher, but this still represents < 10% of VLDL TG (Hellerstein et al., 1991). Currently, some investigators (Howard et al., 1987; Reaven, 1997) propose that the metabolic mechanism of carbohydrate-induced hypertriacylglycerolemia involves an impaired ability of insulin to suppress adipose

tissue lipolysis, which leads to higher free fatty acid flux and increased VLDL production.

Small dense LDL are often observed in persons who consume high-carbohydrate diet. Dreon et al. (1994) analyzed changes in LDL pattern in 105 healthy men consuming high-fat and high-carbohydrate diets for 6 wk each and found that: 1) men exhibiting the pattern B profile of small dense LDL exhibited a 2-fold greater fall in LDL cholesterol than those starting the trial with a pattern A profile when consuming high-carbohydrate diet, 2) that one-third of men exhibiting a pattern A profile while consuming high-fat diet transformed to a pattern B profile while consuming the high-carbohydrate diet. In other words, there was a shift in LDL particle mass from larger, lipid-rich LDL_1 and LDL_2 to smaller, lipid-depleted LDL_3 and LDL_4. These results suggested that the reduction in LDL cholesterol that occurred when a high-carbohydrate diet was consumed was due to a shift from larger, more cholesterol-rich LDL to smaller, cholesterol-depleted LDL without reduction in apoB concentrations. Importantly, when studies were performed under isocaloric conditions, it was reported that hypertriglyceridemia caused by an isocaloric high-carbohydrate intake is not associated with a decrease in LDL particle size (Kasim-Karakas et al., 1997). Weight loss (Lichtenstein et al., 1994) and exercise (Koutsari et al., 2001) under isocaloric conditions also can attenuate the negative effects of high-carbohydrate diet on LDL diameter. Both of these latter factors should reduce adipose-linked free fatty acid concentrations.

Another important consequence of high-carbohydrate diet in human is a lowering of plasma HDL cholesterol, which has been a compelling reason to discourage the

consumption of these diets. Low plasma HDL cholesterol is a major cardiovascular risk factor that is independent of other known risk factors (Rader, 2002). Turley et al. (1998) reported that high-carbohydrate (22%, 6% and 59% energy from total, saturated, and carbohydrate, respectively) consumption was associated with a significant reduction in HDL cholesterol compared with high-fat (36%, 18%, and 43% energy from total, saturated, and carbohydrate, respectively) values. Currently, the proposed mechanism of high carbohydrate-induced lowering of HDL cholesterol in humans involves exchange CE from the core of HDL with TG present in the VLDL core via CETP (Kwiterovich, 2000) than high-fat diet. Interestingly, hamsters fed a high-carbohydrate diet exhibited elevated HDL cholesterol despite increased plasma CETP activity (Remillard et al., 2001).

Carbohydrate-induced ALP characterized by an elevation of plasma TG, a reduction in HDL cholesterol and the presence of small dense LDL is often in association with insulin resistance. Insulin resistance is a common metabolic abnormality that is associated with an increased risk of both atherosclerosis and type 2 diabetes. Studies from humans and animals (Farquhar et al., 1966; Ford et al., 1968; Kasim-Karakas et al., 1996; Taghibiglou et al., 2000) have demonstrated that hyperinsulinemia and glucose intolerance could correlate with the degree of TG elevation during carbohydrate feeding. ALP is often observed in patients with insulin resistance and type 2 diabetes. Fisher et al. (1993) reported that large VLDL are typically overproduced in insulin resistant states such as are found with obesity and type 2 diabetes, characterized by a predominance of small, dense LDL in the plasma compartment.

Insulin has anti-inflammatory and vasodilatory actions on the vasculature under normal circumstances (Garg et al., 2000). Existing data indicate that insulin-mediated vasodilation is blunted in patients with type 2 diabetes (Williams et al., 1996). Maintenance of hemostasis is mediated through factors such as plasmingen activator inhibitor and tissue plasminogen activator. Insulin could increase the levels of plasmingen activator inhibitor and tissue plasminogen activator, diminishing fibrinolytic potential and increasing thrombotic risk (Meigs et al., 2000). The multiple lipoprotein changes observed with ALP commonly aggregate with other ASCVD risk factors, including insulin resistance, hypertension and a procoagulant state to form a syndrome of multiple metabolic risk factors called metabolic syndrome or Syndrome X. Recently, National Cholesterol Education Program Adult Treatment Panel III (NECP-ATP III) defined metabolic syndrome as the second target of risk-reduction therapy after the primary target, LDL cholesterol (NCEP, 2001). The suggestion that insulin resistance represents a major underlying abnormality driving cardiovascular disease has not been well documented, but several mechanisms have been suggested. Ginsberg and his associates (Ginsberg, 2000; Ginsberg and Huang, 2000) proposed that the underlying metabolic abnormality driving this dyslipidemia is an increased assembly and secretion of VLDL particles, leading to an increased plasma level of TG. Hypertriacylglycerolemia, in turn, results in a reduction in the HDL level and the generation of small, dense LDL; these events are mediated by CETP and hepatic lipase. In animals such as rats (Matsui et al., 1997), mice (Kamata et al., 2001) and hamsters (Kasim-Karakas et al., 1996), fructose feeding has been found to cause high TG and

insulin resistance, however, no data to date show that whether LDL particle size becomes small or not in fructose-fed rats or mice that typically lack CETP or whether fructose feeding cause the manifestations of Syndrome X in hamsters that express CETP. Fructose feeding stimulates *de novo* lipogenesis by bypassing a key regulatory step-phosphofructokinase-1 and increases pathway flux through triose phosphates, NADPH and the pentose cycle, increasing the availability of acetyl CoA and NADPH, stimulating fatty acid synthesis (Frayn and Kingman, 1995). Furthermore, it has been shown that high-fructose diets enhance the release of NEFA from adipose tissue (Vrana et al., 1974). The elevation of NEFA concentration in the plasma, in turn, leads to a significant increase of hepatic TG secretion as well as VLDL-TG synthesis. Zammit et al. (2001) proposed that insulin stimulation of hepatic TG secretion is the etiology of insulin resistance. Frequent stimulation of insulin secretion by carbohydrate feeding would result in a chronic stimulation of VLDL secretion, and increase delivery of acyl moieties to muscle. When acyl moieties core provided in excess of the oxidative needs of the tissue, they induce insulin resistance in muscle. Subsequently, insulin resistance in adipose tissue can develop due to the coordinate changes of muscle and adipose tissue caused by increased VLDL-TG. When insulin resistance occurs in adipose tissue, TG not only accumulates in hypertrophied adipocytes, but also in pancreatic β cells, where it is associated with disruption of glucose-induced insulin secretion. In adipose tissue, resistance to the anti-lipolytic effects of insulin would lead to increased concentrations of plasma NEFA. Increased NEFA concentration, which act as substrates for VLDL-TG secretion and induce lipoapoptosis in β cells, would thus link insulin resistance and

obesity to the development of type 2 diabetes. High-carbohydrate diet rather than high fat diet stimulates hepatic VLDL secretion and exacerbates the degree of insulin resistance (Chen et al., 1995; Reaven, 1997). Despite the extensive use of the fructose-fed hamster model, little is known about what changes occur in the physical properties of lipoproteins in those animals.

Summary

Currently, apoB-LP heterogeneity is believed to reflect variation in the atherogenicity of individual apoB-LP subclasses. The physical properties of apoB-LP isolated from blood reflect the summated actions of peripheral metabolism on lipoproteins following particle assembly and secretion. Little is known about the relationship of initial particle composition and structure and the physical properties of circulating apoB-LP. The initial properties of apoB-LP would define their initial substrate properties during peripheral metabolism and could be key determinants of particle metabolism. Specific genetic or dietary mechanisms can regulate the structure-function relations of apoB-LP via changes in the metabolism of circulating lipoproteins and the assembly and secretion of nascent lipoprotein particles.

Objectives of Study

The overall goal of this dissertation was to develop a better understanding of the pathobiological mechanisms of ASCVD. The specific objectives of this research were:

1) To assess several genetic components that impinge on ASCVD through a statistical model that was developed to describe the relations among apoB-LP physical properties, plasma cholesterol concentration and arterial plaque

formation. Independent data for the model were produced by quantifying specific physical properties of apoB-LP in four strains of transgenic mice that differed in the extent of plaque formation, plasma total lipid concentrations and lipoprotein density class distributions when fed a non-purified chow-type diet.

2) To assess certain dietary and metabolic modifiers of ASCVD, mainly the physical properties of circulating apoB-LP in a second rodent model, the Syrian Golden hamster was described and quantified after selected nutritional manipulation. Hamsters were selected as the model system as their native lipoprotein metabolism and response to diet are similar to those of humans in many respects. Specifically, modifications in dietary carbohydrate composition were used to vary insulin responses in order to model the human "Syndrome X" that is associated with increased ASCVD risk.
3) To assess whether altered nascent apoB-LP structure is a component in carbohydrate-induced changes in apoB-LP physiology. ApoB-LP assembly intermediates were isolated from the livers of hamsters fed diets of differing carbohydrate composition for characterization of physical properties.

CHAPTER II

SELECTIVE DELAYS IN APOLIPOPROTEIN B-CONTAINING LIPOPROTEIN CLEARANCE AFFECT CIRCULATING PARTICLE DIAMETER DISTRIBUTION AND PLAQUE FORMATION

Introduction

Apolipoprotein B-containing lipoproteins (apoB-LP) differ with regards to B-isoform, lipid content and composition, particle density and diameter. In clinical populations apoB-LP heterogeneity is associated with differences in ASCVD risk, although the exact changes most associated with increased risk are contentious (Campos et al., 2002; Williams et al., 2003). Dissecting the metabolic mechanisms that create atherogenic apoB–LP in free living human populations is problematic due to incompletely characterized sources of variation. In genetically homogeneous murine models fed identical diets, observed differences in the physical properties of circulating apoB-LP presumably result from the passage of nascent apoB-LP through the intravascular lipolytic cascade and associated remodeling and removal processes. Diet is known to impose additional variation to apoB-LP physical properties even in the setting of homogeneous genetic background (Rudel et al., 1998). Such model systems provide the means to dissect the mechanisms that influence apoB–LP physical properties and atherogenicity.

Delay in apoB-LP clearance was proposed to be a fundamental mechanism that converts native particles into atherogenic species (Walzem et al., 1995). Mice genetically engineered to express exclusively apoB100 or apoB48 showed marked reductions in apoB-LP particle diameter when clearance was delayed by concomitant ablation of the LDL receptor (LDLR) or apolipoprotein E (apoE), respectively (Veniant et al., 1998). apoB isoform *per se* did not affect the extent of arterial plaque formation, which was directly related to plasma cholesterol concentration. Separate studies showed that the LDL receptor related protein (LRP) played no significant role in the clearance of apoB100, while apoB48 was actively removed by both LRP and LDLR (Veniant et al., 1998). This difference in particle biology may underlie observed differences in turnover rates within apoB100 and apoB48 pools (Li et al., 1996) and with the extent of particle diameter change with genetic suppression of particle clearance mechanisms. For example, selective ablation of apoE or LDLR in apoB100-only mice produces similar plasma cholesterol concentrations, but cholesterol was associated with apoB-LP of VLDL diameter (mean, 53.4 nm) with apoE deficiency and LDL diameter (mean, 22.1 nm) with LDLR deficiency. Arterial plaque was much more extensive in apoB100–only mice lacking the LDLR than those lacking apoE. Exacerbation of plaque formation in the LDLR deficient apoB100-only mice resulted from the increased molar concentration of apoB–LP particles represented by smaller particles providing a similar plasma cholesterol concentration.

Relationships observed between particle diameter, cholesterol and apoB concentrations and plaque formation in models expressing exclusively one apoB100 or

apoB48 serve to clarify isoform specific effects, but may not fully replicate more complex interactions possible with heterogeneous apoB isoforms and/or differential rates of particle clearance as occur in free-living humans. As a first step towards development of systematic modeling approaches for these complex interactions we compared relationships between apoB–LP physical properties and arterial plaque formation in apoB wild-type mice relative to apoB100–only mice under in which apoB isoform specific clearance defects were created. Relationships among some of these parameters were reported previously for apoB100-only mice in this same sample set (Veniant et al., 2000).

Materials and Methods

Mice

Creation of these mouse strains was described (Veniant et al., 2001). Briefly, apoB100-only mice were generated by mutating apoB codon 2153 to prevent the expression of a stop codon in mouse embryonic stem (ES) cells (Farese et al., 1996). The genetic background of the mice was 50% C57BL/6 and 50% 129/Sv. The apoB100-only mice were bred with apoE-deficient mice (Piedrahita et al., 1992) to generate apoE-deficient apoB100-only ($Apoe^{-/-}Apob^{100/100}$) mice, and also bred with LDLR-deficient mice (Ishibashi et al., 1993) to generate LDLR-deficient apoB100-only ($Ldlr^{-/-}Apob^{100/100}$) mice. ApoE-deficient mice homozygous for a wild-type apoB allele ($Apoe^{-/-}Apob^{+/+}$) and LDLR-deficient mice homozygous for a wild-type apoB allele ($Ldlr^{-/-}Apob^{+/+}$) were also generated. Genotyping was performed by Southern blot analysis of genomic DNA. Each of the four mouse strains had a 75% C57BL/6 and 25%

129/Sv genetic background. The mice were weaned at 21 d, housed in a barrier facility with 12-h light/dark cycle and fed a chow diet containing 4.5% fat. Experiments were conducted when the mice were 40 wk old.

Blood collection and lipoprotein separation

At 40 wk of age, female mice were fasted 4 h prior to subjecting them to anesthesia and exsanguination via heart puncture. Whole blood was drawn into tubes that contained 1 mg EDTA and 10 U each streptomycin sulfate and procaine penicillin G/mL whole blood. Plasma was isolated by centrifugation at 2500 rpm at 4°C for 20 min, and then held at 4°C before apoB-LP isolation, particle diameter distribution determination and quantitation of apoB isoform concentrations. To minimize proteolytic degradation, 1.0 μL/mL plasma of phenylmethyl sulfonyl fluoride and 5 μL/mL plasma of aprotinin were added to fresh plasma. Total plasma apoB-LP were isolated as the $d < 1.07$ g/mL fraction of plasma (Chapman et al., 1981; Walzem et al., 1994) following 18 h of centrifugation at 40,000 rpm in a TFT 50.3 rotor at 14°C within a Beckman L8-70M ultracentrifuge. Particle diameter distributions were immediately determined in apoB-LP fractions of individual mice. Following analysis, the fractions were stored at –80°C prior to apoB isoform quantification.

Total plasma cholesterol and TG concentrations were measured in plasma samples using colorimetric assays (Spectrum cholesterol assay, Abbott Laboratories, Irving, TX; GB Triacylglycerol Kit, Boehringer Mannheim Biomedicals, Indianapolis, IN) (Veniant et al., 2000)

Apolipoprotein B-containing particle diameter distributions

Apolipoprotein B-containing particle diameters were determined by dynamic light scattering analysis using a Microtrac series 250 Ultrafine Particle Analyzer with a laser probe tip (UPA-250; Microtrac, Clearwater, FL) (Walzem et al., 1994; Veniant et al., 2000). Following ultracentrifugation, samples were carefully removed from the rotor and uncapped. The laser probe was gently placed on the top layer of the supernatant fraction. Great care was taken to not mix the sample layer or allow air bubbles to form at the probe liquid interface. Due to the low lipoprotein content of some samples, a measurement time of 600 sec was used for all samples. Raw particle size distributions were converted to area, number and volume population percentiles, which were used to calculate median particle size for the respective distributions.

Quantitation of apoB100 and apoB48

The concentrations of apoB100 and apoB48 in apoB-LP isolated from $Apoe^{-/-}$ $Apob^{100/100}$, $Apoe^{-/-}Apob^{+/+}$, $Ldlr^{-/-}Apob^{100/100}$ and $Ldlr^{-/-}Apob^{+/+}$ mice were determined by analytical sodium dodecyl sulfate polyacrylamide gel electrophoresis (SDS-PAGE) following Coomassie staining of the separated apolipoproteins (Kotite et al., 1995).

The protein content of isolated apoB-LP was analyzed by a modified Lowry assay (Lowry et al., 1951). Sample volumes containing 50-200 μg protein were combined with 60 μg apotransferritin carrier protein prior to delipidation in order to insure quantitative apolipoprotein recovery (Kotite et al., 1995). Samples were delipidated overnight at –20°C in an ethanol-diethyl ether (3:1 vol/vol) system in which 400–1,200 μL of sample were mixed with 10 vol of ice-cold ethanol-diethyl ether in a 15-mL conical, glass

stoppered tube and thrice inverted. The delipidated mixture was centrifuged for 25 min at 1250 rpm to facilitate removal of the organic phase by a glass transfer pipet. The pellet was then extracted twice with 4 mL cold anhydrous diethyl ether. The resultant whitish pellet was dissolved in 50–100 μL sample buffer containing 10% glycerol, 3% SDS, 1.5% dithiothreitol (DTT), 1% mercaptoacetic acid and 0.02% bromphenol blue in 1 M Tris, pH 6.8. Excess ether was removed under a gentle stream of nitrogen, and the dissolved apolipoproteins were denatured at 100°C for 3 min prior to application to a SDS-PAGE gel.

Individual apoB isoforms were separated using the SDS-PAGE gradient gel and conditions described by Kotite et al. (Kotite et al., 1995) with some modifications. Briefly, the 3–12% gradient polyacrylamide gel was cast using a two-chamber gradient mixer (Bio-Rad Laboratories, Hercules, CA). The 3% polyacrylamide solution contained 3% acrylamide, 0.08% bisacrylamide, 0.1% SDS, 0.03 g/mL glycerol, 0.06% ammonium persulfate (APS) and 0.05% N,N,N,N-tetramethylethylenediamine (TEMED) in 0.376 M Tris, pH 9.2 in the resolving gel, and pH 6.8 in the stacking gel. The 12% polyacrylamide solution contained 12% acrylamide, 0.33% bisacrylamide, 0.1% SDS, 0.10 g/mL glycerol, 0.06% APS and 0.05% TEMED in 0.376 M Tris, pH 9.2. Apolipoprotein separation was effected using a Mini-PROTEIN 2 Vertical gel apparatus (Bio-Rad Laboratories Inc, Hercules, CA) (Laemmli, 1970) containing two minigels in each separation. After loading 50 μL delipidated apoB-LP or standard in each well, a Bio-Rad PowerPAC 300 (Bio-Rad, Laboratories Inc, Hercules, CA) was used to apply 76V to the gels for the first 30 min, followed by 96V until the dye front

was 1 mm from the bottom of the gel. Narrow-cut human LDL served as the source for the apoB100 used as the reference protein within the standard curves.

Following electrophoresis, gels were stained for 15–30 min at 60°C with staining solution containing ethanol:water:glacial acetic acid, 3:8:1 (vol/vol/vol), and 0.15% Coomassie Brilliant Blue R-250 (Sigma Chemical Co., St. Louis, MO). The gels were then destained for 30-60 min at 60°C with a destaining solution of ethanol:water:glacical acetic acid, 3:8:1 (vol/vol/vol). After destaining, the gels were placed between two sheets of cellophane gel wrap (BioDesign Inc. of New York. Carmel, NY), and dried in a fume hood overnight. The dry gels were scanned using a laser scanner (Fluor-STM MultiImage; Bio-Rad, Laboratories Inc, Hercules, CA) equipped with an Image Quant Software Package to automatically integrate the volume of each stained apolipoprotein band. The standard curve for apoB100 was constructed by relating the intensity of dye uptake of each band to its known mass. The line of fit was evaluated by the method at least squares for the power function $y = ax^b$ (Kotite et al., 1995). Because apoB100 and apoB48 have equal chromogenicities (Bergeron et al., 1996), the same standard curve was used to analyze both apoB isoforms. The concentrations of individual apoB species in apoB-LP was calculated from the regression equation relating the absorbance of individual apoB100 standard bands to the amount of apoB100 standard applied to the gel.

Analysis of arterial plaque

Mice arterial plaque was quantified in pinned-out aortas as described by Tangirala et al. (1995). The mice were perfused and the tissues were fixed prior to removal of the

portion of the aorta between the aortic valve and the bracheocephalic artery and then pinned flat on a black wax surface. The image of the pinned-out aortas was recorded with a Polaroid digital microscope camera (Polaroid Corporation, Cambridge, MA), the image was analyzed and plaque was quantified as the percentage of the aortic surface covered by plaque.

Statistical analysis

The results are presented as the mean ± SEM unless otherwise noted. Regression analysis was used to test the strength of association between the percentage of total apoB-LP particles found within individual machine–defined diameter ranges and arterial plaque area. Information regarding those diameter ranges found to have significant associations (positive or negative) with plaque formation was used in subsequent ANOVA models. The arterial plaque area attributable to genotype was tested by one-way ANOVA, while the ability of surrogate markers (e.g. particle diameter, plasma cholesterol concentration) to describe genotype-driven effects on arterial plaque area were modeled by GLM (Proc GLM, SAS Institute, Carey NC). F-testing and partial correlation coefficients were used to determine the significance of individual components of the linear model. Differences among mean values were tested by a least-squares means procedure. Differences were considered significantly different at $P < 0.05$. All these analyses were performed using statistical analysis system procedures (SAS Institute, Inc., Cary, NC)

Results

Plasma lipids and bodyweight

Mice of the $Apob^{+/+}$ $Ldlr^{-/-}$ genotype weighed significantly less than mice of either apoB genotype lacking apoE; bodyweights of apoB100–only mice lacking the LDLR were intermediate (Table 2.1). The plasma total cholesterol concentration was higher in $Apoe^{-/-}Apob^{+/+}$ mice (461 ± 29 mg/dL) than in the other three groups, while there was much lower cholesterol concentration in $Ldlr^{-/-}Apob^{+/+}$ (190 ± 6 mg/dL) mice. $Apoe^{-/-}Apob^{100/100}$ mice (278 ± 7 mg/dL) and $Ldlr^{-/-}$ $Apob^{100/100}$ (296 ± 6 mg/dL) did not have significantly different cholesterol concentrations (Table 2.1). Significant differences were also found in plasma HDL cholesterol concentrations (HDLc, Table 2.1), with $Ldlr^{-/-}Apob^{+/+}$ mice having the greatest concentration (55.5 ± 3 mg/dL), significantly greater than the 42.6 ± 1 mg/dL observed in $Apoe^{-/-}Apob^{100/100}$ mice. That concentration was in turn significantly greater than the 34.8 ± 2 mg/dL observed in $Apoe^{-/-}Apob^{+/+}$ mice or the 32.9 ± 0.7 mg/dL observed in $Ldlr^{-/-}$ $Apob^{100/100}$ mice, the latter two values were not different from one another. Plasma triacylglycerols in $Apoe^{-/-}$ $Apob^{100/100}$ mice, being (127 ± 18 mg/dL) were significantly higher than in any other genotype. Plasma triacylglycerol concentrations in both $Apoe^{-/-}Apob^{+/+}$ mice (87 ± 10 mg/dL) and $Ldlr^{-/-}$ $Apob^{100/100}$ (82 ± 5 mg/dL) mice were similar and significantly higher than that of $Ldlr^{-/-}Apob^{+/+}$ mice (65 ± 6 mg/dL).

TABLE 2.1

Body weight, plasma cholesterol and triacylglycerol concentrations in different mouse genotypes[1]

Genotype	Body weight	Cholesterol	HDL-cholesterol	Triacylglycerol
	g	mg/dL	mg/dL	mg/dL
$Apoe^{-/-}Apob^{100/100}$	28.22 ± 0.81^{a}	278 ± 7^{b}	42.61 ± 1.06^{b}	126.66 ± 17.60^{a}
$Apoe^{-/-}Apob^{+/+}$	29.20 ± 1.25^{a}	461 ± 29^{a}	34.84 ± 2.33^{c}	86.62 ± 9.70^{b}
$Ldlr^{-/-}Apob^{100/100}$	27.86 ± 1.45^{ab}	296 ± 6^{b}	32.85 ± 0.68^{c}	82.42 ± 4.54^{b}
$Ldlr^{-/-}Apob^{+/+}$	25.75 ± 0.52^{b}	190 ± 6^{c}	55.49 ± 2.77^{a}	64.93 ± 5.80^{c}

1 Values are mean ± SEM, n = 14 per genotype. Values sharing a common superscript are significantly different ($P < 0.05$)

TABLE 2.2

apoB-LP particle diameters and percentage of aortic plaque in different mouse genotypes[1]

Genotype	Particle diameter	Plaque
	nm	%
$Apoe^{-/-}Apob^{100/100}$	62.26 ± 1.37^{a}	4.50 ± 0.53^{b}
$Apoe^{-/-}Apob^{+/+}$	38.83 ± 0.14^{b}	6.58 ± 0.96^{b}
$Ldlr^{-/-}Apob^{100/100}$	24.72 ± 0.05^{c}	14.38 ± 0.57^{a}
$Ldlr^{-/-}Apob^{+/+}$	$30.30 \pm 0 .08^{b}$	0.41 ± 0.16^{c}

1 Values are mean ± SEM of the 50th percentile of particle diameter distributions, n = 14 per genotype. Values sharing a common superscript are significantly different ($P < 0.05$).

Arterial plaque analysis

Analysis of the aortas revealed that the $Ldlr^{-/-}Apob^{100/100}$ mice (14.38 ± 0.57%) had significantly more lesions than did $Apoe^{-/-}$ $Apob^{100/100}$ mice (4.5 ± 0.53%) and $Apoe^{-/-}Apob^{+/+}$ mice (6.58 ± 0.96%), whereas the $Ldlr^{-/-}Apob^{+/+}$ mice had no arterial plaque formation (Table 2.2.)

Characterization and concentration of apoB

Individual apoB isoforms in plasma were quantitated optically in stained gels following separation of apoB100 and apoB48 by SDS-PAGE. Figure 2.1 is a representative example of a 3-20% gel prepared to show the total apoprotein profile of the apoB-LP plasma fractions from each mouse genotype. Mouse apoB-LP contained apoB of variable isoform in accordance with genotype in combination with apoA, apoC and apoE. Note that no apoB48 was present in plasma from apoB100-only mice, and similarly that not apoE was present in $apoE^{-/-}$ mice. The image of a typical gel used to separate and quantify apoB isoforms is shown in Figure 2.2. apoB100 was distinctly separated from apoB48 and the apotransferritin carrier protein was apparent at the bottom of the gel. A standard curve for apoB with 44 points was generated over a range of 0.795-27.2 μg apoB100 using 6 individual gels. The linear standard curve is shown in Figure 2.3. The concentration of individual apoB isoforms in individual samples was calculated using this aggregate standard curve for dye uptake. Two standard lanes containing different concentrations of human apoB100 were included in every sample gel. Differences in the MW of apoB100 and apoB48 were corrected and final values

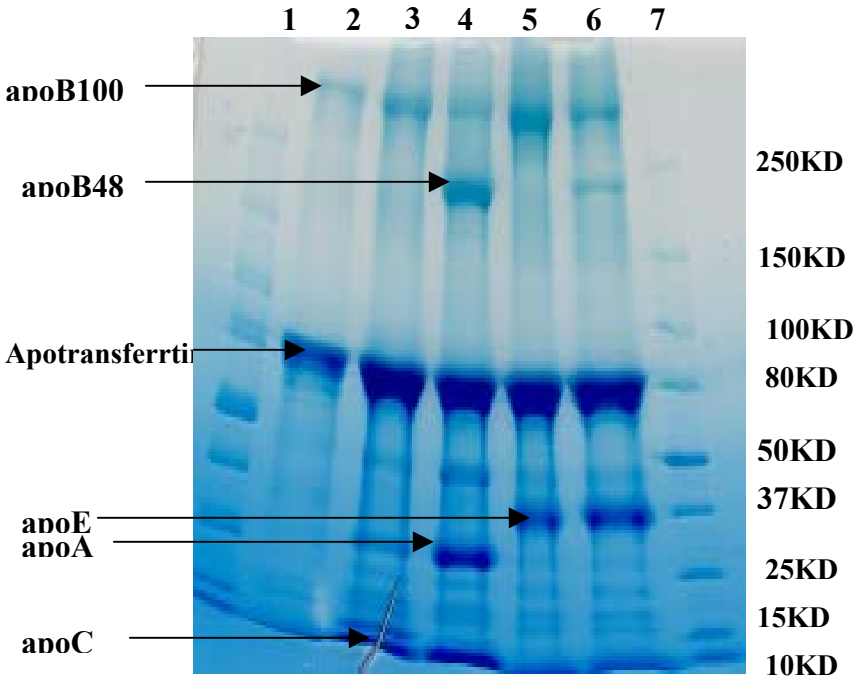

Figure 2.1 Analytical SDS-PAGE (3-20%) of murine plasma apoB-LP apoproteins visualized with Coomassie R250 stain. Lanes 1 and 7, MW standards; 2, apoB100 standard with apotransferrtin carrier protein; 3, $Apoe^{-/-}Apob^{100/100}$ mice; 4, $ApoE^{-/-}Apob^{+/+}$ mice; 5, $Ldlr^{-/-}Apob^{100/100}$ mice; and 6, $Ldlr^{-/-}Apob^{+/+}$ mice.

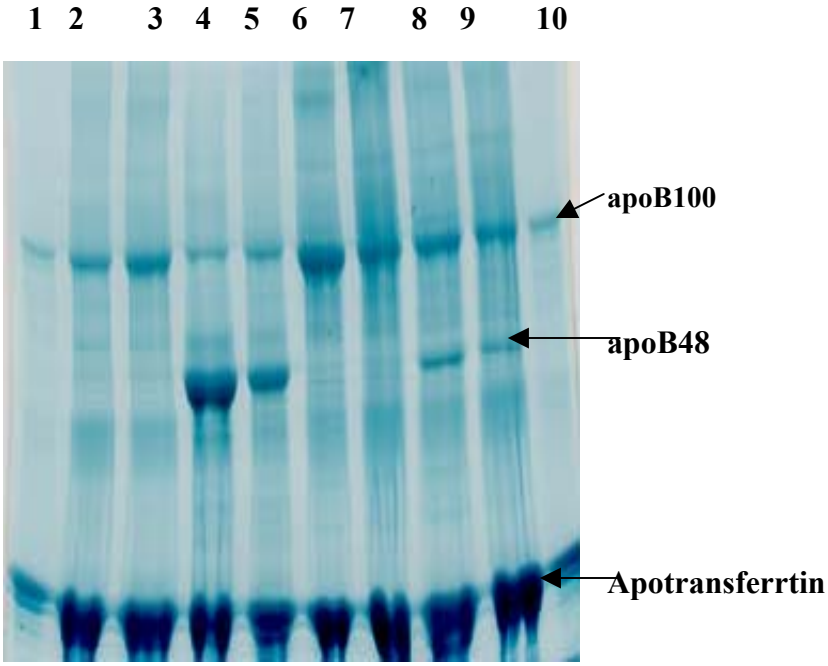

Figure 2.2 SDS-PAGE analysis of apoB100 and apoB48 in the plasma of mice with different genotypes. Mouse apoB–LP samples were analyzed using 3-12% SDS-PAGE as described in methods Lane 1 and10, narrow cut human LDL apoB100 standard with apotransferrtin carrier protein; 2 and 3, $Apoe^{-/-}Apob^{100/100}$mice; 4 and 5 $Apoe^{-/-}Apob^{+/+}$ mice; 6 and 7 $Ldlr^{-/-}Apob^{100/100}$ mice; 8 and 9 $Ldlr^{-/-}Apob^{+/+}$ mice.

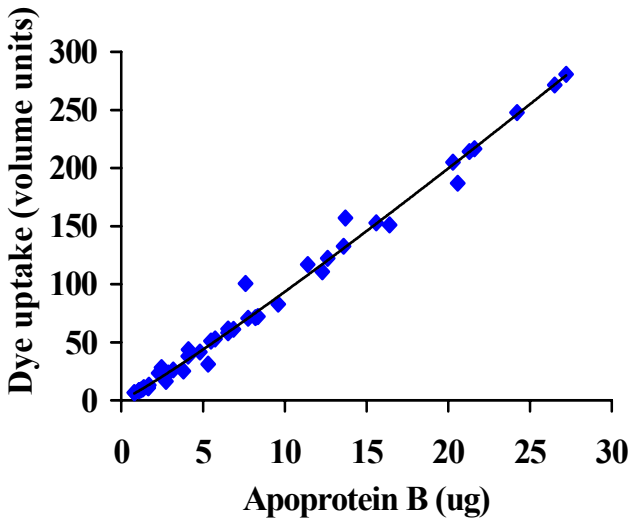

Figure 2.3 Linearity of response for Coomassie stained apoB100. A series of narrow-cut ($1.030 < d < 1.055$ g/mL) human apoB LDL proteins were analyzed by SDS-PAGE. The intensity of staining was quantified by densitometric scanning and related to protein concentration measured by Lowry assay.

LDLapoB100 $y = 7.4982 \text{ x } ^{1.0957}$, $r^2 = 0.9852$

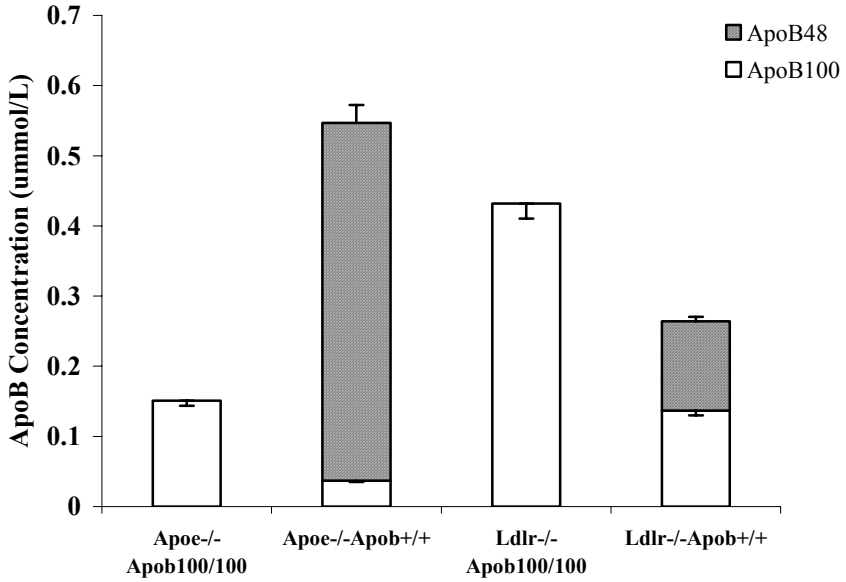

Figure 2.4 Plasma apoB concentrations in different genotype mice.

Values are means ± SEM, n = 14 per group.

were expressed as μmol/L plasma. Figure 2.4 shows the mean concentration of apoB isoforms for each genotype studied. Overall, the greatest difference in total apoB concentration existed between $Apoe^{-/-}Apob^{+/+}$ mice and $Apoe^{-/-}Apob^{100/100}$ mice. The total apoB concentration in plasma from $Apoe^{-/-}Apob^{+/+}$ mice was 0.55 ± 0.08 μmol/L, which is more than three times greater than the 0.15 ± 0.02 μmol/L in plasma from $Apoe^{-/-}Apob^{100/100}$ mice ($P < 0.001$). Notably, the 0.25 ± 0.05 μmol/L total apoB in plasma from $Ldlr^{-/-}Apob^{+/+}$ mice was not significantly different from the amount in plasma from $Apoe^{-/-}Apob^{100/100}$ mice. Similarly, the 0.43 ± 0.03 μmol/L of total apoB in $Ldlr^{-/-}$ $Apoe^{-/-}Apob^{100/100}$ mouse plasma was not significantly different from the amounts of total apoB in the $Apoe^{-/-}Apob^{+/+}$ strain. Thus, $Ldlr^{-/-}Apob^{100/100}$ mice and $Apoe^{-/-}Apob^{+/+}$ mice had similar total apoB concentrations in plasma, with the latter possessing a mixture of apoB100- and B48-containing lipoproteins. The $Apoe^{-/-}Apob^{100/100}$ and $Ldlr^{-/-}Apob^{+/+}$ mice had total apoB concentrations in plasma that were similar to one another and significantly lower than those of the other two genotypes; again, the $apoB^{+/+}$ strain possessed both apoB100 and apoB48.

Total apoB consisted of only apoB100 in $apoB^{100/100}$ mouse strains. The ratio of apoB48/apoB100 was not identical in the $Apob^{+/+}$ strains. Mice of the $Ldlr^{-/-}Apob^{+/+}$ strain possessed an apoB48/apoB100 of 1.0, while the ratio was 17.0 in $Apoe^{-/-}Apob^{+/+}$ mice. Considering only apoB100, mice of the $Ldlr^{-/-}Apob^{100/100}$ strain possessed the greatest amount, 0.43 ± 0.03 μmol/L, while the lowest concentration of apoB100, 0.03 ± 0.01 μmol/L, was observed in plasma from the $Apoe^{-/-}Apob^{+/+}$ mice. Intermediate concentrations of plasma $apoB_{100}$ were present in plasma from $Apoe^{-/-}Apob^{100/100}$ mice,

0.15 ± 0.02 μmol/L, and Ldlr$^{-/-}$Apob$^{+/+}$ mice, 0.14 ± 0.03 μmol/L. No apoB48 was present in plasma from Apoe$^{-/-}$Apob$^{100/100}$ mice. The apoB48 plasma concentration in Apoe$^{-/-}$Apob$^{+/+}$ mice was 0.51 ± 0.29 μmol/L, and was much higher ($P < 0.05$) than the 0.13 ± 0.02 μmol/L in Ldlr$^{-/-}$Apob$^{+/+}$ mice. Thus the total apoB concentration in Apoe$^{-/-}$Apob$^{+/+}$ mice was 0.55 ± 0.08 μmol/L, more than twice as much as the 0.25 ± 0.05 μmol/L in Ldlr$^{-/-}$Apob$^{+/+}$ mice. The fraction of apoB whose clearance was delayed was estimated in Apoe$^{-/-}$Apob$^{+/+}$ mice as [μmol/L apoBtotal x (apoB48/apoBtotal)], in Ldlr$^{-/-}$Apob$^{+/+}$ mice as [μmol/L apoBtotal x (apoB100/apoBtotal)]. Due to the exclusive reliance of native LDL on LDLR for clearance, 100% of the apoB in Ldlr$^{-/-}$Apob$^{100/100}$ mice was assumed to be impaired. In Apoe$^{-/-}$Apob$^{100/100}$ mice, the fraction of apoB whose clearance was delayed was estimated as μmol/L apoBtotal x [(μmol/L apoBtotal in Apoe$^{-/-}$Apob$^{100/100}$ mice - μmol/L apoB$^{100/100}$ in Apoe$^{-/-}$Apob$^{+/+}$ mice)/ μmol/apoBtotal].

Apolipoprotein B-containing particle diameter in transgenic mice

The mean of apoB-LP ($d < 1.07$ g/mL) particle diameter across all mice was 36.9 ± 1.8 nm, with the diameter of particles at the 10th percentile being 24.0 ± 0.9 nm and the 90th percentile being 53.4 ± 3.1 nm. The percentage of apoB-LP with diameters smaller than 75 nm was 94.4 ± 1.2%. There were significant differences in particle diameters of mice with different genotypes (Table 2.2, Fig. 2.5). The 50th population percentile particle diameter was the largest in Apoe$^{-/-}$Apob$^{100/100}$ mice (62.3 nm). This diameter was significantly larger than that of particles from Apoe$^{-/-}$Apob$^{+/+}$ mice (38.8 nm) and Ldlr$^{-/-}$Apob$^{+/+}$ mice (30.3 nm), however the Ldlr$^{-/-}$Apob$^{100/100}$ mice had the smallest particle diameter (24.7 nm).

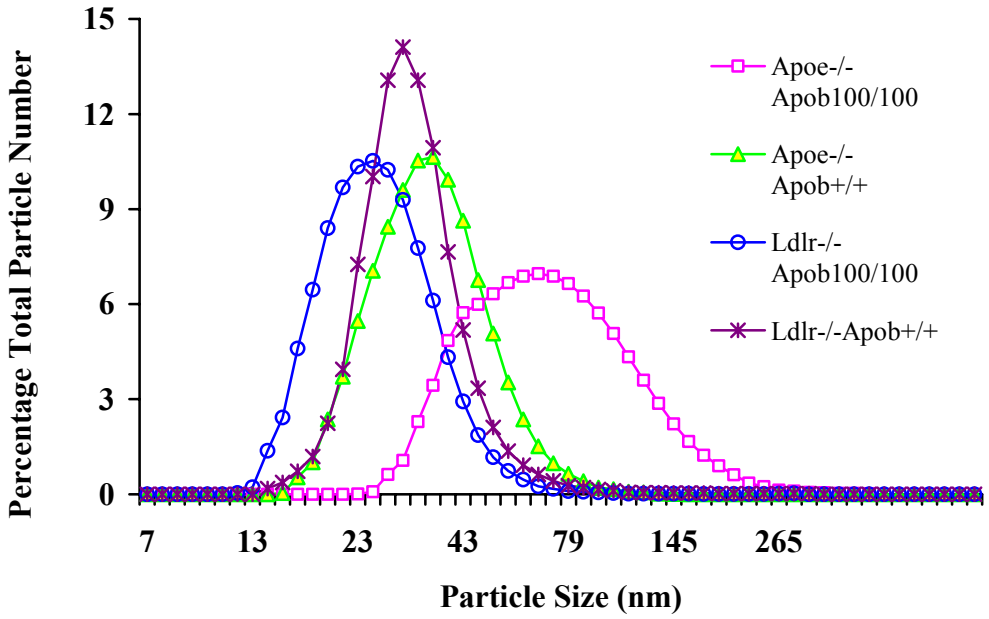

Figure 2.5 Dynamic light scattering-determined diameter distributions of apoB-containing lipoproteins (apoB-LP), d < 1.07 g/mL, isolated from mice of four different genotypes.

A further analysis of apoB-LP size is shown in a histogram plot (Fig. 2.6). Individual correlations were calculated between plaque formation and the fractional amount of apoB-LP that were present in fixed diameter intervals defined by the optics of the Microtrac® instrument. This plot shows that apoB-LP with diameters between 13.9 nm–23.4 nm (PV1) were positively correlated with plaque formation, while apoB-LP with diameters between 33.19 nm-43.0 nm (PV2) were negatively associated with plaque formation. The interval between these two ranges, 23.4–33.1 nm, contained the inflection point of the particle diameter versus plaque severity relationship, but the correlation coefficients in this region were not significant. When all four genotypes were considered together (Figure 2.7), the percentage of total apoB-LP with diameters less than 13.9nm was 7.6%, between 13.9–23.4 was 17.2%, between 25.5–30.4 nm was 21.2%, between 33.1-43 nm was 25.9%, between 43.0-72.3 nm was 18.5%, and particles with diameters larger than 72.3 nm accounted for 9.7% of the total.

Relations among surrogate markers and plaque formation

Mouse genotype could describe nearly all plaque formation ($r^2 = 0.857$, $P < 0.0001$) within the pooled mouse population, suggesting minimal environmental influence on disease development. Seven surrogate markers were used in that analysis, and the pooled population statistics are shown in Table 2.3. General linear models were then developed to test the ability of surrogate markers to model plaque formation using at least 1 and up to 7 markers. Model statements systematically evaluated all combinations of markers both with and without adjustment for variation in apoB clearance. Only two models

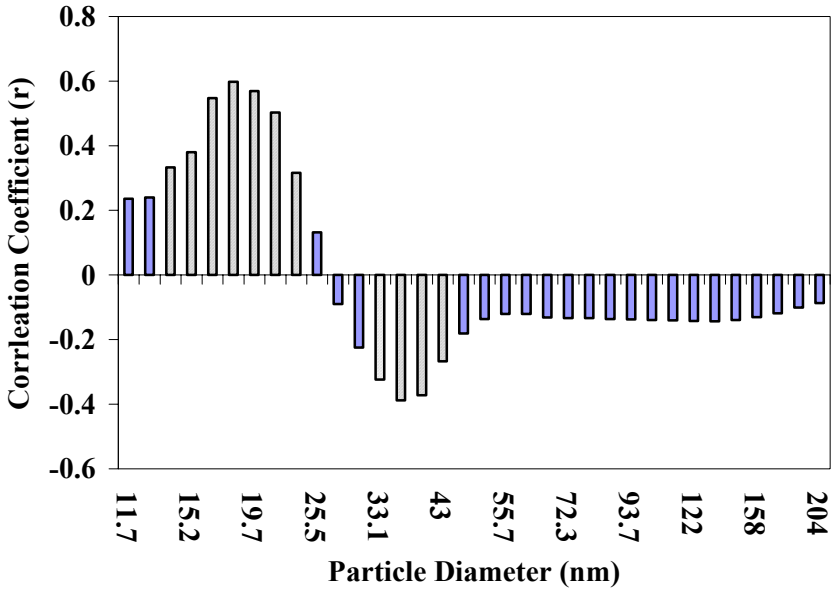

Figure. 2.6 Correlation coefficients for individual particle diameters (number distribution) and arterial plaque. n = 62, Critical value for r = 0.250, $P < 0.05$. Striped bars indicate that the correlations between the percentages of total particles present in a stated diameter interval were significantly correlated to plaque formation (positive values) or lack of plaque (negative values).

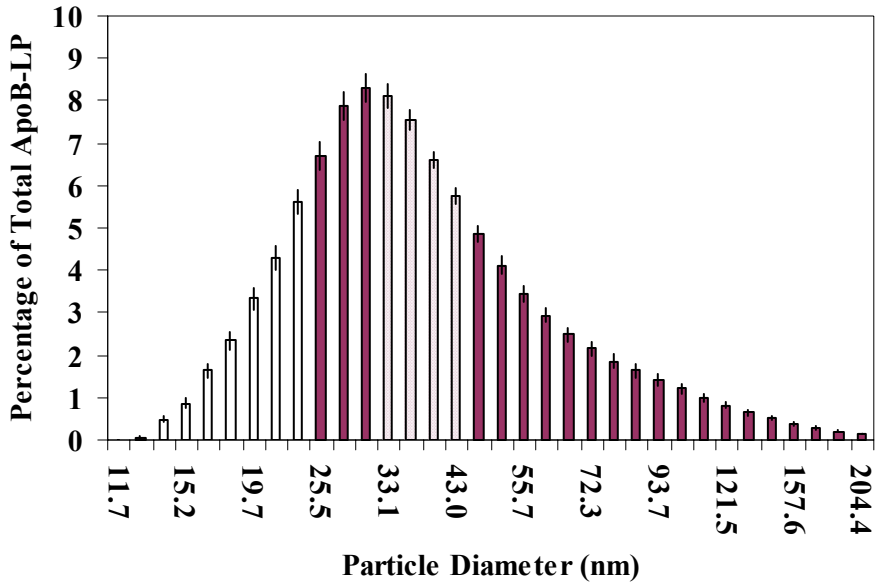

Figure 2.7 Aggregate apoB–LP particle diameter distribution profile. A total of 62 mice from four genotypes were used to construct the curve. Values are means ± SEM. Particle diameters represented by empty bars were significantly associated with plaque formation ($P < 0.05$) while stippled bars represent particle diameters that were negatively associated with plaque formation ($P < 0.05$). Associations to plaque formation were not significant for those particle diameters represented by solid bars.

TABLE 2.3

Best and worst models at different levels of variable inclusion

Rank		Delay in apoB–LP Particle Clearance	
Adj/Unadj	Variable or Model	r^2Adjusted	r^2Unadjusted
1/1	HDL cholesterol (HDLc)	0.392	0.392
2/3	apoB	0.308	0.153
3/2	Cholesterol (Chol)	0.180	0.180
4/4	Moderate Diameter Particles (PV2)	0.038	0.038
5/5	Bodyweight (BW)	0.038	0.038
6/6	Small Diameter Particles (PV1)	-0.008	-0.008
7/7	Triacylglycerols (TG)	-0.014	-0.014
1/1	apoB + HDLc	0.522	0.473
21/21	PV1 + TG	-0.015	-0.015
1/1	PV2 + Chol + HDLc	0.612	0.612
35/35	PV1 + BW + TG	0.026	0.026
1/1	PV1 + PV2 + Chol + HDLc	0.659	0.659
35/34	PV1 + PV2 + BW + TG	0.165	0.165
32/35	apoB + PV1 + BW + TG	0.293	0.144
1/1	PV1 + PV2+ BW + Chol + HDLc	0.683	0.683
4/9	apoB + PV1 + PV2 + BW + HDLc	0.638	0.588
21/21	PV1 + ApoB + BW + TG + Chol	0.358	0.236
1/1	apoB + PV1 + PV2 + BW + Chol + HDLc	0.696	0.687
7/7	apoB + PV1 + BW + TG + Chol + HDLc	0.541	0.516
NA	apoB +PV1 + PV2 + BW +TG +Chol + HDLc	0.691	0.682

based on single surrogate markers (HDLc or apoB) were significant (Appendix 1), and apoB (r^2 = 0.308, P < 0.02) became non-significant when the adjustment for delayed particle clearance was omitted from the model (r^2 = 0.153, P > 0.1). Models containing two or more markers were better able to account for disease formation (Table 2.3, and Appendix 1). Thirteen of the possible twenty-one 2-marker models (62%) were significant, while 30 of 35 possible 3-marker models (85%), and all 5-marker and 6-marker models were significant. However, in each model that included apoB, failure toadjust for delay in particle clearance reduced the ability of the model to account for plaque formation (Table 2.3). Non-adjustment of apoB increased the number of non-significant model statements from (Appendix 1) from19 to 35. Another consistent effect was that removal of HDLc from any model statement reduced the ability of the model to describe plaque formation. For example, a 4 variable model using BW, TG, PV1 and HDLc was better able to account for plaque formation (r^2 = 0.485, P < 0.001), than one where Chol replaced HDLc (r^2 = 0.219, P >0.05). In this case, replacement of PV1 with Chol (BW, TG, Chol, HDLc) improved the model (r^2 = 0.467, P < 0.001). In the full 7 marker model, adjustment for delays in apoB clearance continued to improve model fit, r^2 = 0.691, P < 0.0001, for adjusted, versus r^2 = 0.682, P < 0.001 for unadjusted. A 6-marker model that omitted TG was best able to account for plaque formation, r^2 = 0.696, P < 0.001, and r^2 = 0.687, P < 0.001 for the apoB-clearance adjusted and unadjusted models, respectively.

Correlation analysis was used to assess the strength of association of individual model components within the 7 component model adjusted for delay in apoB-LP

clearance. This analysis found that plasma TG (r^2 = 0.266, P < 0.04), and Chol (r^2 = 0.313, P < 0.02) varied directly with bodyweight, but were weakly related to one another (r^2 = 0.226, P = 0.08). Plasma Chol was inversely related to HDLc (r^2 = -0.355, P = 0.005). Body weight, did not correlate to plaque (r^2 = 0.232, P = 0.071), apoB concentration (r^2 = 0.221, P = 0.084) or PV1 (r^2 = -0.182, P = 0.156) or PV2 (r^2 = 0.247, P = -.053). However PV1 did correlate inversely with PV2 (r^2 = -0.887, P < 0.0001), TG (r^2 = -0.428, P = 0.005), and Chol (r^2 = -0.393, P = 0.006). In contrast, PV2 correlated directly with TG (r^2 = 0.307, P = 0.0005) and Chol (r^2 = 0.510, P < 0.0001) did not correlate with HDLc (r^2 = 0.013, P = 0.919). Plasma total Chol varied directly (r^2 = 0.440, P = 0.003) while plasma HDLc varied inversely (r^2 = -0.630, P < 0.0001) with plaque. Plasma apoB concentration was highly and directly correlated (r^2 = 0.565, P < 0.0001) to plaque formation, as well as Chol (r^2 = 0.630, P < 0.001), but highly inversely correlated to plasma HDLc (r^2 = -0.345, P < 0.0001). If the adjustment for delay in apoB-LP clearance was omitted from the analysis, apoB associations with plaque (r^2 = 0.409, P = 0.001) and Chol (r^2 = 0.519, P < 0.0001) remained significant but were markedly reduced, while correlation with HDLc became non-significant (r^2 = -0.185, P = 0.151)

Discussion

We used gene knock-out and gene-targeting to create strains of mice in which apoB-LP particle clearance was variably impaired. We used several strains in combination in order to develop a population-based model to assess the relation of plaque formation to a number of clinically relevant surrogate markers such as bodyweight, plasma lipid

concentrations and apoB-LP particle diameters. Measurement of individual apoB isoform concentrations allowed us to estimate the fraction of plasma total apoB undergoing prolonged circulation (delayed clearance). Several previous observations led to this approach including: 1) apoB48 and apoB100 are assembled into particles of similar diameters when they are the sole isoform present in the animal (Veniant et al., 1997); 2) particles assembled from either isoform are equally atherogenic and show similar disease causing potential in relation to plasma cholesterol concentration in mice expressing a single isoform and fed identical diets (Veniant et al., 1997); and 3) apoB48–LP are cleared by both LRP and LDLR via apoE, while apoB100 is cleared nearly exclusively by LDLR (Veniant et al., 1998). We assumed that when fed a low-fat chow diet the primary mechanisms influencing particle clearance rates would be those imposed by deliberate genetic modification. This assumption suggested that we could use quantification of apoB100 and apoB48 as an approach to make first approximation estimates of delays in apoB–LP particle clearance within mixed particle populations. Because delays in apoB–LP particle clearance decrease the particle oxidative stability measured *in vitro* (Walzem et al., 1995), we proposed that delayed particle clearance was a fundamental metabolic defect capable of converting native apoB–LP to atherogenic species. We were curious to determine whether adjustment for variable delays in apoB–LP clearance would influence the ability of traditional surrogates to estimate plaque formation within this well defined but highly genetically diverse population of animals. As a corollary question, we were interested to determine whether

information regarding apoB-LP particle diameters could be used to enhance disease risk estimates.

In humans, plasma total cholesterol and LDL cholesterol have a direct relationship to ASCVD risk and are the primary indexes used to detect and evaluate treatment to reduce that risk (NCEP, 2001). Plasma HDL cholesterol concentration varies inversely with ASCVD risk and is an independent risk factor. The results of our studies in mice agree with human-based population estimates in this regard. In the Adult treatment Panel III (ATP III) persons with diabetes without ASCVD were considered to be at equivalent risk to those with overt ASCVD. Diabetes is often presaged or accompanied by the Metabolic syndrome (Reusch, 2002) and an associated atherogenic dyslipidemia characterized by high triacylglycerol, low HDL cholesterol and a predominance of small–diameter LDL particles. In our mouse population apoB–LP particle diameter became smaller when particle clearance was delayed by selective ablation of particle clearance mechanisms. Correlation analysis identified diameter-specific apoB–LP subpopulations that were significantly related to plaque formation in either a positive (diameter = 13.9 – 23.4 nm, PV1) or negative fashion (diameter = 33.1-43 nm, PV2), albeit the range associated directly with plaque formation as not identical to that proposed for humans (Dreon et al., 1994). There were a number of methodological differences in particle diameter measurements that may account for the discrepancy, or it may reflect a species difference. To our knowledge, this is the first time a subpopulation of apoB–LP particles has been identified that is negatively associated with plaque formation and the basis for this association requires further study. In contrast to the

metabolic syndrome, the increase in small–diameter apoB–LP predominance within this population of mice was not correlated to bodyweight and was inversely correlated to plasma TG and Chol. Notably, these mice were not obese, and plasma triacylglycerol concentrations, while generally higher than those found in comparable mice with intact particle clearance mechanisms (Farese et al., 1996), did not reach the 200-300 mg/dL levels associated with murine insulin resistance (Siri et al., 2001). The negative associations between predominance of smaller diameter apoB–LP and plasma cholesterol and triacylglycerol concentrations may be the result of intact hepatic lipase activities (Dichek et al., 1998; Deeb, S. et al., 2003, in press,) in conjunction with normal apoB production rates. In several instances, PV1 appeared in model statements that effectively explained plaque formation (Table 2.3). For example, the best 4-marker model was PV1 + PV2 + Chol + HDLc. However, Chol + HDLc provided most of the explanatory power, as replacement of these markers with BW + TG produced the poorest model. Similarly, combining apoB + PV1 +BW + TG produced the third poorest model. In clinical settings BW, Chol, HDLc, TG and PV1 are associated with increased risk due to metabolic syndrome. The predictive power of a 5-marker model based on these parameters ranked 16th out of 21 possible models. The best 5–marker model was PV1 + PV2 + BW + Chol + HDLc. The degree of mobility in model ranking suggests that the merits of PV1 to improve the explanatory value of a model will be highly situation dependent. For example, it is known that monounsaturated and saturated fat increase LDL particle diameter in several animal models including LDLR-null, human apoB100–overexpressing transgenic mice (Rudel et al., 1998), while LDL diameters

became smaller in similar human apoB100–overexpressing transgenic mice when insulin resistance was imposed by brown adipose tissue ablation (Siri et al., 2001). These latter observations suggest that the apoB–LP particle diameters that will have positive (or negative) associations with plaque formation will differ in different settings. While this speculation remains to be confirmed by experimental data, it seems probable that a fixed particle diameter interval will have a variable relationship to disease rates caused by different underlying pathologies. Indeed as the interactions of different dietary components with the disparate genetic backgrounds present in the human populations become described, new markers of greater or complementary diagnositic value may be identified. In this regard, it would be of interest to compare the outcomes of this study with those of the same mice fed saturated or monounsaturated fat, or under conditions that provoke insulin resistance. If apoB–LP particle diameter proves highly malleable to underlying pathogenic mechanisms it seems unlikely to be suitable as a global independent indicator of disease risk. Indeed apoB–LP particle diameter may have its greatest use in differential diagnosis. In this connection is should be noted that $Apob^{+/+}$, $Ldlr^{-/-}$ mice exhibited plasma apoB100 concentrations equivalent to those of $Apoe^{-/-}$, $Apob^{100/100}$ mice in addition to possessing an equivalent concentration of apoB48, and yet these mice did not develop plaque while the latter did. Thus it seems no single marker is impervious to situational effect.

In this study, correcting for delays in apoB particle clearance improved the ability of the variables measured to explain plaque formation. This observation is consistent with hypothesized mechanisms of atherogenesis (Walzem et al., 1995; Tabas and Krieger,

1999), and would be a common metabolic defect in human genetic disease (as modeled by these mice strains) or diet induced apoB–LP overproduction as occurs with obesity, insulin resistance, or saturated fat intake. Reduced apoB–LP particle diameters may well provide a surrogate estimate of delays in particle clearance in some clinical settings. Interestingly, the frequency of LDL phenotype B (small dense LDL) was not prevalent in a population living on an isolated Mediterranean island, but when the pattern did occur it associated with increases in plasma triacylglycerol concentrations. As in populations in the United States (Dreon et al., 1994), individuals in this Mediterranean population that exhibited LDL phenotype B had higher body mass indexes and prevalence of diabetes and hypertriacylglycerolemia (Rizzo et al., 2003). While more sophisticated turnover methods would improve estimates of delay in apoB–LP particle clearance, the simple approach used here shows that delayed particle clearance is indeed an underlying mechanism to convert native LP species into atherogenic counterparts.

CHAPTER III

EFFECTS OF HIGH-CARBOHYDRATE DIETS ON PHYSICAL PROPERTIES OF PLASMA LIPOPROTEINS IN HAMSTERS

Introduction

Atherosclerotic cardiovascular disease (ASCVD) is a major cause of morbidity and mortality in much of the world (Braunwald, 1997). Lipoprotein profiles provide powerful risk factors for the development of ASCVD. That diet can affect lipoprotein metabolism and atherosclerosis is well documented (Campos et al., 1991; Dreon et al., 1994; Krauss, 1995). Dietary macronutrient composition can influence lipoprotein synthesis, metabolism clearance and arterial retention. Targeting specific dietary habits might lead to reductions in morbidity and mortality associated with ASCVD. Diets that provide more than > 55% energy from carbohydrate are known to decrease plasma LDL cholesterol (LDL-C), a risk factor for ASCVD (Hatch et al., 1955; Krauss et al., 2000). However, as early as 1950, Watkin et al. (1950) observed that reductions in plasma LDL-C concentration caused by high-carbohydrate diets were frequently accompanied by elevations of plasma triacylglycerol (TG), an independent risk factor for ASCVD (Hokanson and Austin, 1996). In humans, a high-carbohydrate diet enhances hepatic TG synthesis (Frayn and Kingman, 1995). Elevated plasma TG concentration is associated with the appearance of atherogenic lipoprotein phenotype (ALP), which consists of high plasma TG, low concentration of high-density lipoproteins (HDL) and small, dense LDL (Austin et al., 1988). When insulin resistance accompanies the ALP, the condition is

termed the "metabolic syndrome" or "Syndrome X," which carries with it a high risk for ASCVD (NCEP, 2001; McKeigue and Davey, 1995; Wingard et al., 1995).

Many studies have been carried out to unravel the mechanism by which high-carbohydrate diets affect lipoprotein metabolism and ALP. Evidence from rat studies demonstrated that diets high in fructose elevate plasma TG concentration and lower HDL concentration (Hwang et al., 1987; Tobey et al., 1982). The hamster has proven to be a good animal model to study the effects of diet on lipoprotein and lipid metabolism (Dietschy et al., 1993). The plasma lipoprotein profile and cholesterol ester transfer protein (CETP) activity of the hamster more closely resemble those of humans than do those of the rat or mouse (Bravo et al., 1994; Stein et al., 1990). The hamster also exhibits a metabolic response to dietary lipids that is similar to the response exhibited by humans (Stein et al., 1990).

The effects of a high-fructose diet on lipid metabolism have been investigated in the hamster. Several investigators observed that diets containing 60% fructose elevate plasma TG concentration in hamsters and cause insulin resistance (Kasim-Karakas et al., 1996; Remillard et al., 2001; Taghibiglou et al., 2000). Distinct from humans and rats, however, hamsters fed a high-fructose diet exhibit increased HDL-C concentration in plasma (Remillard et al., 2001). Elevated plasma HDL-C has been associated with a reduction in coronary events that is independent of changes in LDL-C and TG (Manninen et al., 1988). It is not known whether hamsters fed high-fructose diets exhibit changes in lipoprotein particle diameter and chemical composition indicative of ALP.

An objective of this study was to establish the features of the plasma lipoprotein profile in hamsters fed a fructose-rich diet.

Previous studies of plasma lipoprotein profiles (Remillard et al., 2001; Taghibiglou et al., 2000) compared the effects of a control rodent chow diet with those of a purified fructose-rich diet. Chow is a nonpurified diet comprised of a mixture of intact food. In contrast, purified diets provide macronutrients as purified ingredients. For example, carbohydrate in chow diets is derived from complex mixtures of corn and wheat flakes, wheat middlings, ground corn, and dried whey. In addition to carbohydrate, these ingredients provide variable amounts of protein, fat, vitamins, minerals and various phytochemicals and other nutrients. However, carbohydrate in a fructose-rich diet only consists of a single simple monosaccharide – fructose. Thus, there is a quantifiable but variable difference in composition of any chow and purified diet. Starches can be highly purified but because they are polysaccharides, retain unique chemical and physical characteristics. Starch can be a straight or branched chain polymer comprised of thousands of glucose molecules. Starch polymers must be digested to liberate individual glucose molecules for transport into the bloodstream. Thus, starch-glucose is absorbed more slowly than glucose consumed as a mono or disaccharide producing a lower postprandial rise in insulin and glucose (Truswell, 1994). Furthermore, variation in the glycemic indexes of starchy foods is the result of variations in the ratios of amylose to amylopectin (Jenkins et al., 1981). Amylose, a resistant starch, is incompletely digested in the small intestine and produces smaller increases in postprandial insulin than does amylopectin (Behall and Howe, 1995). In the present study, a cornstarch-rich diet was

used as the control diet, and cornstarch was isocalorically substituted for fructose. Chow diet also was included in this study in order to compare results with those of previous studies. To determine the effect of fructose and starch on the size, lipid and apolipoprotein composition of lipoproteins, hamsters were fed semi-purified diets containing 60% fructose or cornstarch.

Materials and Methods

Animals

Male golden Syrian hamsters (Charles Rivers Laboratory, Wilmington, MA) initially weighing 80–90 g and aged 6–8 wk were housed at 22°C with a 12h light/dark cycle (lights were on 7 a.m. to 7 p.m.) and free access to water and chow diet (#W-8604, Harlan Teklad**,** Madison, WI). After an adaptation period of 2 wk, the animals averaged 115 g. The animals were randomly assigned to one of 3 groups comprised of 15 hamsters each. One group was fed a fructose-rich diet, a second group was fed a cornstarch-rich diet and the third group remained on the chow diet. Food intakes were monitored daily, and body weight was measured twice weekly. At the end of 2 wk, all animals were fasted for 12–16 h, prior to blood collection. The hamsters were anesthetized (isoflurane, 4% in 100% oxygen), and blood was collected via cardiac puncture. All animals were cared for as outlined in "Guide for the Care and Use of Laboratory Animals," prepared by the National Academy of Sciences and published by the National Institutes of Health, Bethesda, MD (NIH publication No. 86-23, revised 1985). Protocols were approved by the University Laboratory Animal Care Committee at Texas A& M University (AUP #9-398).

Diets

The compositions of the purified diets are shown in Table 3.1. The energy compositions of the three experimental diets are shown in Table 3.2. The basal diet was a closed formula cereal-based Rodent chow diet (#W-8604, Harlan Teklad**,** Madison, WI). The fructose-rich diet (#161506, Dyets Inc., Bethlehem, PA) was nutritionally adequate and contained 7.09% cellulose. The starch-rich diet (#161511, Dyets Inc., Bethlehem, PA) was similar to the fructose-rich diet with the exception that the source of carbohydrate was 60% cornstarch. All diets were stored at 4°C.

Blood samples

Cardiac blood was collected individually from the hamsters via heart puncture under isoflurane anesthesia (4% in 100% oxygen). Blood (3 mL/per hamster) was drawn into tubes containing sodium azide (0.01%), Na_2-EDTA (0.12%), pencillin (10,000 U/mL)/streptomycin (10 mg/mL)/neomycin (10 mg/mL) and aprotinin (0.01 TIU/mL). Plasma was separated within 2 hours of blood collection by centrifugation at 1200 × g, for 20 min at 4°C. A cocktail containing reduced glutathione (0.5 mg/mL), leupeptin (0.5 μg/mL) and benzamidine (1 mM) was added to preserve the native lipoprotein structure.

Lipoprotein isolation

Plasma lipoproteins were sub-fractionated based on their hydrated density by sequential density-gradient ultracentrifugation (Chapman et al., 1981; Walzem et al., 1994). Very low-density lipoprotein (VLDL) was isolated from 1 mL plasma at $d <$

TABLE 3.1

Composition of fructose-enriched and starch-enriched diets

Components	Diets	
	Fructose-enriched	Starch-enriched
	g/kg, as fed	
Vitamin free casein	220	220
Cornstarch	0	600
Fructose	600	0
Corn oil	60	60
Cellulose	70.9	70.9
NRC Salt mix	35	35
NRC Vitamin mix	10	10
Choline bitartrate	2	2
L-Arginine	1	1
L-Tryptophane	1.1	1.1

TABLE 3.2

Major composition of the experimental diets

Composition	Chow[1]	Fructose-enriched	Starch-enriched
		%	
Carbohydrate	60.0	60.0[2]	60.0[3]
Protein	24.5	22[4]	22[4]
Fat	4.4	6.0[5]	6.0[5]
Fiber	3.7	7.1[6]	7.1[6]

[1] Harlan Teklad chow diet #W-8604, mixture of intact food.

[2] Purified carbhydrate: fructose; [3] Purified carbhydrate: cornstarch.

[4] Casein; [5] Corn oil; [6] Cellulose.

1.006 g/mL by aspiration with a narrow-bore pipet following 18 h centrifugation at 40,000 rpm in a TFT 50.3 rotor held at 14°C within a Beckman L8-70M ultracentrifuge (Beckman Coulter, Sunnyvale CA). The density was increased to 1.053 g/mL, and LDL were isolated by a second centrifugation for 18 h at 40,000 rpm. The HDL were isolated at *d* 1.053–1.21 g/mL following a third centrifugation for 18 h at 40,000 rpm (Chapman et al., 1981). Particle diameter distributions were immediately determined in each lipoprotein fraction isolated from plasma. Following diameter analysis, the fractions were stored at –80°C prior to compositional analysis.

Metabolic analysis

Plasma TG concentrations were determined enzymatically using a kit from Sigma (Procedure No. 339, Sigma Chemical, Co., St. Louis, MO). Plasma non-esterified fatty acid (NEFA) and glucose concentrations were determined by spectrophotometric method using kits from WAKO (NEFA C Code No. 994-75409; Glucose C2 Code No. 994-90902, WAKO, Richmond, VA). Plasma insulin concentration was measured by ELISA using a rat insulin ELISA kit (Catalog #: INSKR020, Crystal Chem. Inc., Chicago, IL) that has 79% cross-reactivity to hamster insulin.

Lipid analysis

Plasma cholesterol distribution was determined by analytical size-exclusion chromatography (Kieft et al., 1991). Typically, 20 μL of fresh plasma were injected onto a Superose 6 HR 10/30 size-exclusion column (Amersham Pharmacia Biotech, Piscataway, NJ) by an ASI-100 automated sample injector (Dionex Co., Sunnyvale, CA), and eluted with saline containing 0.02% sodium azide at a flow rate of 0.5 mL/min

(Dionex P580 Pump, Dionex Co., Sunnyvale, CA). Plasma total cholesterol distribution was determined enzymatically (Sigma Chemical, Co., St. Louis, MO) using an in line PDA-100 photodiode array detector (Dionex Co. Sunnyvale CA) with primary chromophore detection at 505 nm. Total cholesterol (Tch), free cholesterol (Fch) and phospholipids (PL) were measured enzymatically (Cholesterol CII Cat. No. 276-64909; Free Cholesterol C Cat. No. 274-47109; Phospholipids B Code No. 990-54009, WAKO, Richmond, VA) in plasma, isolated lipoprotein fractions and lipid standards. Cholesterol ester (CE) was calculated by multiplying the difference between Tch and Fch by 1.67.

Analysis of lipoprotein fractions particle size

VLDL particle diameters were determined by dynamic light scattering analysis with a Microtrac series 250 ultrafine particle analyzer with a laser probe tip (UPA-250; Microtrac, Clearwater, FL) (Walzem et al., 1994). Following ultracentrifugation, samples were carefully removed from the rotor and uncapped. The laser probe was gently placed on the top layer of supernatant portion of the sample. It was critical not to mix the sample layer or allow air bubbles at the probe liquid interface. Due to the low lipoprotein content of some samples, a measurement time of 540 sec was used for all samples. The results of primary data collection can be expressed in particle number, particle area or particle volume in order to adequately describe different aspects of the same VLDL particle population with respect to their colloidal properties (Walzem, 1996). Particle number, area and volume distributions are collectively termed density functions of lipoprotein particles. Particle number distribution describes the frequency distribution of VLDL particles of the specified diameter (e.g., a hamster could have

14.3% of all VLDL particles as 55.7-nm particles). Particle volume distribution describes the distribution of total VLDL volume among particles of different diameters (e.g., the same hamster could have 12.6% of all VLDL volume contained within particles 57.7 nm in diameter). The two distributions provide complementary information: the 55.7-nm particles accounted for 12.6% of all VLDL volume, and for 14.3% of all VLDL particle number. Particle volume distribution is sensitive to the presence of large diameter particles because the volume of a sphere increases as a cubic function of particle radius. Particle area distribution is calculated using information from particle number and particle volume distribution. Particle area distribution is calculated first because it is less sensitive to the presence of a few large particles. Raw particle size distributions were converted to area, number and volume population percentiles, which were used to calculate median particle size.

LDL and HDL particle size were measured using non-denaturing gradient gel electrophoresis (NDGGE) (Nichols et al., 1986). Typically, a 15-μL portion of fresh LDL or HDL was applied onto a non-denaturing gradient gel (Alamo Gels Inc., San Antonio, TX). Gels with a linear gradient range of 2–16% polyacrylamide were used to measure the diameter of LDL particles, and gels with a linear gradient range of 4–30% polyacrylamide were used to measure the diameter of HDL particles. A high molecular-weight standard (Amersham Pharmacia Biotech, Piscataway, NJ) was also applied onto each gel. Electrophoresis was performed using a model GE-2/4 LS vertical electrophoresis apparatus (Pharmacia, Uppsala, Sweden) at a constant voltage of 125 V for 24 h at 4°C. Gels were stained with 0.15% Coomassie brilliant blue in

ethanol:water:glacial acetic acid, 3:8:1 (vol/vol/vol) for 15 min at 60°C, and then destained at 60°C in a destaining solution of ethanol:water:glacial acetic acid, 3:8:1 (vol/vol/vol) until backgrounds were clear. Migration of lipoproteins in gel was measured using an Odyssey imager and Odyssey software (LI-COR, Inc., Lincoln, NE). Calibration curves for LDL proteins were constructed by plotting the logarithm of particle diameter against the distance migrated relative to that of Rf (abscissa). Particle sizes were calibrated by comparison with migration distances of standard proteins of known diameter (Shore, 1991).

Quantitation of apolipoprotein B in VLDL

The concentration of apolipoprotein B (apoB100) in VLDL was determined by analytical sodium dodecyl sulfate polyacrylamide gel electrophoresis (SDS-PAGE) with Coomassie blue staining (Kotite et al., 1995). Because apoB100 is the only lipoprotein in hamster LDL particles (data not shown), the concentration of apoB in LDL was determined by a modified Lowry assay (Lowry et al., 1951) using bovine serum albumin (Sigma Chemical Co., St. Louis, MO) as a standard.

The protein concentration of VLDL and LDL were measured by a modified Lowry method (Lowry et al., 1951) using bovine serum albumin as the standard. Sample volumes containing 50–200 μg protein were combined with 60 μg apoferritin carrier protein prior to delipidation to insure quantitative apolipoprotein recovery (Kotite et al., 1995). Samples were delipidated overnight at –20°C in an ethanol-diethyl ether (3:1, v/v) system in which a 400–1,200 μL sample was mixed with 10 volumes of ice-cold ethanol-diethyl ether in a 15-mL conical, glass stoppered tube and inverted. The

delipidated mixture was centrifuged for 25 min at 1250 rpm with a Sorvall TR 6000B centrifuge to facilitate removal of the organic phase. The pellet was extracted twice with 4 ml cold anhydrous diethyl ether. The resultant whitish pellet was dissolved in 50–100 μL sample buffer containing 10% glycerol, 3% SDS, 1.5% dithiothreitol, 1% mercaptoacetic acid and 0.02% bromphenol blue in 1 M Tris, pH 6.8. Excess ether was removed under a gentle stream of nitrogen, and the dissolved apolipoproteins were denatured at 100°C for 3 min prior to application to the SDS–PAGE gel.

Individual apoB isoforms were separated using the SDS-PAGE gradient gel described by Kotite et al. (1995) with some modifications. The 3–12% gradient polyacrylamide gel was cast using a two-chamber gradient mixer (Bio-Rad Laboratories, Hercules, CA). The 3% acrylamide solution contained 3% acrylamide, 0.08% bisacrylamide, 0.1% SDS, 0.03 g/mL glycerol, 0.06% ammonium persulfate (APS) and 0.05% N,N,N,N-tetramethylethylenediamine (TEMED) in 0.376 M Tris, pH 9.2 in resolving gel, and pH 6.8 in the stacking gel. The 12% acrylamide solution contained 12% acrylamide, 0.33% bisacrylamide, 0.1% SDS, 0.10 g/mL glycerol, 0.06% APS and 0.05% TEMED in 0.376 M Tris, pH 9.2. Apolipoprotein separation was effected using a Mini-PROTEIN II Vertical gel apparatus (Bio-Rad Laboratories Inc, Hercules, CA) (Laemmli, 1970) containing two minigels for each separation. After loading 50 μL delipidated VLDL or standard in each well, a Bio-Rad PowerPAC 300 (Bio-Rad, Laboratories Inc, Hercules, CA) was used to apply 76V to the gels for first 30 min, followed by 96V until the dye front was 1 mm from the bottom of the gel. Narrow-cut

human LDL served as the source for the apoB100 used as the reference protein within the standard curves.

The procedures for staining and destaining of SDS-PAGE gels were similar to that of NDGGE gels. After destaining, gels were placed between two sheets of cellophane gel wrap (BioDesign Inc. of New York. Carmel, NY) and dried in a fume hood overnight. The dry gels were scanned using a laser scanner (Fluor-STM MultiImage; Bio-Rad, Laboratories Inc, Hercules, CA) equipped with an Image Quant Software Package to automatically integrate the volume of stained apolipoprotein band. The standard curve for apoB100 was constructed by relating the intensity of dye uptake of each band to its known mass. The line of fit was evaluated (Kotite et al., 1995) at least squares for the power function $y = ax^b$. The concentrations of apoB100 in VLDL and LDL were calculated from the regression equation relating the absorbance of apoB100 standard bands to the amount of apoB100 standard applied to the gel.

Statistical analysis

The results are presented as the mean ± SEM unless otherwise noted. Comparisons among three groups were performed using analysis of variance (one way ANOVA). Difference in mean values was tested by a least-squares means procedure. Values of $P < 0.05$ were considered statistically significant. All analyses were performed using the statistical analysis system procedures (SAS Institute, Inc., Cary, NC).

Results

Physiological and metabolic changes

Final body weight, body weight gain and food intake after 2 wk of consuming the diets were similar among these groups, but the livers of the hamsters fed fructose were about 10% heavier ($P < 0.05$) than those of animals fed starch or chow (Table 3.3). Plasma glucose was not significantly different among the three dietary groups, while fasting insulin was nearly 2-fold higher in the fructose-fed group than in the starch group and chow group. Plasma TG concentration in fructose-fed hamsters was 59% higher ($P < 0.001$) than those from chow-fed, and 72.2% higher than that of starch-fed hamsters ($P < 0.001$). Similarly, fructose-fed animals had significantly higher fasting plasma NEFA concentrations than either starch-fed animals (32%) or chow-fed animals (14%).

Plasma total and lipoprotein cholesterol

Plasma lipoprotein cholesterol profiles were obtained by size-exclusion HPLC. Plasma cholesterol distribution in lipoproteins in hamsters fed chow, fructose and starch diets for 2 wk were shown in Figure 3.1. The fructose-fed hamsters had higher concentrations of total plasma cholesterol ($P < 0.05$), VLDL cholesterol (VLDL-C) ($P < 0.01$) and HDL cholesterol (HDL-C) ($P < 0.05$) compared with those of chow-fed and starch-fed hamsters. Plasma LDL cholesterol (LDL-C) concentration were similar in all diet groups. Animals fed either purified carbohydrate diet had consistently and significantly higher fractional VLDL-C; the values being 6.2% in chow-fed hamsters, 8.7% in starch-fed hamsters and 9.3% in fructose-fed hamsters. The LDL-C fraction accounted for 21.9% of total cholesterol in the chow-fed group. In contrast, LDL-C

TABLE 3.3

Plasma physiological and metabolic changes in hamsters fed chow, fructose-enriched and starch-enriched diets for 2 wk[1]

	Chow	Fructose-enriched	Starch-enriched
Body weight (g)	122.94 ± 4.50	126.19 ± 3.21	123.96 ± 2.40
Weight gain (g)	9.44 ± 1.59	11.06 ± 1.16	9.46 ± 0.90
Food intake (g)	9.77 ± 0.46	9.47 ± 0.34	9.92 ± 0.21
Liver weight (g)	21.50 ± 1.50^{b}	25.03 ± 0.82^{a}	22.42 ± 0.54^{b}
Glucose (mg/dL)	138.78 ± 7.40	125.71 ± 4.70	130.45 ± 5.40
Insulin (ng/mL)	0.64 ± 0.08^{b}	1.10 ± 0.22^{a}	0.68 ± 0.21^{b}
Triacylglycerol (mmol/L)	0.90 ± 0.06^{b}	1.43 ± 0.09^{a}	0.83 ± 0.04^{b}
Free fatty acids (mmol/L)	0.58 ± 0.04^{b}	0.663 ± 0.09^{a}	0.501 ± 0.06^{b}
Cholesterol (mmol/L)	3.13 ± 0.14^{c}	4.22 ± 0.15^{a}	3.59 ± 0.17^{b}

1 Values are means ± SEM, n = 15. Means within a row having different superscripts are significantly different ($P < 0.05$)

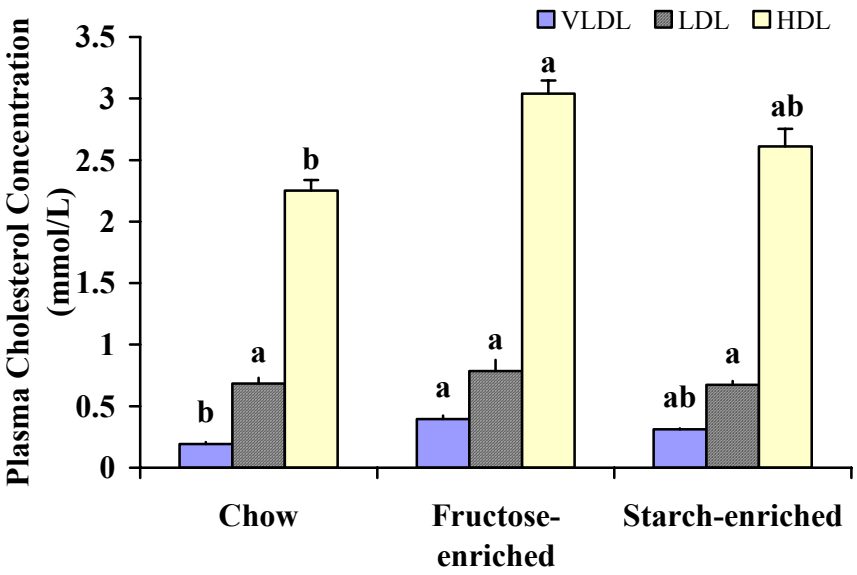

Figure 3.1 Distribution of cholesterol in plasma lipoproteins from hamsters fed chow, fructose-enriched and starch-enriched diets for 2 wk. Values are means ± SEM, n = 15 per treatment group. Values that do not share a letter differ ($P < 0.05$).

accounted for a significantly lower 18.6 and 18.7% of total cholesterol in the fructose and starch fed groups, respectively. There was no significant difference in percentage of HDL-C among the three groups, which averaged 72%. The retention time of VLDL particles from hamsters fed the fructose diet were shorter than those of animals fed either the starch or chow diet ($P < 0.05$) (Table 3.4). Reduced elution times indicate a large particle diameter. LDL particles from the fructose-fed group eluted more slowly than those from either chow-fed or starch-fed animals ($P < 0.05$). HDL eluted more quickly ($P < 0.05$) in animals fed either purified carbohydrate when compared to those fed chow.

Size distributions of lipoprotein fractions

The changes in particle diameter suggested by size-exclusion HPLC were confirmed by independent techniques. The raw density function plot for VLDL particle area distribution is given in Figure 3.2.There was marked heterogeneity in particle diameter of VLDL from plasma of hamsters fed the three diets. Diameter distributions were asymmetric and tailed towards small diameter particles. Chow-fed hamster VLDL particles range from 38 to 89 nm, with median particle diameter = 57 nm; the diameter of VLDL from fructose-fed hamsters ranged from 44 to 96 nm, with the median particle diameter = 63 nm. The diameter of VLDL from starch-fed hamsters ranged from 40 to 91 nm with median = 59 nm. Testing of percentile distributions of VLDL area accumulation plot showed that plasma VLDL particles from fructose feeding group were significantly larger than those of chow and starch feeding groups at the 20^{th} through 60^{th} area percentiles (Figure 3.3).

TABLE 3.4

Retention time of plasma lipoprotein particles after feeding diets for 2 wk[1]

Diets	VLDL	LDL	HDL
		min	
Chow	19.66 ±0.01^{b}	25.63 ±0.04^{b}	33.89 ±0.06^{a}
Fructose-enriched	19.53 ±0.02^{a}	25.90 ±0.05^{a}	33.36 ±0.07^{c}
Starch-enriched	19.61 ± 0.02^{b}	25.55 ±0.15^{b}	33.54 ±0.03^{b}

1 Values represent means ± SEM, n = 15 per treatment group. Means within a column having different superscripts are significantly different ($P < 0.05$).

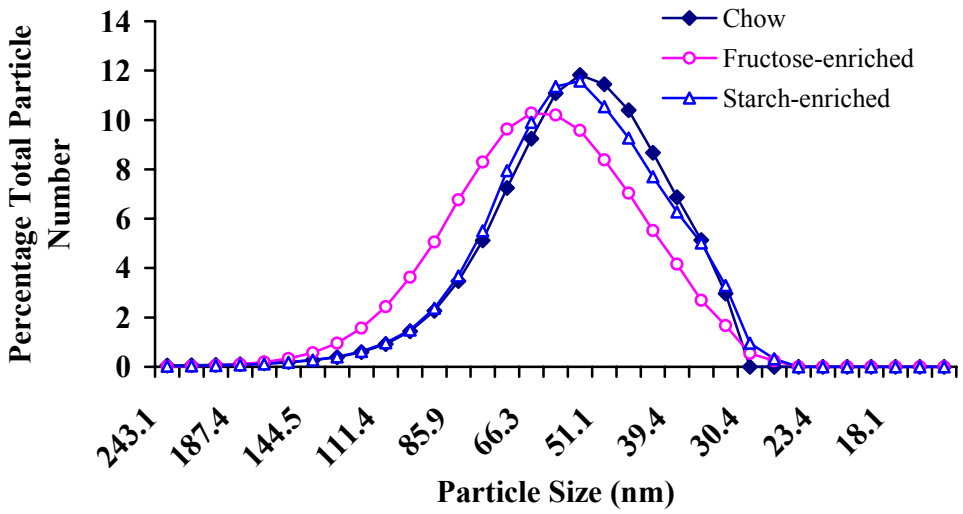

Figure 3.2 Dynamic light scattering-determined diameter distribution of VLDL, d < 1.006 g/mL, isolated from hamsters fed a chow, fructose-enriched or starch-enriched diet for 2 wk.

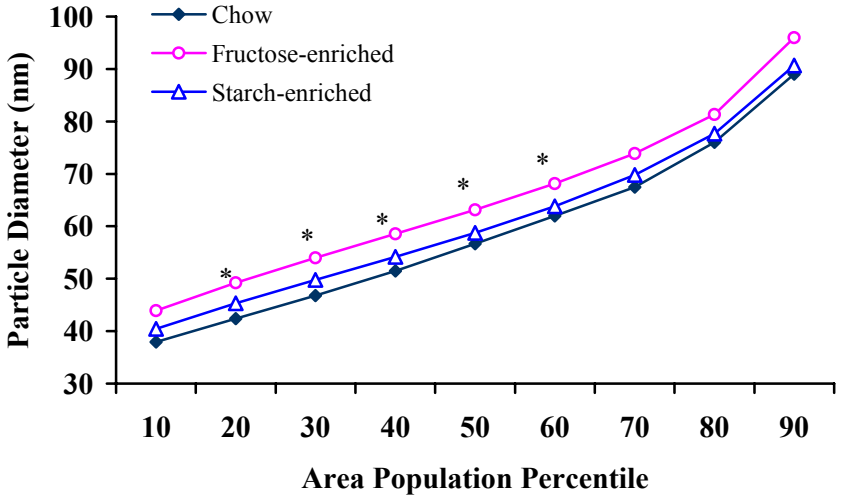

Figure 3.3 Distribution percentile of plasma very low-density lipoprotein (VLDL) particle density function (area) among hamsters fed a chow, fructose-enriched or starch-enriched diet for 2 wk. Within percentile class and density function,* indicates significant difference.

The effect of carbohydrate feeding on the diameter of LDL and HDL particles was analyzed using non-denaturing polyacrylamide gradient gels. All the lipoproteins bands exhibited a polydisperse diameter profile, indicating particle diameter heterogeneity (Figure 3.4). The gradient gel with 2–16% polyacrylamide was used to evaluate the size of LDL particles. LDL particles from fructose-fed hamsters ranged from 21.51 nm to 26.19 nm, with the average of median diameters of 23.61 nm (Table 3.5). These particles were significantly smaller than those in the starch-fed group, which ranged from 22.15 nm to 27.01 nm and averaged 24.40 nm, and those in the chow-fed group, which ranged from 22.10 nm to 25.71 nm and averaged 23.76 nm. Hamster HDL lipoproteins fractions analyzed by electrophoresis in 4–30% gradient gels showed that HDL diameters in hamsters fed the fructose-containing diet were slightly larger as than those of hamsters fed either starch-containing diet ($P = 0.07$) or the chow diet ($P < 0.05$). There was a wide range in HDL particle diameter and overlap in diameter distributions from hamsters fed the different diets. Within HDL gels, a large band averaging 21 nm was noted for a number of animals. The frequency of this LDL-size bands was 12/15 in fructose-fed animals, 3 times and 4 times more frequent than in chow-fed and starch-fed hamsters respectively.

Concentration and chemical composition of plasma lipoprotein fractions

Both the concentration and chemical composition of lipoprotein VLDL fractions varied among the groups of hamsters (Table 3.6). In general, fructose-fed hamsters had the highest concentrations of all VLDL components, with progressive decreases in those

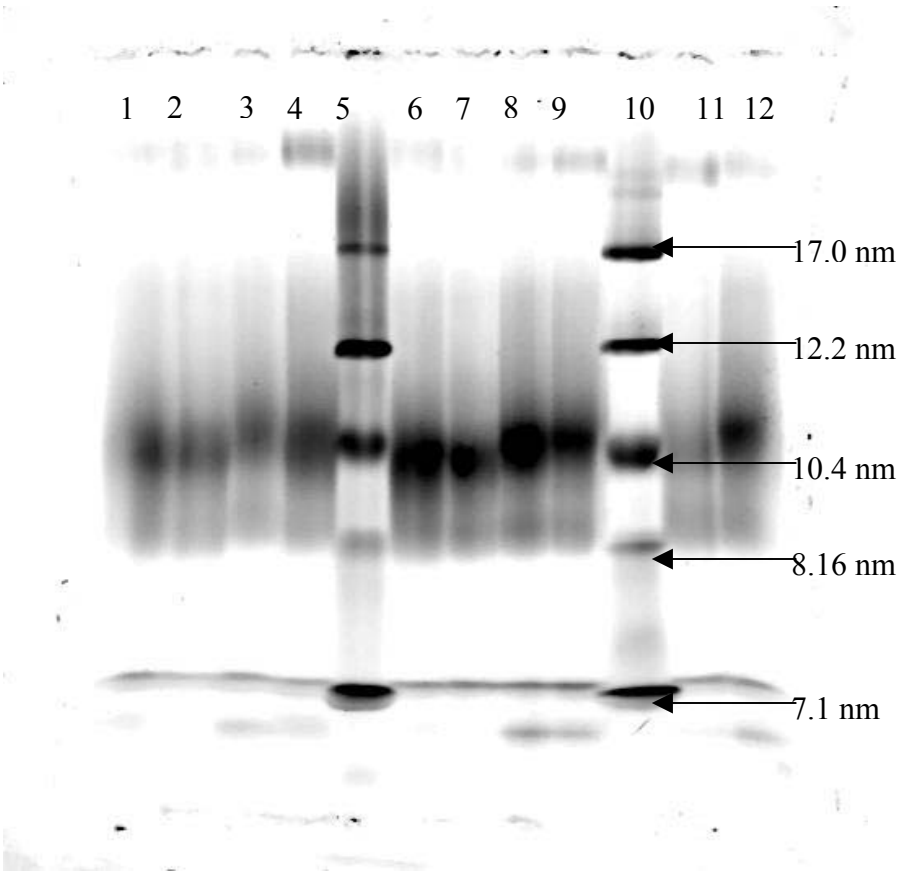

Figure 3.4 4-30% gradient nondenatured PAGE of hamster HDL (1.053 < d < 1.21 g/mL) particles. Gradient nondenatured PAGE was performed using the method described in methods. Lanes 1,2, 6,7 starch feeding HDL; Lanes 3,4,8,9,12 fructose feeding HDL; Lane 11, chow feeding HDL; Lanes 5, 10, molecular weight standard.

TABLE 3.5

Plasma LDL and HDL particle diameters after feeding diets for 2 wk[1]

Diets	LDL	HDL	Frequency of LDL band on HDL gels
	nm	nm	
Chow	23.76 ± 0.07^{a}	10.31 ± 0.08^{a}	4/15
Fructose-enriched	23.61 ± 0.05^{a}	10.53 ± 0.04^{b}	12/15
Starch-enriched	24.40 ± 0.08^{a}	10.45 ± 0.05^{b}	3/15

1 Values are means ± SEM, n = 15 per treatment group. Statistical analysis used a complete weighted least square means analysis. Values across column, not sharing a common superscript, differ at $P < 0.05$.

TABLE 3.6

Concentration and chemical composition of lipoproteins from the d < 1.006 g/mL density fraction (VLDL) separated from plasma of hamsters fed chow, fructose-enriched and starch-enriched diets[1]

Measurement	Chow	Fructose-enriched	Starch-enriched
		µg/mL plasma	
TG[2]	600.03 ± 24.19[b]	1084.77 ± 64.84[a]	596.82 ± 22.83[b]
CE	55.59 ± 4.01[c]	104.54 ± 8.58[a]	84.50 ± 3.75[b]
Fch	30.33 ± 2.41[c]	74.20 ± 8.09[a]	44.01 ± 3.17[b]
PL	97.51 ± 11.24[b]	181.74 ± 21.93[a]	103.16 ± 8.10[b]
PRO	67.75 ± 4.12[b]	91.24 ± 6.21[a]	83.42 ± 4.93[a]
		% Composition	
TG	70.5 ±1.4[a]	70.5 ±1.6[a]	65.4 ±6.0[b]
CE	6.5 ±0.5[b]	6.8 ±0.7[b]	9.3 ±0.7[a]
Fch	3.6 ±0.3[b]	4.8 ±0.5[a]	4.8 ±0.5[a]
PL	14.3 ±1.2[a]	11.8 ±0.6[b]	11.3 ±4.0[b]
PRO	7.9 ±0.8[a]	5.9 ±0.6[b]	9.2 ±1.5[a]

1 Values are means ± SEM, n = 15 per treatment group. Statistical analysis used a complete weighted least square means analysis. Values across rows, not sharing a common superscript differ at $P < 0.05$.

2 Abbreviations: TG, triacylglycerol; Fch, free cholesterol; CE, cholesterol ester; PL, phospholipid; PRO, apolipoprotein.

values seen in starch-fed hamsters and the chow-fed hamsters. Differences in the amount of each chemical component between fructose-fed and chow-fed hamsters were significant ($P < 0.001$). The concentrations of all components except VLDL protein were significantly higher ($P < 0.01$) in fructose-fed hamsters than those in starch-fed hamsters. ApoB100 in VLDL was quantified using a 3–12% gradient SDS-PAGE (Fig. 3.5). The amount of apoB100 in VLDL from fructose-fed hamsters was higher than that in VLDL from either starch-fed (20.6% higher, $P = 0.04$) or chow-fed (68.9% higher, $P = 0.02$). Surprisingly, there was no significant difference in the amount of apolipoprotein in LDL among the three dietary groups, which averaged 0.23 umol/L in all groups. There was similar amount of total apoB in apoB-LP in the plasma from fructose-fed (0.37 umol/L) and starch-fed animals (0.36 umol/L), which were significantly higher than that from chow-fed animals (0.24 umol/L) (Fig. 3.6).

The fractional composition of VLDL from starch-fed hamsters contained 65.4% triacylglycerol (TG), 9.3% cholesterol ester (CE), 4.8% free cholesterol (Fch), 11.3% phospholipids (PL) and 9.2% protein (PRO). The fractional contribution of TG in the fructose-fed group, being 70.5%, was significantly higher than that of starch-fed group. VLDL from the fructose-fed group was poorer in CE (6.8% *versus* 9.3%, $P < 0.05$) than that of the starch-fed group. Starch feeding selectively increased the fractional concentration of VLDL cholesterol (Fch + CE), while not stimulating that of TG. Both purified carbohydrates elevated VLDL fractional content of cholesterol. VLDL from fructose-fed hamsters (5.9%) was significantly poorer in PRO than that from chow-fed (7.9%) and starch-fed animals (9.2%).

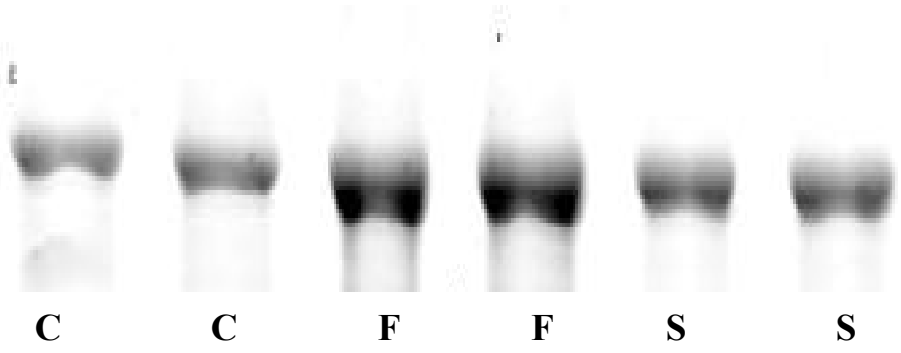

Figure 3.5 Gels from 3–12% gradient SDS-PAGE to quantify hamster plasma VLDL apoB.

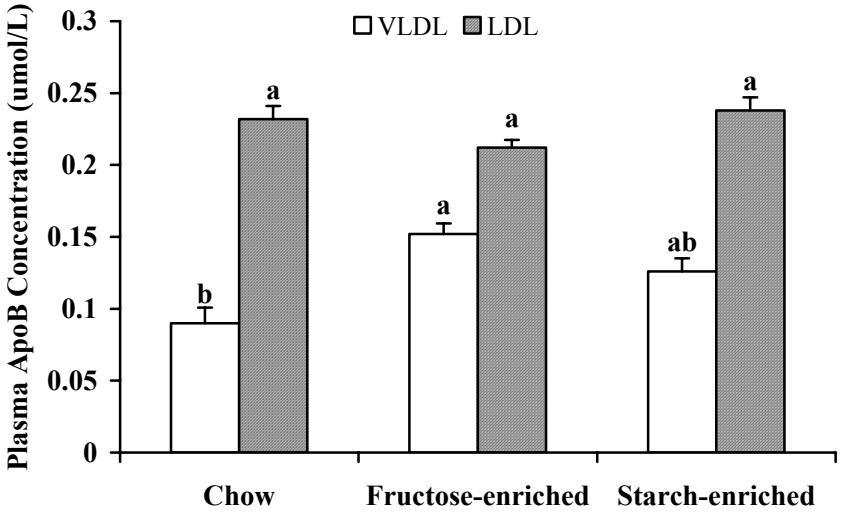

Figure 3.6 apoB concentration in VLDL and LDL particles from plasma hamsters fed chow, fructose-enriched and starch-enriched diets. Values are means ± SEM, n = 15 per treatment group. Comparisons are made among chow, fructose-enriched and starch-enriched diets. Values that do not share a letter differ ($P < 0.05$).

Purified carbohydrate feeding significantly increased the concentration of LDL-Fch and LDL-PL in hamsters (Table 3.7). Fructose significantly increased LDL-TG concentration, producing a 42.5% increase at the expense of a 20% reduction in LDL-CE concentration. The concentration of LDL-CE was significantly higher in starch-fed hamsters than in either fructose-fed or chow-fed hamsters. However, the amount of LDL-PRO in fructose-fed animals was slightly lower than that in the starch-fed and chow-fed groups ($P = 0.08$). The LDL from starch-fed hamsters contained 15.8% TG, 33.6% CE, 10.8% Fch, 22.6% PL and 22.5% PRO. The fractional contribution of TG in the fructose-fed hamsters was higher ($P < 0.01$) than those of the chow-fed and starch-fed hamsters. The ratio of surface (PL + Fch)/ core (TG + CE) lipid is often used to indicate the particle size. However, the ratio of surface/ core in fructose-fed animals (0.74) was smaller than that of the chow-fed (1.11) and starch-fed hamsters (1.18). Again purified carbohydrate significantly increased the fractional content and concentration of Fch. LDL from starch-fed group was CE enriched. However, LDL from fructose-fed (20.5%) and starch-fed animals (22.5%) were significantly poorer in PRO than were those of chow-fed animals (27.1%).

The concentration and chemical composition of lipoproteins in the HDL fraction of plasma from hamsters fed chow, fructose and starch diets are shown in Table 3.8. Fructose-fed animals had the highest concentrations, starch-fed the next highest and chow-fed hamsters the lowest concentrations of HDL-Fch, HDL-CE, HDL-PL and HDL-PRO. Differences between fructose-fed and chow-fed hamsters were significant (P

TABLE 3.7

Concentration and chemical composition of lipoproteins from the 1.006 < d < 1.053 g/mL density fraction (LDL) separated from plasma of hamsters fed chow, fructose-enriched and starch-enriched diets[1]

Meaurement	Chow	Fructose-enriched	Starch-enriched
		μg/mL plasma	
TG[2]	73.74 ± 3.52[c]	119.07 ± 8.27[a]	88.02 ± 6.14[b]
CE	140.80 ± 3.03[b]	151.28 ± 9.80[b]	187.80 ± 8.10[a]
Fch	40.70 ± 7.46[a]	63.40 ± 7.32[a]	60.40 ± 4.20[a]
PL	107.69 ± 1.80[b]	135.40 ± 13.52[a]	126.38 ± 8.80[a]
PRO	134.59 ± 2.78	120.96 ± 7.44	125.56 ± 6.70
		% Composition	
TG	14.8 ±0.8[b]	20.2 ±1.3[a]	15.8 ±0.7[b]
CE	28.2 ±1.2[b]	25.6 ±0.7[b]	33.6 ±0.6[a]
Fch	8.2 ±0.7[b]	10.7 ±0.6[a]	10.8 ±2.3[a]
PL	21.6 ±0.8	22.9 ±0.9	22.6 ±0.5
PRO	27.1 ±3.2[a]	20.5 ±2.8[b]	22.5 ±1.1[b]

1 Values are means ± SEM. n = 15 per treatment group. Statistical analysis used a complete weighted least square means analysis. Values across rows, not sharing a common superscript, differ at $P < 0.05$.

2 Abbreviations were given in legend of Table 3.6.

TABLE 3.8

Concentration and chemical composition of lipoproteins from the 1.053 < d < 1.21 g/mL density fraction (HDL) separated from plasma of hamsters fed chow, fructose-enriched and starch-enriched diets[1]

Measurement	Chow	Fructose-enriched	Starch-enriched
		μg/mL plasma	
TG[2]	68.48 ± 10.20[b]	78.89 ± 3.37[a]	66.61 ± 4.30[b]
Fch	103.01 ± 8.90[c]	215.83 ± 9.54[a]	144.23 ± 9.94[b]
CE	778.40 ± 48.63[c]	1399.82 ± 28.77[a]	990.49 ± 33.23[b]
PL	933.68 ± 73.40[b]	1562.48 ± 50.07[a]	1089.21 ± 70.10[b]
PRO	1089.16 ± 67.49[b]	1363.64 ± 53.37[a]	1082.03 ± 46.59[b]
		%	
TG	2.3 ± 0.3[a]	1.7 ± 0.1[b]	1.9 ± 0.1[b]
CE	26.2 ± 0.6[b]	30.3 ± 0.2[a]	28.7 ± 0.3[b]
Fch	3.5 ± 0.1[b]	4.7 ± 0.1[a]	4.2 ± 0.1[a]
PL	31.4 ± 0.5[b]	33.8 ± 0.1[a]	31.6 ± 0.8[b]
PRO	36.6 ± 0.8[a]	29.5 ± 0.6[c]	33.6 ± 0.7[b]

1 Values are means ± SEM, n = 15 per treatment group. Statistical analysis used a complete weighted least square means analysis. Values across rows, not sharing a common superscript, differ at $P < 0.05$.

2 Abbreviations are given in legend of Table 3.6.

< 0.001). However, the concentration in plasma or fractional content of HDL was not significantly higher in fructose-fed hamsters than in starch-fed and chow-fed hamsters. HDL from starch-fed hamsters contained 1.9% TG, 28.7% CE, 4.2%, Fch 31.6% PL and 33.6% PRO. HDL from the fructose-fed group was significantly richer in Fch, CE and PL than in the chow-fed and starch-fed groups. The fractional contribution of TG in the fructose-fed group (1.7%) was lower than that of chow-fed (2.3%; P = 0.03) and starch-fed (1.9%. P = 0.08) groups. The lower fractional HDL-TG was due to the higher fractional HDL-CE in the fructose-fed group. HDL from fructose-fed animals (29.5%) was poorer in PRO than that of chow-fed (36.6%, P < 0.01) and starch-fed animals (33.6 %) (P = 0.04).

Discussion

Current trends in health promotion emphasize low-fat, high-carbohydrate diets. However, human studies demonstrate that as dietary fat is decreased and carbohydrate is increased, the desired lowered LDL cholesterol can be accompanied by hypertriglycerolemia (HTG) and low HDL cholesterol. Whether low-fat, high-carbohydrate diets offer protection against heart disease is the subject of current debate (Connor and Connor, 1997; Katan et al., 1997; Ornish, 1998; Rudel, 1998). Recently, research relative to fructose-enriched diets, insulin resistance and abnormalities in lipoprotein metabolism has been carried out using the hamster as an animal model (Kasim-Karakas et al., 1996; Taghibiglou et al., 2000). These studies have shown that HTG and insulin resistance develop when hamsters consume fructose-rich diets, however, none of these studies reported detailed lipoprotein profiles of all

lipoprotein species. The objective of the present study was to systemically characterize all plasma lipoproteins in hamsters fed high-carbohydrate diets specifically. The effect of fructose and starch on the physical and biochemical properties of lipoproteins was determined. As in previous studies (Kasim-Karakas et al., 1996; Remillard et al., 2001; Taghibiglou et al., 2000), the fructose feeding induced increased plasma TG concentration in association with hyperinsulinemia and normoglycemia. Taghibiglou et al. (2000) used *in vivo* Triton WR-1339 injection and *in vitro* experiments with primary hamster hepatocytes to demonstrate that both VLDL-TG and VLDL-apoB are over produced in hepatocytes from fructose-fed hamsters as compared with chow-fed animals. Observed changes in lipoproteins in the present study support their results. However, fructose slightly increased the plasma concentration of VLDL-PRO, but significantly decreased the fractional VLDL-PRO. The results indicated that in fructose-fed hamsters, VLDL particle number tended to be slightly higher, but that each VLDL particle contained a greater fraction of lipid, and was significantly larger as compared with those from chow-fed or starch-fed hamsters. The results from retention time and diameter determination were consistent. Circulating particle diameter is determined by initial particle diameter at assembly and subsequent metabolic effects. For example, the particle diameter could decrease due to the TG lipolysis mediated by lipoprotein lipase.

The two major factors responsible for maintenance of the concentrations of VLDL-TG and VLDL-PL are synthesis and secretion of TG and PL by liver and removal of TG by extrahepatic tissues. VLDL-TG synthesis is derived from three sources (Karpe,

1997), plasma NEFA, the main substrate for hepatic TG synthesis; hepatic uptake of partly lipolyzed chylomicron and VLDL remnants; and *de novo* synthesis of TG from carbohydrate. In the present study, fructose significantly elevated plasma NEFA and insulin concentrations indicating that fructose feeding caused insulin resistance. In insulin resistance, increased efflux of NEFA from adipose tissue and impaired insulin-mediated skeletal muscle uptake of NEFA increase hepatic NEFA concentrations (Ginsberg and Huang, 2000). NEFA are the principal substrate for hepatic TG, PL synthesis, and subsequently, the increased production of TG and PL, and the overproduction of TG and PL that could result in abnormal assembly in VLDL particle.

The liver, the principal lipogenic organ, is responsible for the conversion of excess dietary carbohydrates to TG. Feeding a high-carbohydrate diet induces the synthesis of glycolytic and lipogenic enzymes including acetyl-CoA carboxylase, fatty acid synthase, stearoyl-CoA desaturase, glycerol-3-phosphate acyltransferase, ATP citrate lyase, malic enzyme, glucose-6-phosphate dehydrogenase, and pyruvate kinase (Granner and Pilkis, 1990; Ntambi et al., 1988; Sul and Wang, 1998). The coordinated induction of these enzymes is due to sterol regulatory element binding protein (SREBP)-stimulated gene transcription (Horton et al., 1998b; Shimano et al., 1996; Shimano et al., 1999; Shimomura et al., 1998). The induction of lipogenic gene transcription, as a result, increases fatty acid and TG concentration in the liver. The excess TG is incorporated and secreted by the liver as VLDL-TG.

SREBPs are transcription factors that belong to helix-loop-helix leucine zipper family and regulate enzymes responsible for the uptake and synthesis of cholesterol,

fatty acid synthesis and desaturation, TG and phospholipid synthesis, and glucose metabolism (Brown and Goldstein, 1997; Edwards et al., 2000; Foretz et al., 1999a; Horton and Shimomura, 1999). The SREBPs are synthesized as precursors and bound to the ER prior to activation. When activated, SREBPs are released from the membrane and translocate the nucleus as a mature protein following a sequential proteolytic cleavage process (Brown and Goldstein, 1997). Two genes, SREBP-1 and SREBP-2, encode three SREBP isoforms, SREBP-1a, -1c and –2, each with a molecular mass of 125 KD (Brown and Goldstein, 1997). SREBP-1a is a potent activator of all SREBP-responsive genes including those that mediate the synthesis of cholesterol, fatty acids and TG. SREBP-1c, a predominant SREBP-1 isoform in the liver, preferentially enhances transcription of genes required for fatty acid but not cholesterol synthesis (Shimano et al., 1999; Shimomura et al., 1998). Changes in hepatic mature SREBP-1c protein levels were found to parallel those of mRNAs for lipogenic genes in the liver using a dietary manipulation (Horton et al., 1998a). Moreover, targeted disruption of SREBP showed that SREBP-1 is crucial for the carbohydrate mediated stimulation of lipogenic genes in mice (Shimano et al., 1999). SREBP-2 is relatively selective in transcriptionally activating cholesterol biosynthesis (Shimano et al., 1997). Studies showed that the relative expression of SREBP-1a, -1c and –2 *in vivo* is complex and can be affected by the nutritional and hormonal status (Flier and Hollenberg, 1999; Foretz et al., 1999a). These studies linked lipid and carbohydrate metabolism via insulin action and SREBPs. The content of SREBPs in livers from obese ob/ob mice and transgenic aP2-SREBP-1c436 (aP2-SREBP-1c) mice that overexpress nuclear SREBP-1c only in adipose tissue

was investigated (Shimomura et al., 1999). Both lines of mice develop hyperinsulinemia, hyperglycemia, and hepatic steatosis, but aP2-SREBP-1c mice exhibit a syndrome that resembles congenital generalized lipodystrophy in humans. Nuclear SREBP-1c protein levels were significantly elevated in livers from ob/ob and aP2-SREBP-1c mice compared with wild-type mice. Increased nuclear SREBP-1c protein was associated with elevated mRNA levels for known SREBP target genes involved in fatty acid biosynthesis, which led to significantly higher rates of hepatic fatty acid synthesis *in vivo*. Foretz et al. (1999a; 1999b) reported that treatment of isolated hepatocytes with insulin both prevented the decline in SREBP-1 levels and also introduced the genes such as acetyl-CoA carboxylase, fatty acid synthase, glucokinase and pyruvate kinase. Addition of a dominant negative form of SREBP-1c blocked the stimulatory effect of insulin on these target genes. Expression of a dominant positive SREBP –1c stimulated the expression of these same insulin-activated target genes in the absence of insulin (Foretz et al., 1999a). These results indicate that insulin stimulates the transcription of SREBP-1c and that the mature protein, together with a signal derived from glucose, result in enhanced transcription of gene involved in both lipogenesis and glucose metabolism. In this present study, fructose feeding induced insulin resistance, thus elevated insulin levels could increase the transcription of SREBP-1c and SREBP-1c-dependent genes, resulting in increased hepatic synthesis of fatty acids and TG. Starch increased plasma cholesterol level rather than inducing insulin resistance and elevating TG level. Starch feeding appears to induce a different response and may be due to the

effect of starch on SREBP-2. However, the precise mechanism for this action remains unknown.

Despite overproduction of apoB in liver, most apoB will be degraded through three mechanisms (Fisher et al., 2001). Newly synthesized apoB in endoplasmic reticulum (ER) is initially complexed with small amounts of lipid that are shuttled by microsomal triglyceride transfer lipoprotein (MTP). The apoB can be degraded via ER-associated degradation because of lipid deprivation or MTP deficiency. Assembly of VLDL depends on the relative availability of all lipid-cholesterol, PL, TG and CE (Davis, 1999). Davis and Boogaerts (1982) suggested the relative availability of CE to TG determines the relative composition of hydrophobic lipid in the core of newly secreted VLDL. In addition, the availability of free cholesterol may act as a regulator of the assembly of VLDL. These findings may explain why overproduction of TG, PL and apoB but deficiency of cholesterol resulted in formation of TG-rich large diameter VLDL particles instead of overproduction of VLDL particles. The results also indicate that VLDL assembly can be influenced by diet.

Plasma LDL is mainly derived from the plasma VLDL-LDL delipidation cascade (Eisenberg et al., 1973). The present study showed that there was no difference in LDL-PRO mass in plasma from the fructose-fed, starch-fed and chow-fed animals. This suggested that high-carbohydrate diets did not increase LDL particle number. When estrogen was used to treat post-menopausal females, the amount of large diameter VLDL increased in subjects with high–normal plasma TG concentration (Walsh et al., 1991). Large VLDL was postulated to not form LDL to a significant degree (Packard et al.,

1984; Stalenhoef et al., 1984). The studies of these researchers may help to explain the increased VLDL particle diameter and number, in the absence of a change in average LDL particle number in hamsters fed with high-carbohydrate diets in the present study. Characteristic abnormalities in the lipid profile in type-2 diabetes include increased concentrations of small, dense LDL (Feingold et al., 1993; Stewart et al., 1993). The present results showed that fructose feeding also induced the formation of small, dense LDL. However, these LDL were relatively rich in TG and poor in CE. In contrast, increased LDL lipoprotein mass in starch-fed hamsters were enriched in CE. In these short-term studies it is not possible to determine the atherogenicity of large CE-rich LDL associated with starch feeding relative to that of small TG-rich LDL associated with fructose feeding.

HDL play an important role in the prevention and treatment of ASCVD. Epidemiological studies and clinical trials demonstrated that elevated HDL-C has a direct anti-atherosclerotic potential, which is not secondary to its relation to other coronary risk factors (Sacks, 2002). HDL can impede the oxidation of LDL and transfer cholesterol from macrophage back to the plasma. Low plasma concentrations of HDL represent the common abnormality in the metabolic syndrome. Elevated concentrations of TG-rich lipoproteins lower HDL concentrations by promoting exchanges of cholesterol from HDL to VLDL via CETP and catabolizing TG-rich HDL (Bruce et al., 1998; Ginsberg, 2000). Insulin resistance with ASCVD more commonly has the combination of elevated TG and low HDL than elevated total and LDL-C concentrations. Functional defects in HDL may also contribute to ASCVD. In diabetic

patients, HDL does not prevent LDL oxidation as well as it does in non-diabetic patients (Gowri et al., 1999). However, in the fructose-fed hamster model used in the present study, several HDL characteristics were different from those observed in human studies. First, hamsters fed fructose- or starch-containing diets had significantly higher concentrations, not lower concentrations, of plasma HDL-C than did chow-fed hamsters. This result was also observed by Remillard et al. (2001). Also, the concentration and fraction of HDL-C were significantly higher in the fructose-fed hamsters than in starch-fed hamsters. Second, fructose feeding significantly increased all HDL lipid concentrations, but reduced the relative amount of HDL-TG. Third, fructose tended to increase the plasma concentration of HDL-PRO; however, the percentage of HDL-PRO was significantly lower when compared with the plasma concentration in either chow-fed or starch-fed animals in accordance with its observed large diameter. These characteristics suggested that fructose diet resulted in the formation of lipid-rich HDL. Increased HDL mass in both purified carbohydrate-fed groups indicates that hamsters have a different response to simple carbohydrates than other model species. The mechanism for the response is under investigation.

The following factors are thought to affect HDL cholesterol or particle number. First, apoAI is the major apolipoprotein component, which indicates the concentration of HDL-C or particle number. The composition and gel results showed that apoAI increased in fructose- and starch-fed hamsters. Mooradian et al. (1997) reported that plasma apoA1 and hepatic apoA1 mRNA concentrations in young rats or aged rats fed either a 60% fructose diet or a 60% glucose diet were significantly higher than in rats fed

rat chow. These investigators suggested that apoA1 expression in rats is modulated by factors related to the nature of dietary carbohydrates rather than insulin resistance being associated with feeding a high-fructose diet. Second, transgenic overexpression of LCAT in mice substantially increased HDL cholesterol and increased the plasma concentration of CE-rich, large HDL to an even greater extent (Francone et al., 1997; Vaisman et al., 1995). apoAI activates LCAT (Francone et al., 1997), thus, more apoAI means greater LCAT activation. Third, transfer of CE from HDL to apoB-LP in exchange for TG by CETP is the major pathway by which HDL cholesterol is returned to liver in humans (Tall, 1990). Remillard et al. (2001) reported a significant increase in the concentration and activity of CETP, both in plasma and adipose tissue of fructose-fed hamsters. In hamsters, adipose tissue and muscle are the major sources of CETP (Jiang et al., 1991), and lipoprotein composition analysis (Goulinet and Chapman, 1993) also demonstrated that the hamster is partially deficient in neutral lipid (CE, TG) transfer activity. Thus, fructose-fed hamsters produced large CE-rich HDL, increased HDL-C and particle number rather than lowering HDL-C. Third, both cellular protein ABCA1, which facilitates cholesterol and PL transport between HDL particles and peripheral cells, and SR-BI, which facilitates the uptake of HDL-CE by liver, can affect HDL-C and particle number. Species differences or specific HDL metabolic pathways are also likely to contribute to the different responses. Whether the increased HDL plays the protective role for ASCVD is not clear. HDL isolated from subjects with non-insulin-dependent diabetes mellitus exhibited a decreased capacity to induce cholesterol efflux (Gowri et al., 1999). The composition and protective effects of HDL_2, but not of HDL_3,

differed significantly between control and diabetic subjects. HDL_2 from diabetics, which were TG-enriched and cholesterol depleted compared with those from control subjects, were less able to protect LDL from oxidation and oxidation induced apoB100 fragmentation. In the present study, HDL types were not separated, nor was HDL function measured. It is not clear whether the hamsters fed a fructose-rich diet had HDL_2 enriched with TG and depleted of cholesterol while total HDL were enriched with cholesterol and depleted of TG.

Plasma lipoprotein and lipid metabolism are important in understanding the mechanism of ASCVD. The metabolism of plasma lipoproteins is highly interrelated, and it is critical to consider the entire lipoprotein and lipid profiles, rather than to focus on one or two lipoproteins. It is concluded that a high-carbohydrate diet significantly changes the entire lipoprotein and lipid profiles, as well as the physical properties of plasma lipoprotein particles. Further studies will be needed to define the role of HDL (type and function) and the mechanism of induction of a high HDL concentration in plasma. Further investigations will provide new insight into lipoprotein metabolism and the effect of high-carbohydrate diets on ASCVD in hamsters.

CHAPTER IV

DIETARY EFFECTS ON THE ASSEMBLY AND SECRETION OF apoB-CONTAINING LIPOPROTEINS IN HAMSTERS

Introduction

apoB-containing lipoproteins (apoB-LP) including chylomicrons, very low-density lipoproteins (VLDL), intermediate-density lipoproteins (IDL) and low-density lipoproteins (LDL) serve to deliver essential lipid and energy through out the body. The assembly of apoB-LP occurs in liver, small intestine, human heart and mammalian yolk-sac endoderm. (Young et al., 1995; Farese et al., 1996; Nielsen et al., 1998). Pathologies of abetalipoproteinaemia (Sharp et al., 1993) and familial hypobetalipoproteinaemia (Innerarity et al., 1990) are linked to genetic dysfunction in apoB-LP. Both VLDL and chylomicrons are metabolized to their remnants (IDL, LDL and chylomicron remnants) Convincing evidence indicates that apoB-LP are a major determinant of atherosclerotic cardiovascular disease (ASCVD) risk (Young, 1990; Packard and Shepherd, 1997). Specific changes in the physical properties (mass, composition, size, etc.) of apoB-LP constitute a metabolic profile that is closely associated with the incidence of ASCVD. For example, larger VLDL are cleared more rapidly, and produce fewer LDL than do smaller VLDL (Packard and Shepherd, 1997). Small dense LDL are more susceptible to oxidative damage than are large, less dense LDL (Chait et al., 1993). Intracellular and probably plasma membrane-associated processes control the physical properties of circulating apoB-LP, which define the features of apoB-LP for lipolytic and remodeling

proteins. Diets influence the physical properties of circulating apoB-LP, thus the dietary effect on apoB-LP is probably exerted during assembly and secretion processes.

The assembly of apoB-LP is a complex, multi-step process that occurs within the rough and smooth endoplasmic reticulum (ER) and subsequent compartments of the secretory pathway in the Golgi complex in hepatocytes. The process of particle assembly can be divided into two general steps, precursor formation and precursor joining (Alexander et al., 1976; Boren et al., 1994; Hamilton et al., 1998). Within the first step, two precursors are formed. First, a lipid-poor apoB-containing apoB-LP precursor is assembled within the rough ER, and a lipid-rich apoB-deficient apoB-LP precursor (a VLDL-sized lipid droplet) forms within the smooth ER. During the second step, these two precursors combine by as yet undescribed processes to form nascent apoB-LP particles. Some molecular details for the formation of the apoB-containing apoB-LP precursor are known (Boren et al., 1992; Rustaeus et al., 1995; Hamilton et al., 1998; Rustaeus et al., 1998). For example, apoB destined for assembly can translocate across the ER membrane to generate a transmembrane apoB in which the bulk of the protein mass is situated on the cytosolic side of the ER membrane (Rustaeus et al., 1999). If lipid becomes available, transmembrane apoB can undergo a process of post-translational lipid-facilitated translocation into the lumen of the ER (Sakata et al., 1993). Little is known about the processes involved in formation of the apoB-deficient lipid core, but these processes appear to depend on microsomal triacylglycerol transfer protein (MTP). However, combination of the two precursors to form mature nascent apoB-LP may not depend on MTP (Gordon et al., 1996).

It is known that the consumption of a high-carbohydrate diet can induce the formation of small dense LDL in the bloodstream. small dense LDL are thought to be more atherogenic than their larger counterparts (Dreon et al., 1994). In contrast, consumption of a high-fat diet can cause large, less dense LDL to appear in the blood (Rudel, unpublished data). It is not known whether high-carbohydrate-induced small dense LDL are more atherogenic than high-fat-induced large, less dense LDL in humans. It is also not clear whether changes in the physical properties of circulating lipoproteins stem solely from pathological intravascular metabolism or whether they result from changes to the physical properties of apoB-LP during assembly and prior to secretion into systemic circulation. Most studies of apoB-LP assembly have been performed *in vitro* in cell lines (e.g., HepG2 and McA-RH 7777 cells) or primary hepatocytes (Boren et al., 1992; Cianflone et al., 1992; Hamilton et al., 1998; Taghibiglou et al., 2000b). Studies *in vitro* showed that some defects in HepG2 cells resulted in defective triacylglycerol (TG) mobilization (Wu et al., 1996). Human studies *in vivo* (Parks et al., 1999) showed that a high-carbohydrate diet could alter rates of VLDL secretion, e.g., a high-carbohydrate diet induced VLDL-TG and VLDL-apoB overproduction and secretion. However, because of complicated effects of human multiple genes and environmental factors (e.g. diet, exercise), It is difficult to define the impact of physical properties of metabolic origin of apoB-LP on that of circulating apoB-LP in human studies. Using animal models, an investigator can easily define some factors (e.g. genes) and keep experimental conditions as similar as possible. Recently, (Taghibiglou et al., 2000a) introduced a fructose-fed hamster model for VLDL study. Studies with this

model showed that fructose feeding increased the concentration of VLDL and their components, enhanced TG percentage, increased VLDL particle size and small dense LDL (see Chapter III). That work demonstrated that high-carbohydrate diets changed the physical and biochemical features of circulating lipoproteins in Golden Syrian hamsters. However, little is known about how a high-carbohydrate diet impacts the size and composition of apoB-LP assembly intermediate particles; these are features that could influence the subsequent metabolism of nascent particles and their atherogenic potential. In hamsters, lipemia and insulin resistance are directly related to the content of fructose in the diet. The present study assessed whether nascent apoB-LP structure is altered by high-carbohydrate diets. The physical and biochemical features of nascent apoB-LP and apoB-LP assembly intermediates were characterized in livers from hamsters fed diets differing in carbohydrate composition.

Materials and Methods

Animals

Male golden Syrian hamsters from Charles Rivers laboratory (Wilmington, MA), aged 6 wk and weighing 90 g were housed in pairs at 22°C with a 12 h light/dark cycle (lights were on 7 a.m. to 7 p.m.) and had free access to water and food over an adaptation period of 2 wk. The average weight of the animals at this time was 110 g, and they were randomly assigned into 3 groups of 40 hamsters each and were fed either a closed formula cereal-based Harlan Teklad rodent chow (#W-8604, Harlan Teklad, Madison, WI), a 60% fructose-rich diet (#161506, Dyets Inc, Bethlehem, PA) or a 60% corn starch-rich diet (#161511, Dyets Inc, Bethlehem, PA). The animals had free access

to the experimental diets for 2 wk. At this time, 10 animals from each group were assigned to the secretion study, and 30 hamsters were assigned to the assembly study. Food intakes were monitored every day, and body weight was measured twice a week. All experiments were carried out on animals fasted for 16 h. All animals were cared for as outlined in "Guide for the Care and Use of Laboratory Animals," prepared by the National Academy of Sciences and published by the National Institutes of Health, Bethesda, MD (NIH publication No. 86-23, revised 1985). All experimental procedures were approved by the University Laboratory Animal Care Committee at Texas A& M University.

Triton WR-1339 injection and isolation of nascent VLDL

After 2 wk on the diets, blood for measurement of plasma TG was obtained from the periorbital venous sinus of hamsters under isoflurane (4% in 100% oxygen) anesthesia and then were injected Triton WR-1339 (20% solution in saline) through cardiac puncture at a dose of 600 mg/kg body weight. Sixty minutes after Triton injection, the animals were anesthetized and blood was collected via cardiac puncture into tubes that contained sodium azide (0.01%), Na_2-EDTA (0.12%), pencillin (10,000 U/mL)/streptomycin (10 mg/mL)/neomycin (10 mg/mL) and aprotinin (0.01 TIU/mL). Within 2 h of blood collection, plasma was separated by Sorvall TR 6000B centrifuge (Sorvall-Dupont, Wilmington, DE) at 2500 rpm, for 20 min at 4°C, and a mixture of reduced glutathione (0.5 mg/mL plasma), Leupeptin (0.5 μg/mL plasma) and benzamidine (0.16 mg/mL plasma) was added to preserve the native lipoprotein structure. VLDL was isolated from 1 mL plasma at $d < 1.006$ g/mL by aspiration with a

narrow-bore pipet following 18 h centrifugation at 40,000 rpm in a TFT 50.3 rotor at 14°C within a Beckman L8-70M (Beckman Coulter, Sunnyvale, CA) ultracentrifuge.

Triton WR-1339 is an alkaline polyether anionic detergent that blocks the removal of VLDL from plasma (Otway and Robinson, 1967). The hepatic secretion rate of VLDL fraction is proportional to the rate of increase in plasma concentration of VLDL component over time (Kazumi et al., 1986). The secretion rate of VLDL, in μg/100 g body weight/min, from liver into plasma was calculated using the following formula:

$$\text{VLDL-X secretion rate} = (\text{VLDL-X}_{60} - \text{VLDL-X}_{0})/60 \times V \times W/100$$

where VLDL-X_0 is plasma VLDL component concentration (μg/mL plasma) before Triton administration, VLDL-X_{60} is plasma VLDL component concentration (μg/mL plasma) 60 min after Triton injection, V is plasma volume (mL) and W is body weight. Plasma volume was determined as 3.86 mL/100 g body weight (Holt and Dominguez, 1980). Plasma concentrations of VLDL components were determined colorimetrically as described below. Triton injection enhances the secretion of VLDL and blocks the removal of VLDL, resulting in nascent VLDL accumulation in plasma. Thus, VLDL isolated from hamster plasma after Triton injection was assumed to represent nascent or Golgi VLDL, so called "nascent VLDL" or "nascent apoB-LP."

Isolation of rough endoplasmic reticulum

As described above, after the 2-wk feeding period, the hamsters were anesthetized with isoflurane and exsanguinated by cardiac puncture. Livers were removed immediately and rinsed in ice-cold saline. Rough ER was isolated by calcium precipitation (Hamilton et al., 1999). Livers were minced finely and 10–12 g were

suspended in 2 mL/g of ice-cold 140 mM KCl and homogenized by using a Polytron® PT3100 (KINEMATICA AG, Lucern, Switzerland) at setting 10 for 30 sec. The homogenized liver was divided equally into two 50-mL Sorvall centrifuge tubes and mixed with additional ice-cold 140 mM KCl to a volume of 40 mL. The homogenate was centrifuged in a Sorvall SS-34 rotor (Sorvall-Dupont, Wilmington, DE) at 8,000 rpm for 10 min at 4°C. After centrifugation, air bubbles and floating fat were removed by water aspiration, the supernatant solution was decanted into another centrifuge tube and the volume was adjusted to 40 mL with 140 mM KCl. This procedure was repeated until there was no visible floating fat. The final supernatant portion from each group livers was titrated with ice-cold 8 mM $CaCl_2$ at 20–25 mL/min. Rough ER pellets were obtained by centrifugation in a SS-34 Sorvall rotor at 8,000 rpm for 10 min at 4°C. To remove any lipid droplets, rough ER pellets were washed with KCl via resuspention of ER pellets in KCl (final concentration of 0.5 M) and centrifugating for 62 min at 34,000 rpm in a TFT 50.3 rotor at 21 C° (Kulinski et al., 2002).

Isolation of apoB-containing lipoprotein assembly intermediates from rough ER

Rough ER lumen contents were separated from the membrane of the rough ER after membrane rupture with 100 mM Na_2CO_3, pH 11.2 and centrifugation for 18 h at 35,000 rpm in a TFT50.3 rotor at 4 C°. apoB-containing lipoprotein assembly intermediate particles were recovered from the lumen contents. After centrifugation, the top layer was cut with a tube cutter to collect the top fraction, and the bottom fraction (floating yellow cloud next to pellet) was drawn up with pasteur pipette. The top layer fraction contained putative apoB-deficient assembly intermediates (second-step particle), while the bottom

fraction contained putative apoB-containing assembly intermediates (first-step particle). Both fractions were further purified by centrifugation at 30,000 rpm in a TFT 50.3 rotor at 4°C for 18 h. For apoB-deficient assembly intermediates, overlayed 4 mL/each tube 0.9% saline slowly without mixing to the top layer fraction (2.5 mL/each tube) prior to centrifugation. For apoB-containing assembly intermediates, overlayed 4 mL/each tube with1.053 g/mL NaCl/ NaBr density solution, slowly without mixing to the bottom fraction followed by adjusting the density of the bottom fraction with solid dessicated KBr to 1.3 g/mL. After ultracentrifugation, both intermediate particles were collected and dialyzed against saline with 0.01% EDTA for 24 h at 4°C.

Electron microscopy

To identify rough ER and assess homogeneity, rough ER pellets were fixed, dehydrated, embedded and stained as described by Hamilton et al. (1999) Pieces of pellets were punched with a pasteur pipette into fresh fixative (2 % glutaraldehyde–1% paraformaldehyde in 0.1 M sodium cacodylate buffer, pH 7.4) and fixed for 24 h. After the fixed samples were washed with buffer, they were transferred into 2% osmium tetroxide overnight, then dehydrated in acetone and embedded in Epon. The sample sections were stained with 0.8% lead citrate for 5 min and examined with a Siemens 101 electron microscope (Siemens/CTI Corp., Knoxville, TN).

Analysis of biochemical markers

To assess purity of the ER, biochemical markers for rough ER and other membranes were assayed in whole liver homogenate and in the rough ER fraction. The activities of glucose-6-phosphatase (deDuve et al., 1955) and diacylglycerol acyltransferase (DGAT),

a major enzyme in the synthesis of TG (Ozasa et al., 1989) were measured as markers of ER. 3-hydroxy-3-methylglutaryl co-enzyme A (HMG-CoA) reductase , a rate-limiting enzyme of cholesterol biosynthesis, was determined as a smooth ER marker (Erickson et al., 1990). RNA was extracted from rough ER (Quantum Prep Aquapure RNA Isolation Kit Cat # 732-6370; Bio-Rad Laboratories, Hercules CA) and RNA concentration was estimated by measuring absorbance at 260 nm. To assess contamination of the ER by other membranes, succinate INT reductase was measured as a mitochondrial marker (Pennington, 1961), 5'-nucleotidase as a plasma membrane marker (Emmelot et al. (1964), acid phosphatase as a marker enzyme for lysozyme (deDuve et al., 1955) and GM130 as a marker of the Golgi complex (Nakamura et al. (1997), Golgi matrix protein of 130 KDa, is a protein isolated from Triton-insoluble Golgi matrix and associated with the *cis*-compartment. GM130 functions as a structural element of the Golgi complex. To measure GM130, proteins were separated by SDS-PAGE following in-gel Western blotting. Liver homogenates (40 μg) and rough ER pellets (40 μg) were fractioned by SDS-PAGE on a 4–15% gel. Following electrophoresis, the gels were washed with 50% isopropanol and ultrapure water, and blocked in Odyssey Blocking Buffer (LI-COR, Inc., Lincoln, NE). IRDye700™-labeled goat anti-mouse secondary antibody (LI-COR, Inc., Lincoln, NE) was used to detect mouse anti-rat primary antibody (BD Biosciences, San Diego, CA). Bands were visualized by an Odyssey imager and calculations were made using Odyssey software (LI-COR, Inc., Lincoln, NE).

Size analysis of nascent VLDL and apoB-containing lipoprotein assembly intermediate particles

The particle diameters of nascent VLDL and apoB-containing lipoprotein assembly intermediates were measured by dynamic laser light-scattering analysis using a Microtrac series 250 ultrafine particle analyzer with a laser probe tip (UPA-250; Microtrac, Clearwater, FL), and Microtrac software (Honeywell, Inc., Ft. Washington, PA) (Walzem et al., 1994; Mack et al., 1994). Following ultracentrifugation, the centrifuge tubes containing the samples were removed from the rotor and uncapped. The laser probe was gently placed on the top layer of supernatant portion. It is critical not to mix the sample layer or prevent air bubbles at the probe liquid interface. Due to the low lipoprotein content of some samples, a measurement time of 540 sec was used for all samples. The results of primary data collection can be expressed in particle number, particle area or particle volume in order to adequately describe different aspects of the same particle population with respect to their colloidal properties (Walzem, 1996). Particle number distribution describes the frequency distribution of particles of the specified diameter. Particle volume distribution describes the distribution of total particle volume among particles of different diameter. Particle volume distribution is sensitive to the presence of large diameter particles because the volume of a sphere increases as a cubic function of particle radius. In this chapter, particle number will be used to describe the particle diameter in order to compare particle diameter from different sources. Raw particle diameter distributions were converted to area, number and volume population percentiles, which were used to calculate median particle diameter.

Composition analysis of nascent VLDL and apoB-containing lipoprotein assembly intermediate particles

Nascent VLDL and dialyzed apoB-containing lipoprotein assembly intermediate particles were used in composition studies. Protein (PRO) was measured by a modified Lowry method (Lowry et al., 1951) using bovine serum albumin as the standard. Triacylglycerol concentration was determined enzymatically using a kit from Sigma (Procedure No. 339, Sigma Chemical Co., St. Louis, MO). Total cholesterol (Tch), free cholesterol (Fch) and phospholipids (PL) were measured by use of enzymatic kits (Cholesterol CII Cat. No. 276-64909; Free Cholesterol C Cat. No. 274-47109; Phospholipids B Code No. 990-54009, WAKO, Richmond, VA). Esterified cholesterol (CE) was calculated by multiplying the difference between Tch and Fch by 1.67 (Chapman et al., 1981). The assay for total cholesterol or free cholesterol depends on the 1) hydrolysis of CE, which releases Fch, 2) the oxidation of Fch in a reaction that generates hydrogen peroxide and 3) the colorimetric measurement of the hydrogen peroxide produced (Richmond, 1973). In the assay of phospholipids, choline-containing phospholipids are hydrolyzed by phopholipase D to free choline, which is subsequently oxidized with the production of hydrogen peroxide, which is measured colorimetrically (Takayama et al., 1977). Non-esterified fatty acid (NEFA) of apoB-LP assembly intermediate particles was determined by a spectrophotometric method using kits (NEFA C Code No. 994-75409, WAKO, Richmond, VA). This method depends on the acylation of coenzyme A (CoA) by the fatty acids in the presence of acyl-CoA synthetase. The

acyl-CoA produced is oxidized with generation of hydrogen peroxide and the hydrogen peroxide is measured colorimetrically (Elphick, 1968).

Electrophoretic analyses of apolipoproteins

Isolation of apoB. Apolipoprotein B in isolated assembly intermediates was identified by SDS-PAGE and subsequent in-gel Western blotting. The protein concentration of assembly intermediates was determined by a modified Lowry assay (Lowry et al., 1951). Sample volumes containing 50-200 μg protein were combined with 60 μg apoferritin carrier protein prior to delipidation to insure quantitative apolipoprotein recovery (Kotite et al., 1995). Samples were delipidated overnight at –20°C after mixing 400–1200 μL sample with 10 volumes of ice-cold ethanol-diethyl ether in a 15-mL conical, glass-stoppered tube. The delipidated mixture was centrifuged for 25 min at 1250 rpm in a Sorvall TR 6000B centrifuge to facilitate removal of the organic phase. The pellet was extracted twice with 4 mL cold anhydrous diethyl ether. The resultant pellet was dissolved in 50–100 μL sample buffer containing 3% SDS, 1.5% dithiothreitol, and 1% mercaptoacetic acid. Excess ether was removed under a gentle stream of nitrogen, and the dissolved apolipoproteins were denatured at 100°C for 3 min prior to application to the SDS–PAGE gel.

Apolipoproteins were separated using the SDS-PAGE gradient gel described by Kotite et al. (1995) with some modifications. The 3–12% and 3–20% gradient polyacrylamide gels were cast using a two-chamber gradient mixer (Bio-Rad Laboratories, Hercules, CA). A 3–12% gradient polyacrylamide gel was used to identify and quantify apoB, while a 3–20% gradient polyacrylamide gel was used to observe the

apolipoprotein profile in the assembly intermediate particles. Apolipoprotein separation was effected using a Mini-PROTEIN II Vertical gel apparatus (Bio-Rad Laboratories Inc., Hercules, CA) (Laemmli, 1970) containing two minigels for each separation. After loading 50 μL delipidated VLDL or apoB100 standard in each well, a Bio-Rad PowerPAC 300 (Bio-Rad, Laboratories Inc, Hercules, CA) was used to apply 76V to the gels for 30 min, followed by 96V until the dye front was 1 mm from the bottom of the gel. Narrow-cut human LDL served as the source for the apoB100 used as the reference protein within the standard curves.

Identification of apoB in assembly intermediate particles. In-gel Western blotting was employed in this study to identify apoB in assembly intermediate particles. Aliquots of 0.3-2 ug of sample (first-step particle, second-step particle and plasma VLDL) and apoB100 standard proteins were subjected to SDS-PAGE electrophoresis. Following electrophoresis, one of the gels was washed with 50% isopropanol and ultrapure water, and subsequently blocked in Odyssey Blocking Buffer (LI-COR, Inc., Lincoln, NE) After phosphate buffer saline (PBS) (0.1% Tween-20 in PBS) washing, the gel was incubated for 1 h with a rabbit antiserum specific for hamster apoB (Lampire Biological Laboratories, Pipersville, PA) Following PBS washing, the gel was incubated with an IRDye700™-labeled goat anti-rabbit secondary antibody (LI-COR, Inc., Lincoln, NE). After PBS washing, the gel was screened using an Odyssey™ Infrared Imaging System (LI-COR, Inc., Lincoln, NE) equipped with an Odyssey Software Package.

Quantification of apoB. apoB was quantitatively characterized by analytical SDS-PAGE with Coomassie brilliant blue staining (Kotite et al., 1995). Aliquots of 30-

40 ug of sample (first-step particle, second-step particle and plasma VLDL) and apoB100 standard proteins were subjected to SDS-PAGE electrophoresis. Following electrophoresis, gels were stained with 0.15% Coomassie brilliant blue in staining solution for 15 min at 60°C, and then destained at 60°C in a destaining solution until backgrounds were clear. The gels were scanned using an Odyssey™ Infrared Imaging System (LI-COR, Inc. Lincoln, NE) equipped with an Odyssey Software Package to automatically integrate the volume of stained apolipoprotein bands. The standard curve for apoB was constructed by relating the intensity of dye uptake of each band to its known mass. The line of fit was evaluated (Kotite et al., 1995) at least squares for the power function $y = ax^b$. The concentrations of apoB in assembly intermediate particles were calculated from the regression equation relating the absorbance of apoB standard bands to the amount of apoB standard applied to the gels.

Statistical analysis

The results are presented as the mean ± SEM unless otherwise noted. Comparisons among three groups were performed using analysis of variance (ANOVA). Difference in mean values was tested by a least-squares means procedure. P values less than 0.05 was considered statistically significant. All analyses were performed using the statistical analysis system procedures (SAS Institute, Inc., Cary, NC).

Results

Morphology of isolated rough endoplasmic reticulum

The electron micrograph of the rough ER isolated from hamster liver is shown in Figure. 4.1. Rough ER membrane consisted of many short strips of curved or parallel

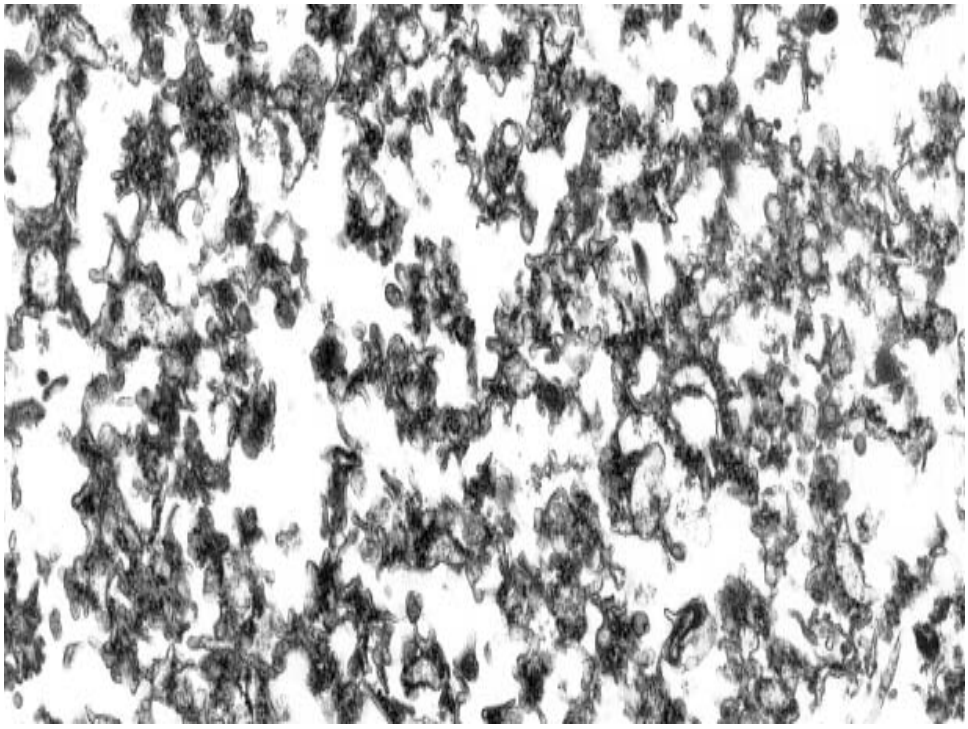

Figure 4.1 Electron micrograph of the rough endoplasmic reticulum (ER) isolated from hamster livers. Rough ER fractions consisted of many short strips of curved or parallel non-vesiculated membrane fragments. Electron dense ribosomes are on the outside surface. (× 40.000)

non-vesiculated membrane fragments. The electron dense ribosomes were on the outside surface of the ER. For some rough ER fragments, inside the sac (cisterna) was flocculent material-the newly synthesized proteins.

Analyses of biochemical markers

Table 4.1 presents the data for biochemical markers measured in homogenate and rough ER fraction from hamster livers. The rough ER fraction was enriched 3.7-fold in glucose-6-phosphatase, 3-fold in RNA and 3.8-fold in DGAT as compared with activities in the homogenate. However, mitochondria marker succinate INT reductase and smooth ER marker HMG-CoA reductase activities were barely detectable in rough ER fraction compared with homogenate, and the activities of plasma membrane marker 5' nucleotidase (10-fold), lysozme marker acid phosphatase (5-fold) and Golgi complex maker GM130 (13-fold) were lower than their activities in homogenate.

Effects of diet on hepatic secretion of VLDL

The plasma VLDL mass from hamsters fed chow, fructose-enriched and starch-enriched diets was increased about 2-fold in all dietary groups 60 min following the administration of Triton WR-1339 (Figure 4.2). The mean increase was greater for VLDL mass from the starch-fed (2.6-fold) compared with the chow- (2.1-fold) or fructose-fed (2.2-fold) animals, however, the differences were not significant. After Triton injection, the plasma concentration of all VLDL components increased in all animals (Figure 4.3). However, the increase was greater for VLDL-triacylglycerol (VLDL-TG), VLDL-cholesteryl ester (VLDL-CE), VLDL-phospholipid (VLDL-PL) and VLDL-protein (VLDL-PRO) (2-fold) compared with VLDL-free cholesterol

TABLE 4.1

Biochemical marker analyses of subcellular fractions from hamster liver[1]

Markers[3]	Homogenate[2]	Rough ER[2]	Fold Change
G-6-Pase (ug/mg protein)	0.85 ± 0.17	3.10 ± 0.32	3.6↑
RNA (ug/mg protein)	32.32 ± 7.61	95.63 ± 19.20	3.0↑
DGAT (pmoL/mg/min)	82 ± 15	22 ± 7	3.7↑
HMG-CoA red (nmoL/mg/min)	25.30 ± 0.32	0.17 ± 0.01	149↓
succ INT red (pmoL/mg/min)	401 ± 8	10 ± 3	40↓
5' nuc (ug Pi/mg protein/min)	0.78 ± 0.23	0.06 ± 0.01	13↓
acid phosph (nmoL/mg/min)	0.05 ± 0.002	0.01 ± 0.004	5↓
GM130 (ug/mg protein)	6.73 ± 0.35	0.50± 0.24	13↓

1 Values are expressed as means ± SEM, n = 10.

2 Homogenate, whole hamster liver homogenate; Rough ER, rough ER membrane from hamster liver.

3 G-6-Pase, Glucose-6-phosphatase; DGAT, acyl coenzyme A: diacylglycerol acyltransferase; HMG-CoA red, HMG-CoA reductase; succ INT red, succinate-INT dehydrogenase; 5' nuc, 5' nucleotidase; acid phosph, acid phosphatase. The data are expressed as fold change over whole hamster liver homogenate.

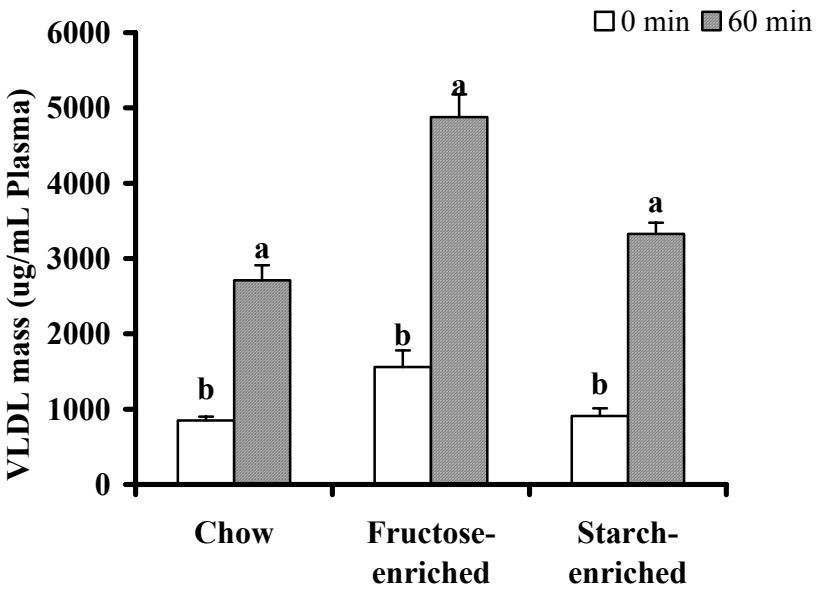

Figure 4.2 Plasma VLDL mass from hamsters fed chow, fructose-enriched and starch-enriched diets 60 min after the administration of Triton WR-1339. Values are expressed as means ± SEM, n = 10 per treatment group. Values that do not share a letter differ ($P < 0.05$).

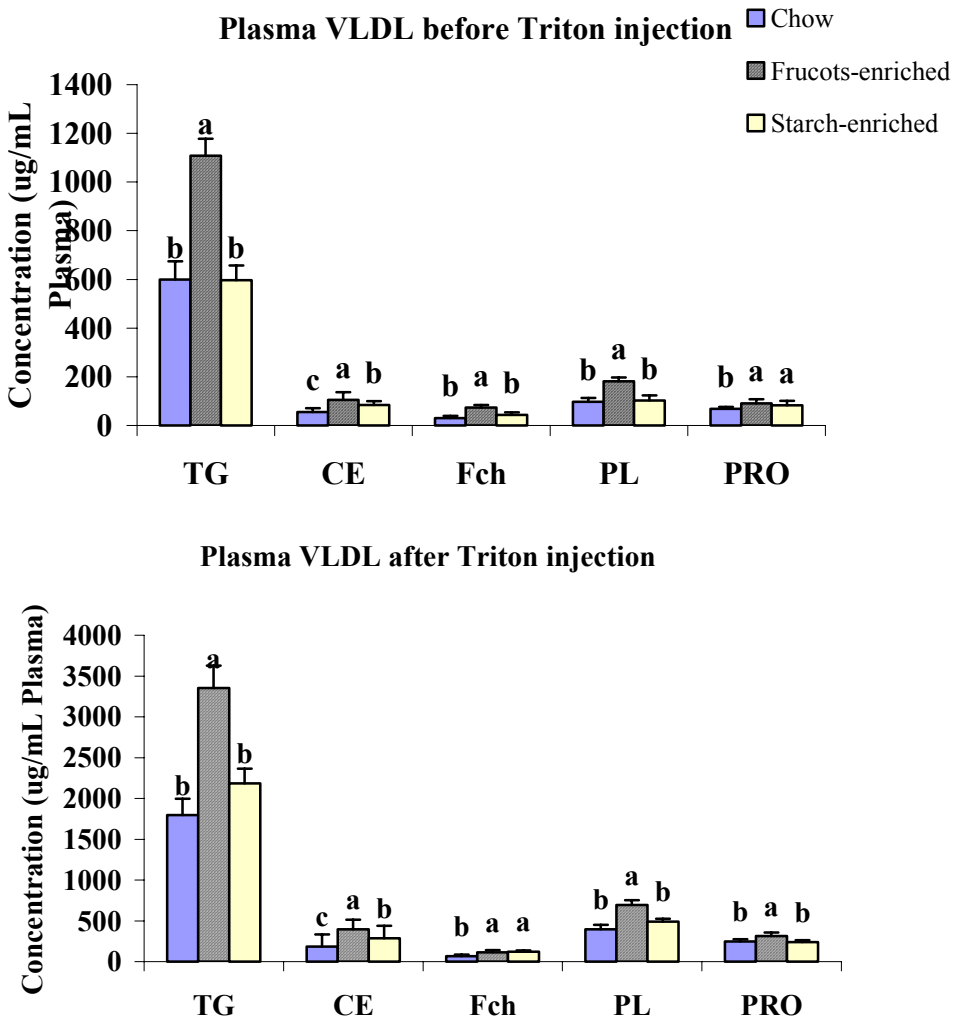

Figure 4.3 Concentration of components of plasma VLDL from hamsters fed chow, fructose-enriched and starch-enriched diets after intracardial injection of Triton. Values are expressed as means ± SEM, n = 10 per treatment group. Abbreviations: TG, triacylglycerol; Fch, free cholesterol; CE, cholesterol ester; PL, phospholipid; PRO, apolipoprotein. Values that do not share a letter differ ($P < 0.05$).

(VLDL-Fch) (1-fold) for the chow- and fructose-fed hamsters. Calculation of hepatic VLDL secretion rate based on an individual VLDL fraction showed higher hepatic secretion rates for fructose-fed compared with chow- and starch-fed animals (Figure 4.4). The difference in hepatic secretion rate between fructose fed and hamsters fed either chow or starch diet was statistically significant for VLDL-TG, VLDL-CE, VLDL-PL and VLDL-PRO.

Composition and concentration of nascent VLDL and apoB-containing lipoprotein assembly intermediate particles

The contents of the rough ER were fractioned by ultracentrifugation into two fractions, those separating at $d < 1.006$ g/mL and those separating at $1.006 < d < 1.053$ g/mL. The chemical composition of these two fractions and VLDL isolated from plasma before and after Triton injection is shown in Table 4.2 for chow-fed hamsters, Table 4.3 for fructose-fed hamsters and Table 4.4 for starch-fed hamsters. For animals in all dietary groups, the fraction isolated at $d < 1.006$ g/mL (second-step particle) was TG-rich; compared with VLDL isolated from plasma before or after Triton injection. This fraction from animals in all dietary groups had an increased percentage of TG, and a decreased percentage of Fch and PRO compared with VLDL isolated from plasma before and after Triton injection. However, these second-step particles had an increased percentage of CE in chow- and starch-fed animals, but not in fructose-fed animals. The particles from fructose-fed hamsters were richer in TG than that from either chow- or starch-fed animals ($P < 0.05$). Fructose and starch feeding caused a higher Fch and a lower PRO in this VLDL fraction compared with chow feeding. These differences were

TABLE 4.2

Composition of VLDL and lipoprotein assembly particles isolated from hamsters fed chow diet[1]

	d < 1.006 g/mL[3]			1.006 < d < 1.053 g/mL[3]
	Plasma	Plasma after triton injection	Rough ER	Rough ER
			%	
TG[2]	70.5 ± 1.4	65.0 ± 1.3	72.2 ± 2.7	35.7 ± 3.7
CE	6.5 ± 0.5	6.8 ± 0.6	8.0 ± 0.3	3.4 ± 0.2
Fch	3.6 ± 0.6	2.4 ± 0.3	1.1 ± 0.3	3.8 ± 0.3
PL	14.3 ± 1.2	14.8 ± 0.3	14.1 ± 1.4	29.4 ± 3.7
PRO	7.9 ± 0.8	10.9 ± 1.9	4.6 ± 0.1	27.7 ± 2.6

1 Values are means ± SEM, n = 15 per treatment group.

2 See Figure 4.3 for abbreviations.

3 Rough ER d < 1.006 d/mL particle NEFA 0.024 mmol/L; 1.006 < d <1.053 g/mL particle NEFA 0.0086 mmol/L

TABLE 4.3

Composition of VLDL and lipoprotein assembly particles isolated from hamsters fed fructose-enriched diet[1]

	d < 1.006 g/mL			1.006 < d < 1.053 g/mL
	Plasma	Plasma after triton injection	Rough ER	Rough ER
			%	
TG[2]	70.5 ± 1.6	68.6 ± 0.9	73.4 ± 3.6	29.6 ± 2.1
CE	6.8 ± 0.7	8.1 ± 0.7	3.5 ± 0.3	10.3 ± 0.3
Fch	4.8 ± 0.5	2.3 ± 0.3	5.4 ± 0.1	8.7 ± 0.3
PL	11.8 ± 0.6	14.1 ± 0.3	13.9 ± 2.9	29.6 ± 0.9
PRO	5.9 ± 0.6	6.9 ± 0.8	4.0 ± 0.1	22.3 ± 2.6

1 Values are means ± SEM, n = 15 per treatment group.

2 See Figure 4.3 for abbreviations

TABLE 4.4

Composition of VLDL and lipoprotein assembly particles isolated from hamsters fed starch-enriched diet[1]

	d < 1.006 g/mL			1.006 < d < 1.053 g/mL
	Plasma	Plasma after triton injection	Rough ER	Rough ER
			%	
TG[2]	65.4 ± 6.0	64.1 ± 1.3	69.7 ± 0.9	24.9 ± 0.8
CE	9.3 ± 0.7	8.6 ± 0.4	8.5 ± 0.5	10.5 ± 0.4
Fch	4.8 ± 0.5	3.7 ± 0.4	3.6 ± 0.5	5.4 ± 0.5
PL	11.3 ± 4.0	14.8 ± 0.4	13.9 ± 2.1	33.95 ± 0.8
PRO	9.2 ± 1.5	8.8 ± 0.7	4.3 ± 0.1	25.21 ± 3.7

1 Values are means ± SEM, n = 15.

2 See Figure 4.3 for abbreviations.

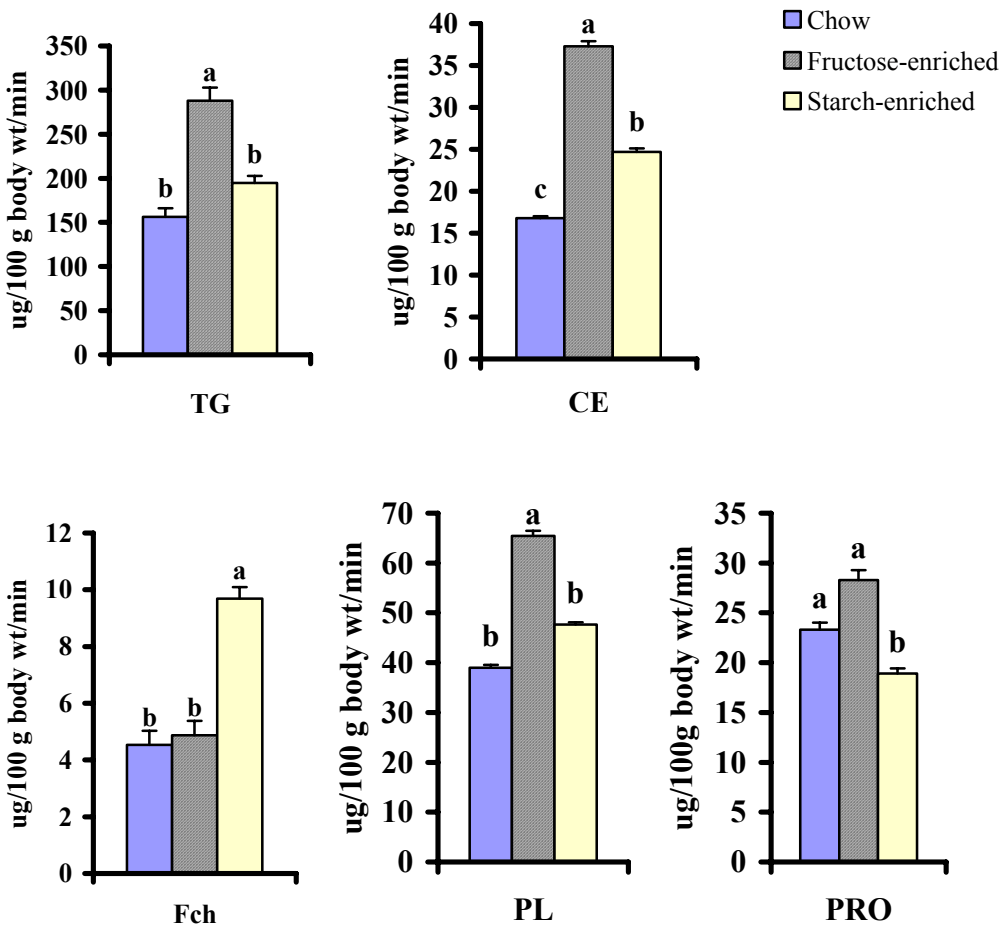

Figure 4.4 Secretion rates of VLDL components in hamsters fed chow, fructose-enriched and starch-enriched diets. Values are means ± SEM, n = 10 per treatment group. See Figure 4.3 for abbreviations. Values that do not share a letter differ ($P < 0.05$).

significant in fructose feeding, but not in starch feeding. Comparing the mass of lipoprotein assembly intermediate particles in the three groups, the increase was significantly greater (80%) in the fructose-fed than that in chow- or starch-fed animals.

The fraction isolated at $1.006 < d < 1.053$ g/mL (first-step particle) of lipoproteins had little core material-TG and CE-but was rich in Fch, PL and PRO compared with the core material in the second-step particle. These first-step particles from fructose-and starch-fed hamsters were richer in CE ($P < 0.01$) and Fch ($P < 0.05$), but poorer in PRO ($P < 0.05$) compared with those from chow-fed hamsters. These particles from starch-fed group were richer in PL, but poorer in TG ($P < 0.05$) compared with the first-step particles in the other two groups. However, comparing the lipoprotein mass of particles in the three groups, the increase was significantly greater for all core material components in the fructose-fed than for the chow- or starch-fed animals (Figure 4.5). The increase in mass of first-step particles from rough ER was consistent with that in plasma before and after Triton injection (Figure 4.3, Figure 4.5) By 3-10% SDS-PAGE, the second-step particles from the rough ER contained apoE but not apoB100, These first-step particles contained apoB100 and apoE. Some protein bands were consistently observed, but these proteins were not identified (Figure 4.6). The Western blot analysis of apoB in the fractions released from liver rough ER are shown in Figure 4.7. An apoB100 band was found in blots of the first-step particle, but not the second-step particle. The quantification of apoB from the first-step particle recovered from rough ER and plasma VLDL before and after Triton injection is shown in Figure 4.8 and Figure 4.9, respectively. The apoB concentration of the first-step particles from fructose-fed

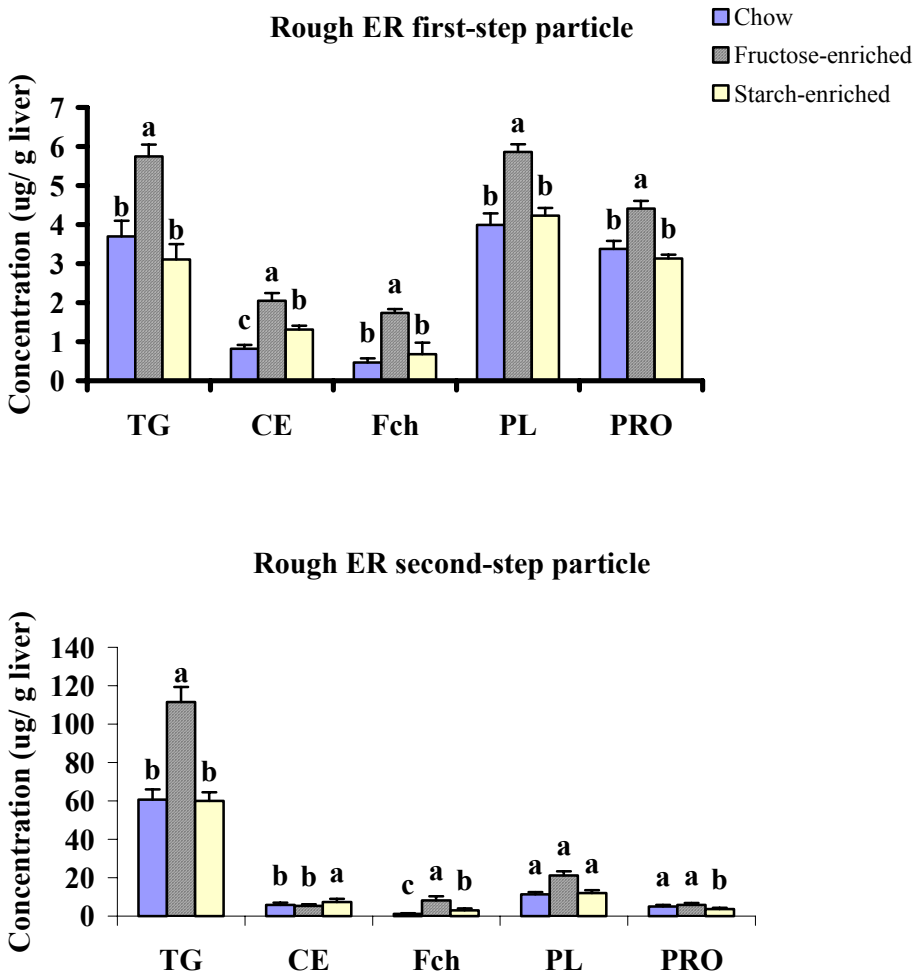

Figure 4.5 Comparison of the concentration of components of particles from liver rough ER from hamsters fed chow, fructose-enriched and starch-enriched diets. Values are means ± SEM, n = 6 per treatment group. Abbreviations were given in Figure 4.3. Values that do not share a letter differ ($P < 0.05$).

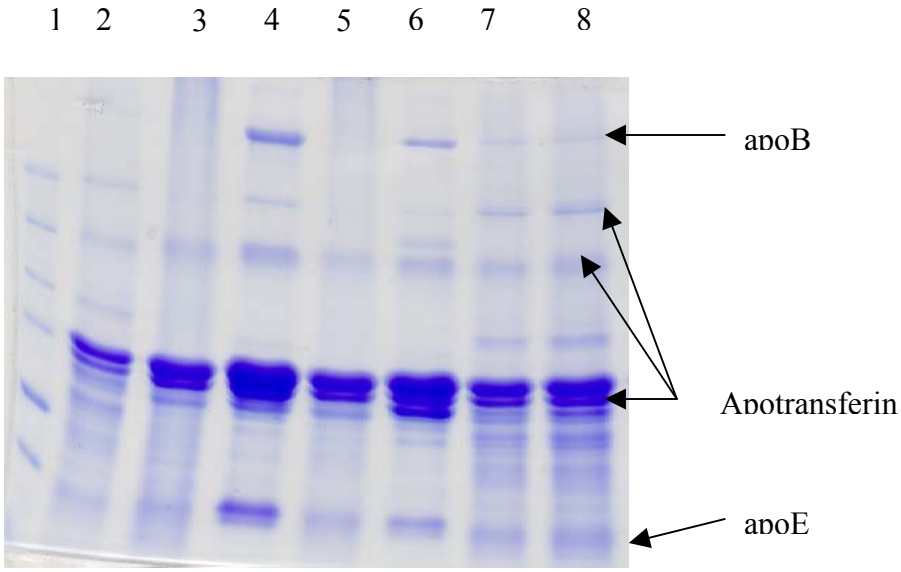

Figure 4.6 Analytical SDS-PAGE (3-12%) of hamster plasma VLDL and lipoprotein assembly intermediate particles from rough ER visualized with Coomassie R250 stain. Lane:1, MW standard; 2, first-step particle (35 μg), chow-fed hamsters; 3, second-step particle (45 μg), chow-fed hamsters; 4, first-step particle (45 μg), fructose-fed hamsters; 5, second-step particle (40 μg), fructose-fed hamsters; 6, first-step particle (45 μg), starch-fed hamsters; 7, plasma VLDL (40 μg), fructose-fed hamsters; 8, plasma VLDL (42 μg), chow-fed hamsters.

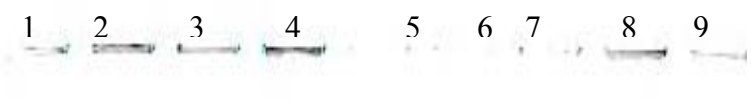

Figure 4.7 In-gel Western blot identification of apoB in lipoprotein assembly intermediate particles from hamster liver rough ER. Lane: 1, first-step particle (1 μg), chow-fed hamsters; 2, first-step particle (1.3 μg), fructose-fed hamsters; 3, first-step particle (1.3 μg), starch-fed hamsters; 4, apoB100 standard (1 μg); 5, second-step particle (2 μg), chow-fed hamsters; 6, second-step particle (2 μg), fructose-fed hamsters; 7, second-step particle (2 μg), starch-fed hamsters; 8, plasma VLDL (1 μg), chow-fed hamsters; 9, apoB100 standard (0.3 μg).

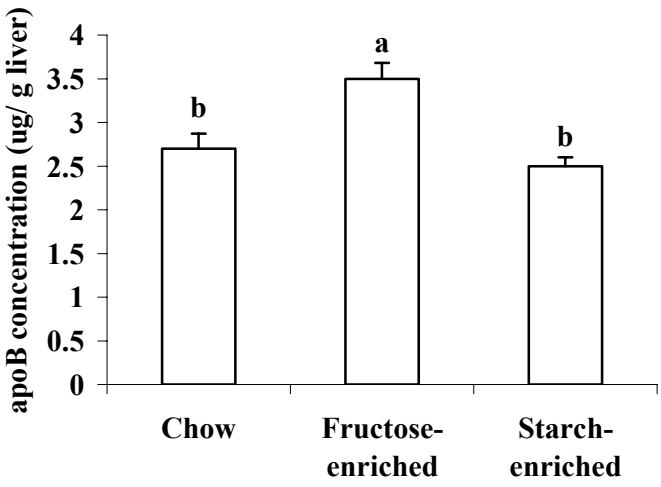

Figure 4.8 Comparison of the concentration of apoB in first-step particles isolated from hamsters fed chow, fructose-enriched and starch-enriched diets. Values are means ± SEM, n = 6 per treatment group. Values that do not share a letter differ ($P < 0.05$).

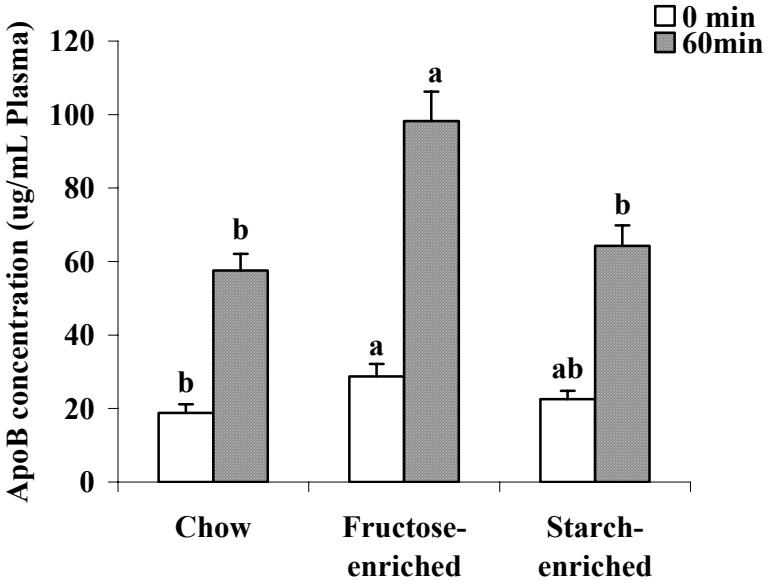

Figure 4.9 Quantification of apoB from plasma VLDL isolated from hamsters before and 60 min after Triton injection. Values are means ± SEM, n = 15 per treatment group. Comparisons are made among chow, fructose-enriched and starch-enriched diets. Values that do not share a letter differ ($P < 0.05$).

hamsters was significantly greater than their concentration in particles from the other groups. The increase in VLDL-apoB for fructose-fed (2.4-fold) was greater compared with chow- (2.1-fold) or starch-fed (1.9-fold) animals.

Particle size distribution of nascent VLDL and apoB-containing lipoprotein assembly intermediate particles

After Triton injection, the diameter of nascent VLDL isolated from plasma was significantly smaller in all hamsters compared with the size of VLDL from plasma before Triton injection (Figure 4.10). Fructose-fed hamsters had average diameters of 49 nm, slightly larger than the diameters of chow- (47 nm) or starch-fed (48 nm) hamsters, however, there was no significant difference among the three groups. The second-step particles from chow-fed hamsters averaged 53 nm in diameter, with particle sizes ranging from 38 to 238 nm (Figure 4.10). Fructose feeding was associated with a larger second-step particle (63 nm) compared with chow or starch (51 nm) feeding (Figure 4.11). There was no significant difference in second-step particle diameters between chow and starch feeding. For chow- and starch-fed hamsters, the diameter of second-step particles was larger than that of nascent VLDL, but smaller than that of circulating VLDL (Figure 4.10). However, the size of second-step particles from fructose-fed animals was not larger than that of nascent VLDL. Consistent with their density and composition, the first-step particles from chow-fed hamsters were smaller than second-step particles. Their diameters ranged from 11 to 22 nm, and averaged 13.4 nm, while the diameters of these particles from the fructose-fed group were significantly larger (16 nm) than those of either chow- or starch-fed (12.6 nm) group (Figure 4.11).

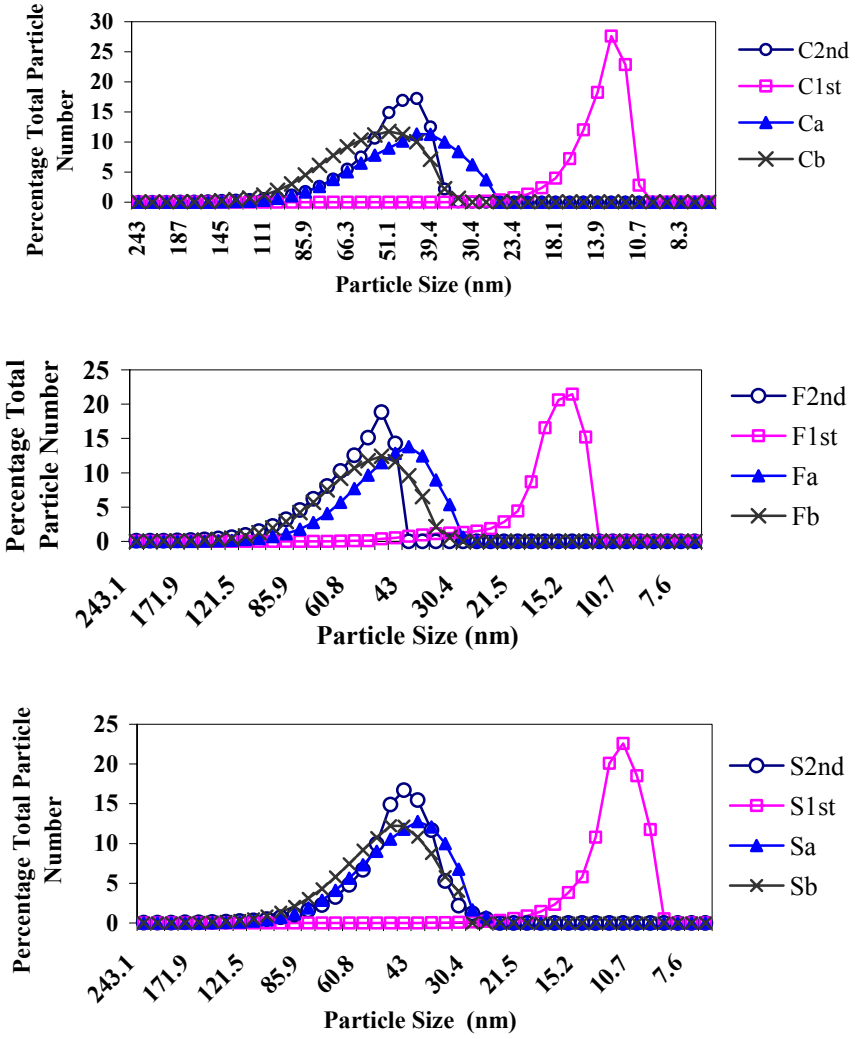

Figure 4.10 Dynamic light scattering-determined diameter distribution of VLDL, d < 1.006 g/mL, isolated from hamsters before and 60 min after Triton injection, and particles d < 1.006 g/mL and 1.006 < d > 1.053 isolated from rough ER. 2nd, second-step particles; 1st, first –step particles; a, VLDL after Triton injection; b, VLDL before injection. C, F and S: hamsters fed from chow, fructose-enriched and starch-enriched diets.

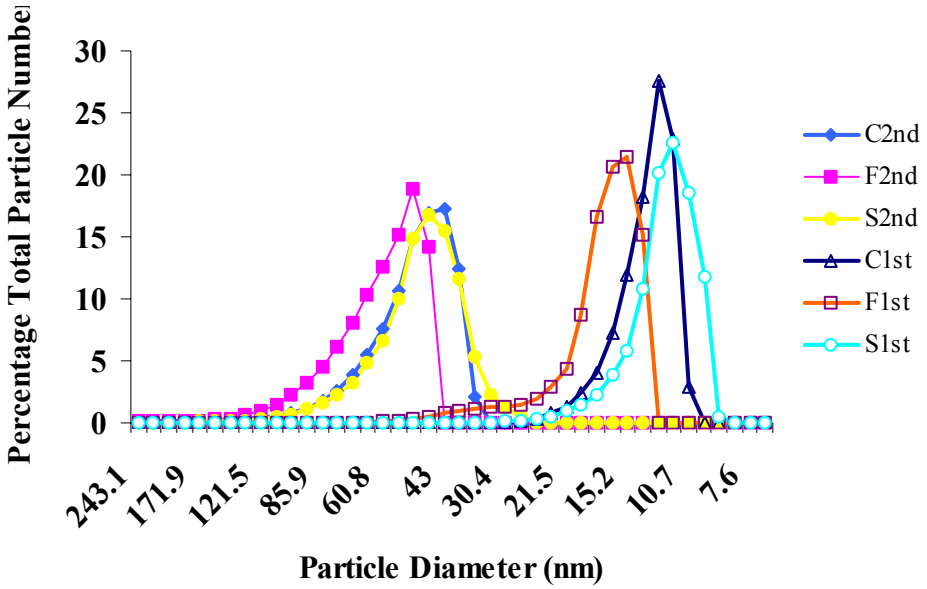

Figure 4.11 Dynamic light scattering-determined diameter distribution of particles d < 1.006 g/mL (second-step particle) and 1.006 < d > 1.053 g/mL (first-step particle) isolated from hamster liver rough ER. 2nd, second-step particles; 1st, first – step particles. C, F and S: hamsters fed chow, fructose-enriched and starch-enriched diets.

Discussion

The purpose of the present study was to investigate nutrient effects on the assembly and secretion of apoB-containing lipoproteins in hamster liver by isolating and characterizing intermediates in the assembly pathway and nascent VLDL after Triton WR-1339 injection. The results from chapter III showed that fructose feeding could induce insulin resistance, elevated plasma TG concentration, apoB overproduction and small dense LDL in hamsters. Elevated plasma TG concentration, apoB overproduction and small dense LDL are collectively termed atherogenic lipoprotein profile (ALP). Do assembly particle physical properties change with diet? Are manifestations of ALP solely the result of metabolic differences post secretion or are nascent particles different? Extensive research relative to apoB-LP assembly and secretion in vitro has been carried out in primary rat hepatocytes (Boren et al., 1992; Boren et al., 1994; Hamilton et al., 1998; Rusinol et al., 1993). However, few studies have been performed in vivo because of technical difficulties. Liver rough ER is the major organelle for lipoprotein synthesis and assembly. Recently, Hamilton et al. (1999) introduced a novel technique for isolating rough ER membrane from liver. The rapid and non-ultracentrifugal method can recover large amounts of highly pure hepatocyte rough ER, which is a valuable method that can be used to study in vivo the assembly of apoB-LP, as well as secretion and membrane protein translation, translocation and folding. The hamster is a good model for the study of lipoprotein metabolism because its lipoprotein metabolism appears to resemble that of humans. Hamster liver secretes VLDL containing only apoB100 with a density close to that of human apoB100 (Arbeeny et al., 1992). As in humans, hamster

LDL receptor plays a key role in LDL metabolism (Spady and Dietschy, 1985). The hamster develops insulin resistance in association with a marked hyper-triacyglycerolmia when fed a fructose-enriched diet (Kasim-Karakas et al., 1996). However, unlike the human, the hamster is a HDL-cholesterol-rich animal. Hamster lipoproteins are primarily distinguished by their lipoprotein core lipid content compared with their human counterparts. Both hamster plasma VLDL and LDL are CE-deficient and TG-rich, whereas HDL are CE-rich and TG-poor (Goulinet and Chapman, 1993). Recently, Taghibiglou et al. (2000a) introduced a fructose-fed hamster model to investigate the mechanisms mediating the overproduction of VLDL in the insulin-resistant state. These investigators demonstrated that hepatic VLDL-apoB overproduction in fructose-fed hamsters resulted from intracellular stability of nascent apoB and enhanced expression of MTP. However, whether core lipid availability determines the efficiency of the VLDL assembly process is currently unknown. In the present study, employing the fructose-fed hamster model and the calcium precipitation method of recovering rough ER membrane, the author investigated dietary effects on the physical properties of apoB-LP particles during the assembly and secretion pathway. The author also suggested the value of establishing the effect of high fructose on the assembly and secretion of apoB-LP in the fructose-fed hamster model so as to systemically characterize hepatic apoB-LP.

Two lipoprotein fractions were isolated from the contents of rough ER by ultracentrifugation. The second-step particles (d < 1.006 g/mL) were TG-rich, PRO-poor, they were slightly larger than nascent VLDL recovered 1 h post Triton WR-1339

injection, but smaller than plasma VLDL. They contained proportionately less protein and no apoB, indicating that these particles were lipid-rich, apoB-deficient apoB-LP precursors. Fructose-fed hamsters had 80% more particle mass compared with those fed a chow diet or a starch diet. The results in this study revealed particles with a greater mass of large lipid-rich, apoB-deficient apoB-LP precursors synthesized by liver when fed a fructose-containing diet.

The first-step particles recovered between the densities 1.006 and 1.053 g/mL were rich in PL and protein, and contained apoB, but a lower percentage of TG and CE than that of second-step particles. These particles were small, consistent with their chemical composition, indicating that they were apoB-containing lipid-poor lipoprotein precursors. Like second-step particles, the lipoprotein mass of first-step particles from fructose-fed hamsters was much greater than that of particles from hamsters fed a chow diet or starch diet, however, the particles from fructose-fed animals contained proportionately less protein. These results indicate that liver produced larger, lipid-rich, first-step apoB-LP precursors under the fructose feeding condition. The composition and size of second-step particles and first-step particles were different among the three groups, which suggested that diet did affect the formation of liver lipoprotein precursors and assembly of apoB-LP.

It has been suggested that in the first step, apoB might be associated with lipid as it is translated and translocated across the membrane of the rough ER (Boren et al., 1992). The primary lipid involved in the apoB-containing particles is PL, TG and cholesterol. Newly synthesized apoB may have two fates: assembly and secretion, or degradation

depending on the lipid availability (Davis, 1999). Fructose feeding increased the concentrations of TG, PL and cholesterol, which provided more available lipid to apoB to assemble and decreased the chance of apoB degradation. Thus, hamsters fed fructose have more apoB-containing apoB-LP precursors. In the second step, at the smooth surface ends of the rough ER, the apoB-containing particle and TG-rich apoB-deficient particle could join and convert to nascent VLDL, Golgi VLDL and eventually to plasma VLDL (Hamilton et al., 1998). More apoB-containing apoB-LP precursors fuse with TG-rich apoB-deficient particles, leading to more mature apoB-LP formation in fructose-fed animals.

In order to further investigate the changes in physical properties of VLDL particles that occur during the secretion pathway, hamsters were injected via cardiac puncture with Triton WR-1339 to block not only the removal of VLDL from plasma but also the intravascular conversions that occur as a result of lipase-mediated events (Steiner et al., 1984). This indirect method has been used successfully to study the rate of secretion of VLDL from liver (Holt and Dominguez, 1980; Taghibiglou et al., 2000a). Comparing the chemical composition and size among nascent VLDL, second-step particles and first-step particles from animals in all dietary groups, the chemical composition of nascent VLDL was between that of second-step particles and that of first-step particles, and the size of nascent VLDL was slightly smaller than that of second-step particles, but significantly larger than that of first-step particles. The present study, for the first time, reported the plasma VLDL particle diameter after Triton injection. Feeding a fructose diet resulted in a higher percentage of TG in nascent VLDL compared with feeding a

starch or chow diet. These results suggest that a lipid-rich, second-step particle might be added to an apoB-containing first-step particle to form a VLDL particle. Different assembly precursors led to production of different nascent VLDL. The interaction of lipid and protein during the assembly of the two particles assembly may result in the changes in composition and size. Such an interaction could explain why there was no significant difference in the size of nascent VLDL isolated from animals in the three dietary groups.

The study on VLDL secretion rate based on individual VLDL components clearly indicates that hepatic secretion of VLDL-TG, VLDL-CE and VLDL-PL were significantly elevated in fructose-fed hamsters as compared with chow- or starch-fed hamsters. Fructose feeding caused greater secretion rates of VLDL-Fch and VLDL-PRO compared with chow feeding, however, the differences were not statistically significant. This indicates that fructose feeding induces the increase in secretion rate for all VLDL components, but that the increase in secretion rate for individual components differs. Fructose feeding induces insulin resistance in hamster (see Chapter III). Hepatic overproduction of VLDL in the metabolic state may result from direct hepatic effects of insulin and the effects of the increased availability of free fatty acids for certain lipid synthesis (Lewis et al., 1995). The increased concentration of plasma free fatty acids in fructose-fed animals suggests that the increased flux of free fatty acids into the liver may contribute to overproduction of VLDL-TG, VLDL-CE and VLDL-PL (see Chapter III). Regulation of apoB-LP assembly and secretion mainly depends on the availability of lipid (Dixon and Ginsberg, 1993). Overproduction of hepatic lipid may result in reduced

the degradation of apoB (Zhou et al., 1995) and an increased expression of MTP (Taghibiglou et al., 2000a), which can in turn facilitate the assembly and secretion of apoB-LP.

Interestingly, in hamster, the size of nascent VLDL was smaller than that of circulating VLDL although the concentration of VLDL-TG in nascent VLDL was 2-fold greater than that in circulating VLDL, which also occurs in hens from immature to laying (Griffin et al., 1982). However, this did not occur in overfed laying hens (Walzem et al., 1994). In hamsters, the concentrations of both VLDL-TG and VLDL-PL in nascent VLDL were significantly higher than that in circulating VLDL, and the increased rate of VLDL-PL was greater than that of VLDL-TG. Overfeeding of laying hens led to accumulation of TG (concentration and composition) but not PL (Walzem et al., 1994), thus overfeeding can increase hen VLDL particle size. VLDL metabolism appears to respond differently in the metabolic state of overproduction of TG and may be due to species differences. The species difference may also explain why hens do not have insulin resistance in spite of having a high concentration of TG.

The present study provides the first characterization of nascent apoB-LP and apoB-LP precursors from rough ER in hamster. The data indicate that apoB-containing apoB-LP precursor and lipid-rich apoB-deficient apoB-LP precursor are synthesized independently by liver. At the smooth surface ends of the rough ER, these two precursors join and convert to nascent apoB-LP. The nascent apoB-LP modified by further addition of lipid during the secretion process, but the source of lipid and the mechanism by which the lipid is added to the particles are not clear. This study also

showed that diets affected apoB-LP precursor formation and assembly, and apoB-LP secretion. Further work is necessary to delineate the steps in apoB-LP secretion and to define the interaction of nascent apoB-LP and lipid in the secretion process.

CHAPTER V

SUMMARY AND CONCLUSIONS

Summary of Research Findings

Understanding of the pathobiological mechanisms of atherosclerotic cardiovascular disease is necessary to effectively prevent and treat ASCVD. Elevated concentrations of circulating apoB-LP are strongly associated with the risk of ASCVD. In this dissertation research, the author investigated three aspects in pathobiological mechanisms of ASCVD related to apoB-LP: 1). the role of several genetic components that impinge on ASCVD through use of a statistical model; 2). the role of certain dietary components as metabolic modifiers of the concentrations and physical properties (i.e., mass, particle diameter and composition) of circulating apoB-LP in hamsters; and 3). the role of apoB-LP assembly and secretion in nutritionally induced changes to the physical properties of circulating apoB-LP.

Selective delays in apolipoprotein B-containing lipoprotein clearance affect circulating particle diameter distribution and plaque formation

In humans, lipoprotein profiles differ with regards to concentrations of individual particle type that vary in pro-atherogenicity. Such variation is the result of differences in genotype and environment. Lipoprotein phenotypes produce a number of different pro-athergenicities and antiatherogenicity due to genetic drivers. Numerous investigators have studied the relationship among apoB-LP physical properties and atherogenesis in transgenic and knockout mouse models. In these models, tests have been designated to isolate single factors whereas observed variables have numerous factors for which risk

must be assayed. The uniqueness of the approach is the availability and use of numerous transgenic models simultaneously to verify the mechanistic drivers of phenotypes observed in free populations. Little is known whether complex mixtures of apoB-LP types found in humans occur systemically in these same mouse models. Results of the studies described in Chapter II demonstrate for the first time the associations of apoB concentration, genotype, apoB-LP particle diameter, and plasma cholesterol concentration with arterial plaque formation in transgenic mice. The major findings are summarized as follows:

1. Plasma total apoB concentration explained 30.8% of arterial lesions when adjusted for delayed particle clearance, while only 15.3% of arterial lesions without the adjustment. Moreover, in each model that included apoB, failure to adjust for delay in particle clearance reduced the ability of themodel to account for plaque formation. These results indicate that delayed clearance is a significant driver in the formation of atherogenic lipoprotein species.
2. In the mouse population, apoB-LP particle diameter became smaller when particle clearance was delayed. Correlation analysis identified diameter-specific apoB-LP subpopulations that were significantly related to plaque formation in either a positive or negative fashion.. This is the first time a subpopulation of apoB-LP particles has been identified that negatively associated with plaque formation..
3. Genotype alone can explain 87% of the arterial lesions that developed. Adding plasma cholesterol concentration, apoB concentration, and particle diameter did

not significantly change the explanation for arterial lesions. Plasma total cholesterol alone explained 18% of arterial plaque formation, while genotype explained 74% of the variation in total plasma cholesterol that had little relationship to apoB-LP diameter. These results clearly indicate that genotype probably dictated the metabolic conditions under which apoB-LP accumulation occurs critically influences arterial lesion formation in this transgenic model.

Effects of high-carbohydrate diets on physical properties of plasma lipoproteins in hamsters

High-carbohydrate diets can affect lipoprotein metabolism, and induce an atherogenic lipoprotein profile (ALP) and insulin resistance that are associated with atherosclerosis in humans and animals. The hamster fed a fructose-enriched diet is a widely used model in studies of ALP, insulin resistance. However, little is known about the changes in physical properties of lipoprotein that occur under these metabolic conditions in hamster. Results of the studies described in Chapter III show for the first time features of the physical properties of plasma lipoprotein in hamsters fed high-carbohydrate diets. The major findings from this study are summarized as follows:

1. Fructose feeding significantly increased hamster VLDL lipoprotein mass and decreased the percentage of VLDL-PRO. VLDL particle diameter increased in the 20-60th population percentiles in hamsters fed a fructose-enriched diet. This is the first report of large, TG-rich plasma VLDL in hamsters fed this type of

diet. The large, TG-rich plasma VLDL may be the result of limited lipolysis prior to the conversion from VLDL to LDL and/or altered assembly of VLDL.

2. Fructose feeding significantly increased plasma LDL lipoprotein mass and the concentrations of LDL-Fch and LDL-PL. The fructose-fed group of hamsters had a significant increase in LDL-TG at the expense of a reduction in LDL-CE, while the starch-fed group had a significant increase in LDL-CE. LDL particle diameter was smaller in fructose-fed hamsters than in starch-fed hamsters. These results demonstrate for the first time that fructose feeding induces small, TG-rich LDL, while starch feeding produces large, CE-rich LDL in hamsters.
3. ApoB-containing lipoproteins exhibit similar physical properties in fructose-fed hamsters and in humans with an atherogenic lipoprotein phenotype.
4. Increased plasma HDL lipoprotein mass and HDL-cholesterol during fructose and starch feeding indicate that hamsters have a different response to simple carbohydrates than that of other animal species. It may be possible to develop an intervention to increase HDL in insulin resistant humans with ALP.

Dietary effects on the assembly and secretion of apoB-containing lipoproteins in hamsters

The profiles of circulating lipoproteins result from the interactions of several factors, including the physical properties of nascent lipoproteins. Dietary effects on the physical properties of circulating lipoproteins were presented in Chapter III. Chapter IV presented a study of whether the changes in the physical properties of circulating lipoproteins arise from changes in the physical properties of nascent lipoprotein assembly intermediates

during apoB-LP assembly and/or during their secretion. This study was pursued via isolating lipoprotein assembly intermediate particles from rough ER and measurement of plasma VLDL secretion rates and particle physical properties after Triton injection. The major findings from this study are summarized as follows:

1. Two types of lipoprotein assembly intermediate particles were isolated from rough ER. One set of particles was TG-rich, apoB-deficient and VLDL-sized, putative second-step, The other type of particle was small, lipid-poor, and apoB-containing, putative first-step. The composition of nascent VLDL was between that of second-step particle and that of first-step particle. These results suggest that two sets of particles are independently synthesized in liver then and assemble to produce a nascent VLDL particle. The odds further support the "two-step" theory of apoB-LP assembly.
2. This is first report that the diameter of first-step particles in fructose-fed hamsters is larger than that of either chow-fed or starch-fed animals. Increased diameter in first-step particles suggests there is decreased chance for apoB degradation, which is physical basis for apoB oversecretion.
3. The concentrations of the lipoprotein mass and individual components of both second-step particles and first-step particles recovered from liver were higher in fructose-fed than in either chow-fed or starch-fed hamsters. The composition and size of the two particle types were different among the three dietary groups. Changes observed in lipoprotein assembly intermediate particles are consistent with those in plasma VLDL. These data demonstrate for the first time that diets

do affect the formation of lipoprotein assembly precursors and that changes in the physical properties of circulating lipoproteins can stem from the changes in the physical properties of lipoprotein assembly precursors.

4. VLDL from post-Triton plasma differed in both circulating VLDL composition (low TG and high PRO) and diameter. The fructose-fed group of hamsters had a greater secretion rate of VLDL components in comparison with the other groups. These findings suggest that lipid is added to the nascent VLDL and the nascent VLDL is further modified during the secretory pathway. For the first time, fructose feeding of hamsters was shown to increase the secretion rates not only of VLDL-TG, and VLDL-apoB but also of VLDL-CE, VLDL-Fch, and VLDL-PL.

Conclusions

The metabolism and physical properties of apoB-containing lipoproteins play an important role in the atherogenicity of apoB-LP. The results of this research show that both genetic factors and dietary factors can affect the metabolism and physical properties of apoB-LP. Genetic factors are a major determinant of metabolism in such a complex transgenic model. Metabolic conditions under which apoB-LP accumulate critically influence the physical properties of apoB-LP and further enhance arterial lesion formation. Diet is the other important factor that determines the metabolism and physical properties of lipoproteins. Diet can change the physical properties of apoB-LP during the processes of assembly and secretion, and subsequently alter the physical properties and further metabolism of circulating apoB-LP. The completion of the dissertation research may have important implications for explaining the mechanism of atherosclerosis and

identifying the targets of intervention against which food and food ingredients could regulate lipid and lipoprotein metabolism to improve health.

LITERATURE CITED

Alexander, C. A., Hamilton, R. L., & Havel, R. J. (1976) Subcellular localization of B apoprotein of plasma lipoproteins in rat liver. J. Cell Biol. 69: 241-263.

Anber, V., Griffin, B. A., McConnell, M., Packard, C. J., & Shepherd, J. (1996) Influence of plasma lipid and LDL-subfraction profile on the interaction between low density lipoprotein with human arterial wall proteoglycans. Atherosclerosis 124: 261-271.

Appel, B., & Fried, S. K. (1992) Effects of insulin and dexamethasone on lipoprotein lipase in human adipose tissue. Am. J. Physiol. 262: E695-699.

Arbeeny, C. M., Meyers, D. S., Bergquist, K. E., & Gregg, R. E. (1992) Inhibition of fatty acid synthesis decreases very low density lipoprotein secretion in the hamster. J. Lipid Res. 33: 843-851.

Assmann, G., Schulte, H., von Eckardstein, A., & Huang, Y. (1996) High-density lipoprotein cholesterol as a predictor of coronary heart disease risk. The PROCAM experience and pathophysiological implications for reverse cholesterol transport. Atherosclerosis 124 Suppl: S11-20.

Atzel, A., & Wetterau, J. R. (1993) Mechanism of microsomal triglyceride transfer protein catalyzed lipid transport. Biochemistry (Mosc). 32: 10444-10450.

Austin, M. A., Breslow, J. L., Hennekens, C. H., Buring, J. E., Willett, W. C., & Krauss, R. M. (1988) Low-density lipoprotein subclass patterns and risk of myocardial infarction. JAMA 260: 1917-1921.

Austin, M. A., Hokanson, J. E., & Edwards, K. L. (1998) Hypertriglyceridemia as a cardiovascular risk factor. Am. J. Cardiol. 81: 7B-12B.

Austin, M. A., King, M. C., Vranizan, K. M., & Krauss, R. M. (1990) Atherogenic lipoprotein phenotype. A proposed genetic marker for coronary heart disease risk. Circulation 82: 495-506.

Bannykh, S. I., & Balch, W. E. (1997) Membrane dynamics at the endoplasmic reticulum-Golgi interface. J. Cell Biol. 138: 1-4.

Bantle, J. P., Raatz, S. K., Thomas, W., & Georgopoulos, A. (2000) Effects of dietary fructose on plasma lipids in healthy subjects. Am. J. Clin. Nutr. 72: 1128-1134.

Barter, P. J., & Rye, K. A. (1996) Molecular mechanisms of reverse cholesterol transport. Curr. Opin. Lipidol. 7: 82-87.

Behall, K. M., & Howe, J. C. (1995) Effect of long-term consumption of amylose vs amylopectin starch on metabolic variables in human subjects. Am. J. of Clin. Nutr. 61: 334-340.

Bell-Quint, J., & Forte, T. (1981) Time-related changes in the synthesis and secretion of very low density, low density and high density lipoproteins by cultured rat hepatocytes. Biochim. Biophys. Acta 663: 83-98.

Bennett, A. J., Bruce, J. S., Salter, A. M., White, D. A., & Billett, M. A. (1996) Hepatic microsomal triglyceride transfer protein messenger RNA concentrations are increased by dietary cholesterol in hamsters. FEBS Lett. 394: 247-250.

Bergeron, N., Kotite, L., & Havel, R. J. (1996) Simultaneous quantification of apolipoproteins B-100, B-48, and E separated by SDS-PAGE. Methods Enzymol. 263: 82-94.

Berriot-Varoqueaux, N., Aggerbeck, L. P., Samson-Bouma, M., & Wetterau, J. R. (2000) The role of the microsomal triglygeride transfer protein in abetalipoproteinemia. Annu. Rev. Nutr. 20: 663-697.

Betteridge, D. J., Illingworth, D. R., & Shepherd, J. (1999) Lipoproteins in Health and Disease. Arnold, London, UK.

Boogaerts, J. R., Malone-McNeal, M., Archambault-Schexnayder, J., & Davis, R. A. (1984) Dietary carbohydrate induces lipogenesis and very-low-density lipoprotein synthesis. Am. J. Physiol. 246: E77-83.

Boren, J., Graham, L., Wettesten, M., Scott, J., White, A., & Olofsson, S. O. (1992) The assembly and secretion of ApoB 100-containing lipoproteins in Hep G2 cells. ApoB 100 is cotranslationally integrated into lipoproteins. J. Biol. Chem. 267: 9858-9867.

Boren, J., Rustaeus, S., & Olofsson, S. O. (1994) Studies on the assembly of apolipoprotein B-100- and B-48-containing very low density lipoproteins in McA-RH7777 cells. J. Biol. Chem. 269: 25879-25888.

Braun, J. E., & Severson, D. L. (1992) Regulation of the synthesis, processing and translocation of lipoprotein lipase. Biochem. J. 287: 337-347.

Braunwald, E. (1997) Shattuck lecture--cardiovascular medicine at the turn of the millennium: triumphs, concerns, and opportunities. N. Engl. J. Med. 337: 1360-1369.

Bravo, E., Cantafora, A., Calccabrin, i. A., & Ortu, G. (1994) Why prefer the Golden Syrian hamster (*Mesocritus auratus*) to the Wistar rat in experimental studies on plasma lipoprotein metabolism? Comp. Biochem. Physiol. 107: 347-355.

Brown, M. S., & Goldstein, J. L. (1997) The SREBP pathway: regulation of cholesterol metabolism by proteolysis of a membrane-bound transcription factor. Cell 89: 331-340.

Bruce, C., Chouinard, R. A., Jr., & Tall, A. R. (1998) Plasma lipid transfer proteins, high-density lipoproteins, and reverse cholesterol transport. Annu. Rev. Nutr. 18: 297-330.

Calabresi, L., Franceschini, G., Sirtori, C. R., De Palma, A., Saresella, M., Ferrante, P., & Taramelli, D. (1997) Inhibition of VCAM-1 expression in endothelial cells by reconstituted high density lipoproteins. Biochem. Biophys. Res. Commun. 238: 61-65.

Callow, M. J., Stoltzfus, L. J., Lawn, R. M., & Rubin, E. M. (1994) Expression of human apolipoprotein B and assembly of lipoprotein(a) in transgenic mice. Proc. Natl. Acad. Sci. U. S. A. 91: 2130-2134.

Callow, M. J., Verstuyft, J., Tangirala, R., Palinski, W., & Rubin, E. M. (1995) Atherogenesis in transgenic mice with human apolipoprotein B and lipoprotein (a). J. Clin. Invest. 96: 1639-1646.

Campos, H., Moye, L. A., Glasser, S. P., Stampfer, M. J., & Sacks, F. M. (2002) Low-density lipoprotein size, pravastatin treatment, and coronary events. JAMA 286: 1468-1474.

Campos, H., Willett, W. C., Peterson, R. M., Siles, X., Bailey, S. M., Wilson, P. W., Posner, B. M., Ordovas, J. M., & Schaefer, E. J. (1991) Nutrient intake comparisons between Framingham and rural and Urban Puriscal, Costa Rica. Associations with lipoproteins, apolipoproteins, and low density lipoprotein particle size. Arterioscler. Thromb. 11: 1089-1099.

Chait, A., Brazg, R. L., Tribble, D. L., & Krauss, R. M. (1993) Susceptibility of small, dense, low-density lipoproteins to oxidative modification in subjects with the atherogenic lipoprotein phenotype, pattern B. Am. J. Med. 94: 350-356.

Chapman, M. J., Goldstein, S., Lagrange, D., & Laplaud, P. M. (1981) A density gradient ultracentrifugal procedure for the isolation of the major lipoprotein classes from human serum. J. Lipid Res. 22: 339-358.

Chapman, M. J., Guerin, M., & Bruckert, E. (1998) Atherogenic, dense low-density lipoproteins. Pathophysiology and new therapeutic approaches. Eur. Heart J. 19 Suppl A: A24-30.

Chen, Y. D., Coulston, A. M., Zhou, M. Y., Hollenbeck, C. B., & Reaven, G. M. (1995) Why do low-fat high-carbohydrate diets accentuate postprandial lipemia in patients with NIDDM? Diabetes Care 18: 10-16.

Cianflone, K., Dahan, S., Monge, J. C., & Sniderman, A. D. (1992) Pathogenesis of carbohydrate-induced hypertriglyceridemia using HepG2 cells as a model system. Arterioscler. Thromb. 12: 271-277.

Cianflone, K. M., Yasruel, Z., Rodriguez, M. A., Vas, D., & Sniderman, A. D. (1990) Regulation of apoB secretion from HepG2 cells: evidence for a critical role for cholesteryl ester synthesis in the response to a fatty acid challenge. J. Lipid Res. 31: 2045-2055.

Cockerill, G. W., Rye, K. A., Gamble, J. R., Vadas, M. A., & Barter, P. J. (1995) High-density lipoproteins inhibit cytokine-induced expression of endothelial cell adhesion molecules. Arterioscler. Thromb. Vasc. Biol. 15: 1987-1994.

Connor, W. E., & Connor, S. L. (1997) Should a low-fat, high-carbohydrate diet be recommended for everyone? The case for a low-fat, high-carbohydrate diet. N. Engl. J. Med. 337: 562-563.

Criqui, M. H., Heiss, G., Cohn, R., Cowan, L. D., Suchindran, C. M., Bangdiwala, S., Kritchevsky, S., Jacobs, D. R., Jr., O'Grady, H. K., & Davis, C. E. (1993) Plasma triglyceride level and mortality from coronary heart disease. N. Engl. J. Med. 328: 1220-1225.

Dashti, N. (1992) The effect of low density lipoproteins, cholesterol, and 25-hydroxycholesterol on apolipoprotein B gene expression in HepG2 cells. J. Biol. Chem. 267: 7160-7169.

Dashti, N., Williams, D. L., & Alaupovic, P. (1989) Effects of oleate and insulin on the production rates and cellular mRNA concentrations of apolipoproteins in HepG2 cells. J. Lipid Res. 30: 1365-1373.

Davidson, N. O., Anant, S., & MacGinnitie, A. J. (1995) Apolipoprotein B messenger RNA editing: insights into the molecular regulation of post-transcriptional cytidine deamination. Curr. Opin. Lipidol. 6: 70-74.

Davis, R. A. (1999) Cell and molecular biology of the assembly and secretion of apolipoprotein B-containing lipoproteins by the liver. Biochim. Biophys. Acta 1440: 1-31.

Davis, R. A., & Boogaerts, J. R. (1982) Intrahepatic assembly of very low density lipoproteins. Effect of fatty acids on triacylglycerol and apolipoprotein synthesis. J. Biol. Chem. 257: 10908-10913.

deDuve, C., Pressman, B. C., Gianetto, R., Wattiaux, R., & F., A. (1955) Tissue fractionation studies. 6. Intracellular distribution patterns of enzymes in rat liver tissue. Biochem J. 60: 604-617.

Demant, T., & Packard, C. (1998) In vivo studies of VLDL metabolism and LDL heterogeneity. Eur. Heart J. 19 Suppl H: H7-10.

Dichek, H. L., Brecht, W., Fan, J., Ji, Z. S., McCormick, S. P., Akeefe, H., Conzo, L., Sanan, D. A., Weisgraber, K. H., Young, S. G., Taylor, J. M., & Mahley, R. W. (1998) Overexpression of hepatic lipase in transgenic mice decreases apolipoprotein B-containing and high density lipoproteins. Evidence that hepatic lipase acts as a ligand for lipoprotein uptake. J. Biol. Chem. 273: 1896-1903.

Dietschy, J. M., Turley, S. D., & Spady, D. K. (1993) Role of liver in the maintenance of cholesterol and low density lipoprotein homeostasis in different animal species, including humans. J. Lipid Res. 34: 1637-1659.

Dixon, J. L., & Ginsberg, H. N. (1993) Regulation of hepatic secretion of apolipoprotein B-containing lipoproteins: information obtained from cultured liver cells. J. Lipid Res. 34: 167-179.

Donaldson, J. G., Finazzi, D., & Klausner, R. D. (1992) Brefeldin A inhibits Golgi membrane-catalysed exchange of guanine nucleotide onto ARF protein. Nature 360: 350-352.

Dreon, D. M., Fernstrom, H. A., Miller, B., & Krauss, R. M. (1994) Low-density lipoprotein subclass patterns and lipoprotein response to a reduced-fat diet in men. FASEB J. 8: 121-126.

Dreon, D. M., Fernstrom, H. A., Williams, P. T., & Krauss, R. M. (1997) LDL subclass patterns and lipoprotein response to a low-fat, high- carbohydrate diet in women. Arterioscler. Thromb. Vasc. Biol. 17: 707-714.

Edwards, P. A., Tabor, D., Kast, H. R., & Venkateswaran, A. (2000) Regulation of gene expression by SREBP and SCAP. Biochim. Biophys. Acta 1529: 103-113.

Eisenberg, S., Bilheimer, D. W., Levy, R. I., & Lindgren, F. T. (1973) On the metabolic conversion of human plasma very low density lipoprotein to low density lipoprotein. Biochim. Biophys. Acta 326: 361-377.

Ellsworth, J. L., Erickson, S. K., & Cooper, A. D. (1986) Very low and low density lipoprotein synthesis and secretion by the human hepatoma cell line Hep-G2: effects of free fatty acid. J. Lipid Res. 27: 858-874.

Elphick, M. C. (1968) Modified colorimetric ultramicro method for estimating Nefa in serum. J. Clin. Pathol. 21: 567-570.

Emmelot, P., Bos, C. J., Benedetti, E. L., & Rumke, P. (1964) Studies on plasma membranes. 1. Chemical composition and enzyme content of plasma membranes isolated from rat liver. Biochim. Biophys. Acta 90: 126-145.

Erickson, S. K., Lear, S. R., Barker, M. E., & Musliner, T. A. (1990) Regulation of cholesterol metabolism in the ethionine-induced premalignant rat liver. J. Lipid Res. 31: 933-945.

Farese, R. V., Jr., Cases, S., Ruland, S. L., Kayden, H. J., Wong, J. S., Young, S. G., & Hamilton, R. L. (1996a) A novel function for apolipoprotein B: lipoprotein synthesis in the yolk sac is critical for maternal-fetal lipid transport in mice. J. Lipid Res. 37: 347-360.

Farese, R. V., Jr., Ruland, S. L., Flynn, L. M., Stokowski, R. P., & Young, S. G. (1995) Knockout of the mouse apolipoprotein B gene results in embryonic lethality in homozygotes and protection against diet-induced hypercholesterolemia in heterozygotes. Proc. Natl. Acad. Sci. U. S. A. 92: 1774-1778.

Farese, R. V., Jr., Veniant, M. M., Cham, C. M., Flynn, L. M., Pierotti, V., Loring, J. F., Traber, M., Ruland, S., Stokowski, R. S., Huszar, D., & Young, S. G. (1996b) Phenotypic analysis of mice expressing exclusively apolipoprotein B48 or apolipoprotein B100. Proc. Natl. Acad. Sci. U.S.A. 93: 6393-6398.

Farquhar, J. W., Frank, A., Gross, R. C., & Reaven, G. M. (1966) Glucose, insulin, and triglyceride responses to high and low carbohydrate diets in man. J. Clin. Invest. 45: 1648-1656.

Feingold, K. R., Grunfeld, C., Pang, M., Doerrler, W., & Krauss, R. M. (1992) LDL subclass phenotypes and triglyceride metabolism in non-insulin- dependent diabetes. Arterioscler. Thromb. 12: 1496-1502.

Feingold, K. R., Krauss, R. M., Pang, M., Doerrler, W., Jensen, P., & Grunfeld, C. (1993) The hypertriglyceridemia of acquired immunodeficiency syndrome is associated with an increased prevalence of low density lipoprotein subclass pattern B. J. Clin. Endocrinol. Metab. 76: 1423-1427.

Fisher, E. A., Pan, M., Chen, X., Wu, X., Wang, H., Jamil, H., Sparks, J. D., & Williams, K. J. (2001) The triple threat to nascent apolipoprotein B. Evidence for multiple, distinct degradative pathways. J. Biol. Chem. 276: 27855-27863.

Fisher, E. A., Zhou, M., Mitchell, D. M., Wu, X., Omura, S., Wang, H., Goldberg, A. L., & Ginsberg, H. N. (1997) The degradation of apolipoprotein B100 is mediated by the ubiquitin- proteasome pathway and involves heat shock protein 70. J. Biol. Chem. 272: 20427-20434.

Fisher, R. M., Coppack, S. W., Gibbons, G. F., & Frayn, K. N. (1993) Post-prandial VLDL subfraction metabolism in normal and obese subjects. Int. J. Obes. Relat. Metab. Disord. 17: 263-269.

Fisher, W. R. (1983) Heterogeneity of plasma low density lipoproteins manifestations of the physiologic phenomenon in man. Metabolism: Clinical & Experimental 32:283-291.

Flier, J. S., & Hollenberg, A. N. (1999) ADD-1 provides major new insight into the mechanism of insulin action. Proc. Natl. Acad. Sci. U.S.A. 96: 14191-14192.

Ford, S., Jr., Bozian, R. C., & Knowles, H. C., Jr. (1968) Interactions of obesity, and glucose and insulin levels in hypertriglyceridemia. Am. J. Clin. Nutr. 21: 904-910.

Foretz, M., Guichard, C., Ferre, P., Foufelle, F. (1999a) Sterol regulatory element binding protein-1c is a major mediator of insulin action on the hepatic expression of glucokinase and lipogenesis- related genes. Proc. Natl. Acad. Sci. U.S.A. 96: 12737-12742.

Foretz, M., Pacot, C., Dugail, I., Lemarchand, P., Guichard, C., Le Liepvre, X., Berthelier-Lubrano, C., Spiegelman, B., Kim, J. B., Ferre, P., & Foufelle, F. (1999b) ADD1/SREBP-1c is required in the activation of hepatic lipogenic gene expression by glucose. Mol. Cell. Biol. 19: 3760-3768.

Francone, O. L., Haghpassand, M., Bennett, J. A., Royer, L., McNeish, J. (1997) Expression of human lecithin:cholesterol acyltransferase in transgenic mice: effects on cholesterol efflux, esterification, and transport. J. Lipid Res. 38: 813-822.

Frayn, K. N., & Kingman, S. M. (1995) Dietary sugars and lipid metabolism in humans. Am. J. Clin. Nutr. 62: 250S-261S.

Galeano, N. F., Milne, R., Marcel, Y. L., Walsh, M. T., Levy, E., Ngu'yen, T. D., Gleeson, A., Arad, Y., Witte, L., al-Haideri, M. (1994) Apoprotein B structure and receptor recognition of triglyceride-rich low density lipoprotein (LDL) is modified in small LDL but not in triglyceride-rich LDL of normal size. J. Biol. Chem. 269: 511-519.

Garg, R., Kumbkarni, Y., Aljada, A., Mohanty, P., Ghanim, H., Hamouda, W., & Dandona, P. (2000) Troglitazone reduces reactive oxygen species generation by leukocytes and lipid peroxidation and improves flow-mediated vasodilatation in obese subjects. Hypertension 36: 430-435.

Gaw, A., Packard, C. J., Lindsay, G. M., Griffin, B. A., Caslake, M. J., Lorimer, A. R., & Shepherd, J. (1995) Overproduction of small very low density lipoproteins (Sf 20-60) in moderate hypercholesterolemia: relationships between apolipoprotein B kinetics and plasma lipoproteins. J. Lipid Res. 36: 158-171.

Ginsberg, H. N. (2000) Insulin resistance and cardiovascular disease. J. Clin. Invest. 106: 453-458.

Ginsberg, H. N., & Huang, L. S. (2000) The insulin resistance syndrome: impact on lipoprotein metabolism and atherothrombosis. J. Cardiovasc. Risk 7: 325-331.

Ginsberg, H. N., Le, N. A., Melish, J., Steinberg, D., & Brown, W. V. (1981) Effect of a high carbohydrate diet on apoprotein-B catabolism in man. Metabolism. 30: 347-353.

Glaumann, H., Bergstrand, A., & Ericsson, J. L. (1975) Studies on the synthesis and intracellular transport of lipoprotein particles in rat liver. J. Cell. Biol. 64: 356-377.

Glickman, R. M., Rogers, M., & Glickman, J. N. (1986) Apolipoprotein B synthesis by human liver and intestine in vitro. Proc. Natl. Acad. Sci. U.S.A. 83: 5296-5300.

Gofman, J. W., Lindgren, F., Elliott, H., Mantz, W., Hewitt, J., Strisower, B., & Herring, V. (1950) The role of lipids and lipoproteins in atherosclerosis. Science 111: 166-186.

Goldstein, J. L., Brown, M. S., & Stone, N. J. (1977) Genetics of the LDL receptor: evidence that the mutations affecting binding and internalization are allelic. Cell 12: 629-641.

Gordon, D. (1999) Epidemiology of Lipoproteins. In: Lipoproteins in Health and Disease (Betteridge, D., Illingworth, D., & Shepherd, J. eds.), pp.587-595. Arnold, New York, NY.

Gordon, D. A., Jamil, H., Gregg, R. E., Olofsson, S. O., & Boren, J. (1996) Inhibition of the microsomal triglyceride transfer protein blocks the first step of

apolipoprotein B lipoprotein assembly but not the addition of bulk core lipids in the second step. J. Biol. Chem. 271: 33047-33053.

Gordon, D. A., Jamil, H., Sharp, D., Mullaney, D., Yao, Z., Gregg, R. E., & Wetterau, J. (1994) Secretion of apolipoprotein B-containing lipoproteins from HeLa cells is dependent on expression of the microsomal triglyceride transfer protein and is regulated by lipid availability. Proc. Natl. Acad. Sci. U.S.A. 91: 7628-7632.

Gordon, D. J., Knoke, J., Probstfield, J. L., Superko, R., & Tyroler, H. A. (1986) High-density lipoprotein cholesterol and coronary heart disease in hypercholesterolemic men: the Lipid Research Clinics Coronary Primary Prevention Trial. Circulation 74: 1217-1225.

Gordon, D. J., Probstfield, J. L., Garrison, R. J., Neaton, J. D., Castelli, W. P., Knoke, J. D., Jacobs, D. R., Jr., Bangdiwala, S., & Tyroler, H. A. (1989) High-density lipoprotein cholesterol and cardiovascular disease. Four prospective American studies. Circulation 79: 8-15.

Gordon, D. J., & Rifkind, B. M. (1989) High-density lipoprotein--the clinical implications of recent studies. N. Engl. J. Med. 321: 1311-1316.

Gordon, T., Castelli, W. P., Hjortland, M. C., Kannel, W. B., & Dawber, T. R. (1977) High density lipoprotein as a protective factor against coronary heart disease. The Framingham Study. Am. J. Med. 62: 707-714.

Goulinet, S., & Chapman, M. J. (1993) Plasma lipoproteins in the golden Syrian hamster (*Mesocricetus auratus*): heterogeneity of apoB- and apoA-I-containing particles. J. Lipid Res. 34: 943-959.

Gowri, M. S., Van der Westhuyzen, D. R., Bridges, S. R., & Anderson, J. W. (1999) Decreased protection by HDL from poorly controlled type 2 diabetic subjects against LDL oxidation may be due to the abnormal composition of HDL. Arterioscler. Thromb. Vasc. Biol. 19: 2226-2233.

Granner, D., & Pilkis, S. (1990) The genes of hepatic glucose metabolism. J. Biol. Chem. 265: 10173-10176.

Greeve, J., Altkemper, I., Dieterich, J. H., Greten, H., & Windler, E. (1993) Apolipoprotein B mRNA editing in 12 different mammalian species: hepatic expression is reflected in low concentrations of apoB- containing plasma lipoproteins. J. Lipid Res. 34: 1367-1383.

Griffin, B. A., Freeman, D. J., Tait, G. W., Thomson, J., Caslake, M. J., Packard, C. J., & Shepherd, J. (1994) Role of plasma triglyceride in the regulation of plasma low density lipoprotein (LDL) subfractions: relative contribution of small, dense LDL to coronary heart disease risk. Atherosclerosis 106: 241-253.

Griffin, H., Grant, G., & Perry, M. (1982) Hydrolysis of plasma triacylglycerol-rich lipoproteins from immature and laying hens (*Gallus domesticus*) by lipoprotein lipase in vitro. Biochem. J. 206: 647-654.

Grundy, S. M. (1986) Comparison of monounsaturated fatty acids and carbohydrates for lowering plasma cholesterol. N. Engl. J. Med. 314: 745-748.

Grundy, S. M. (1997) Small LDL, atherogenic dyslipidemia, and the metabolic syndrome. Circulation 95: 1-4.

Grundy, S. M., Nix, D., Whelan, M. F., & Franklin, L. (1986) Comparison of three cholesterol-lowering diets in normolipidemic men. JAMA. 256: 2351-2355.

Gurr, M. I., Harwood, J. L., & Frayn, K. N. (2002) Lipid Biochemistry. Blackwell Science, Oxford, UK.

Hamilton, R. L., Moorehouse, A., Lear, S. R., Wong, J. S., & Erickson, S. K. (1999) A rapid calcium precipitation method of recovering large amounts of highly pure hepatocyte rough endoplasmic reticulum. J. Lipid Res. 40: 1140-1147.

Hamilton, R. L., Wong, J. S., Cham, C. M., Nielsen, L. B., & Young, S. G. (1998) Chylomicron-sized lipid particles are formed in the setting of apolipoprotein B deficiency. J. Lipid Res. 39: 1543-1557.

Harris, S. G., Sabio, I., Mayer, E., Steinberg, M. F., Backus, J. W., Sparks, J. D., Sparks, C. E., & Smith, H. C. (1993) Extract-specific heterogeneity in high-order complexes containing apolipoprotein B mRNA editing activity and RNA-binding proteins. J. Biol. Chem. 268: 7382-7392.

Hatch, F. T., Abell, L. L., & Kendall, F. E. (1955) Effects of restriction of dietary fat and cholesterol upon serum lipids and lipoproteins in patients with hypertension. Am. J. Med. 19: 48-60.

Heinecke, J. W., Kawamura, M., Suzuki, L., & Chait, A. (1993) Oxidation of low density lipoprotein by thiols: superoxide-dependent and -independent mechanisms. J. Lipid Res. 34: 2051-2061.

Hellerstein, M. K., Christiansen, M., Kaempfer, S., Kletke, C., Wu, K., Reid, J. S., Mulligan, K., Hellerstein, N. S., & Shackleton, C. H. (1991) Measurement of de novo hepatic lipogenesis in humans using stable isotopes. J. Clin. Invest. 87: 1841-1852.

Hennessy, L. K., Osada, J., Ordovas, J. M., Nicolosi, R. J., Stucchi, A. F., Brousseau, M. E., & Schaefer, E. J. (1992) Effects of dietary fats and cholesterol on liver lipid content and hepatic apolipoprotein A-I, B, and E and LDL receptor mRNA levels in cebus monkeys. J. Lipid Res. 33: 351-360.

Henriksen, T., Mahoney, E. M., & Steinberg, D. (1981a) Enhanced macrophage degradation of low density lipoprotein previously incubated with cultured endothelial cells: recognition by receptors for acetylated low density lipoproteins. Proc. Natl. Acad. Sci. U. S. A. 78: 6499-6503.

Henriksen, T., Mahoney, E. M., & Steinberg, D. (1981b) Enhanced macrophage degradation of low density lipoprotein previously incubated with cultured endothelial cells: recognition by receptors for acetylated low density lipoproteins. Proc. Natl. Acad. Sci. U. S. A. 78: 6499-6503.

Hodis, H. N., Mack, W. J., Krauss, R. M., & Alaupovic, P. (1999) Pathophysiology of triglyceride-rich lipoproteins in atherothrombosis: clinical aspects. Clin. Cardiol. 22: II15-20.

Hokanson, J. E., & Austin, M. A. (1996) Plasma triglyceride level is a risk factor for cardiovascular disease independent of high-density lipoprotein cholesterol level: a meta- analysis of population-based prospective studies. J. Cardiovasc. Risk 3: 213-219.

Holt, P. R., & Dominguez, A. A. (1980) Triton-induced hyperlipidemia: a model for studies of intestinal lipoprotein production. Am. J. Physiol. 238: G453-457.

Horton, J. D., Bashmakov, Y., Shimomura, I., & Shimano, H. (1998a) Regulation of sterol regulatory element binding proteins in livers of fasted and refed mice. Proc. Natl. Acad. Sci. U. S. A. 95: 5987-5992.

Horton, J. D., & Shimomura, I. (1999) Sterol regulatory element-binding proteins: activators of cholesterol and fatty acid biosynthesis. Curr. Opin. Lipidol. 10: 143-150.

Horton, J. D., Shimomura, I., Brown, M. S., Hammer, R. E., Goldstein, J. L., & Shimano, H. (1998b) Activation of cholesterol synthesis in preference to fatty acid synthesis in liver and adipose tissue of transgenic mice overproducing sterol regulatory element-binding protein-2. J. Clin. Invest. 101: 2331-2339.

Howard, B. V., Abbott, W. G., Egusa, G., & Taskinen, M. R. (1987) Coordination of very low-density lipoprotein triglyceride and apolipoprotein B metabolism in humans: effects of obesity and non- insulin-dependent diabetes mellitus. Am. Heart J. 113: 522-526.

Huff, M. W., & Nestel, P. J. (1982) Metabolism of apolipoproteins CII, CIII1, CIII2 and VLDL-B in human subjects consuming high carbohydrate diets. Metabolism. 31: 493-498.

Hussain, M. M., Maxfield, F. R., Mas-Oliva, J., Tabas, I., Ji, Z. S., Innerarity, T. L., & Mahley, R. W. (1991) Clearance of chylomicron remnants by the low density lipoprotein receptor-related protein/alpha 2-macroglobulin receptor. J. Biol. Chem. 266: 13936-13940.

Hwang, I. S., Ho, H., Hoffman, B. B., & Reaven, G. M. (1987) Fructose-induced insulin resistance and hypertension in rats. Hypertension 10: 512-516.

Innerarity, T. L., Mahley, R. W., Weisgraber, K. H., Bersot, T. P., Krauss, R. M., Vega, G. L., Grundy, S. M., Friedl, W., Davignon, J., & McCarthy, B. J. (1990) Familial defective apolipoprotein B-100: a mutation of apolipoprotein B that causes hypercholesterolemia. J. Lipid Res. 31: 1337-1349.

Ishibashi, S., Brown, M. S., Goldstein, J. L., Gerard, R. D., Hammer, R. E., & Herz, J. (1993) Hypercholesterolemia in low density lipoprotein receptor knockout mice and its reversal by adenovirus-mediated gene delivery. J. Clin. Invest. 92: 883-893.

Jamil, H., Chu, C. H., Dickson, J. K., Jr., Chen, Y., Yan, M., Biller, S. A., Gregg, R. E., Wetterau, J. R., & Gordon, D. A. (1998) Evidence that microsomal triglyceride transfer protein is limiting in the production of apolipoprotein B-containing lipoproteins in hepatic cells. J. Lipid Res. 39: 1448-1454.

Jenkins, D. J., Wolever, T. M., Taylor, R. H., Barker, H., Fielden, H., Baldwin, J. M., Bowling, A. C., Newman, H. C., Jenkins, A. L., & Goff, D. V. (1981) Glycemic index of foods: a physiological basis for carbohydrate exchange. Am. J. Clin. Nutr. 34: 362-366.

Jiang, X. C., Moulin, P., Quinet, E., Goldberg, I. J., Yacoub, L. K., Agellon, L. B., Compton, D., Schnitzer-Polokoff, R., & Tall, A. R. (1991) Mammalian adipose tissue and muscle are major sources of lipid transfer protein mRNA. J. Biol. Chem. 266: 4631-4639.

Kamata, K., Kanie, N., & Inose, A. (2001) Mechanisms underlying attenuated contractile response of aortic rings to noradrenaline in fructose-fed mice. Eur. J. Pharmacol. 428: 241-249.

Karpe, F. (1997) Postprandial lipid metabolism in relation to coronary heart disease. Proc. Nutr. Soci. 56: 671-678.

Kasim-Karakas, S. E., Lane, E., Almario, R., Mueller, W., & Walzem, R. (1997) Effects of dietary fat restriction on particle size of plasma lipoproteins in postmenopausal women. Metabolism. 46: 431-436.

Kasim-Karakas, S. E., Vriend, H., Almario, R., Chow, L. C., & Goodman, M. N. (1996) Effects of dietary carbohydrates on glucose and lipid metabolism in golden Syrian hamsters. J. Lab. Clin. Med. 128: 208-213.

Katan, M. B., Grundy, S. M., & Willett, W. C. (1997) Should a low-fat, high-carbohydrate diet be recommended for everyone? Beyond low-fat diets. N. Engl. J. Med. 337: 563-566.

Kazumi, T., Vranic, M., & Steiner, G. (1985) Changes in very low density lipoprotein particle size and production in response to sucrose feeding and hyperinsulinemia. Endocrinology 117: 1145-1150.

Kazumi, T., Vranic, M., & Steiner, G. (1986) Triglyceride kinetics: effects of dietary glucose, sucrose, or fructose alone or with hyperinsulinemia. Am. J. Physiol. 250: E325-330.

Kieft, K. A., Bocan, T. M., & Krause, B. R. (1991) Rapid on-line determination of cholesterol distribution among plasma lipoproteins after high-performance gel filtration chromatography. J. Lipid Res. 32: 859-866.

Kim, E., Ambroziak, P., Veniant, M. M., Hamilton, R. L., & Young, S. G. (1998) A gene-targeted mouse model for familial hypobetalipoproteinemia. Low levels of apolipoprotein B mRNA in association with a nonsense mutation in exon 26 of the apolipoprotein B gene. J. Biol. Chem. 273: 33977-33984.

Kotite, L., Bergeron, N., & Havel, R. J. (1995) Quantification of apolipoproteins B-100, B-48, and E in human triglyceride-rich lipoproteins. J. Lipid Res. 36: 890-900.

Koutsari, C., Karpe, F., Humphreys, S. M., Frayn, K. N., & Hardman, A. E. (2001) Exercise prevents the accumulation of triglyceride-rich lipoproteins and their remnants seen when changing to a high-carbohydrate diet. Arterioscler. Thromb. Vasc. Biol. 21: 1520-1525.

Krauss, R. M. (1994) Heterogeneity of plasma low-density lipoproteins and atherosclerosis risk. Curr Opin in Lipidol 5: 339-349.

Krauss, R. M. (1995) Dense low density lipoproteins and coronary artery disease. Am. J. Cardiol. 75: 53B-57B.

Krauss, R. M. (1997) Genetic, metabolic, and dietary influences on the atherogenic lipoprotein phenotype. World Rev. Nutr. Diet. 80: 22-43.

Krauss, R. M. (1998) Atherogenicity of triglyceride-rich lipoproteins. Am. J. Cardiol. 81: 13B-17B.

Krauss, R. M., & Burke, D. J. (1982) Identification of multiple subclasses of plasma low density lipoproteins in normal humans. J. Lipid Res. 23: 97-104.

Krauss, R. M., & Dreon, D. M. (1995) Low-density-lipoprotein subclasses and response to a low-fat diet in healthy men. Am. J. Clin. Nutr. 62: 478S-487S.

Krauss, R. M., Eckel, R. H., Howard, B., Appel, L. J., Daniels, S. R., Deckelbaum, R. J., Erdman, J. W., Jr., Kris-Etherton, P., Goldberg, I. J., Kotchen, T. A., Lichtenstein, A. H., Mitch, W. E., Mullis, R., Robinson, K., Wylie-Rosett, J., St Jeor, S., Suttie, J., Tribble, D. L., & Bazzarre, T. L. (2000) AHA Dietary Guidelines: revision 2000: A statement for healthcare professionals from the Nutrition Committee of the American Heart Association. Circulation 102: 2284-2299.

Krempler, F., Kostner, G., Bolzano, K., & Sandhofer, F. (1979) Lipoprotein (a) is not a metabolic product of other lipoproteins containing apolipoprotein B. Biochim. Biophys. Acta 575: 63-70.

Kulinski, A., Rustaeus, S., & Vance, J. E. (2002) Microsomal triacylglycerol transfer protein is required for lumenal accretion of triacylglycerol not associated with ApoB, as well as for ApoB lipidation. J. Biol. Chem. 277: 31516-31525.

Kwiterovich, P. O., Jr. (2000) The metabolic pathways of high-density lipoprotein, low-density lipoprotein, and triglycerides: a current review. Am. J. Cardiol. 86: 5L-10L.

Kwiterovich, P. O., Jr. (2002a) Clinical relevance of the biochemical, metabolic, and genetic factors that influence low-density lipoprotein heterogeneity. Am. J. Cardiol. 90: 30i-47i.

Kwiterovich, P. O., Jr. (2002b) Lipoprotein heterogeneity: diagnostic and therapeutic implications. Am. J. Cardiol. 90: 1i-10i.

Laemmli, U. K. (1970) Cleavage of structural proteins during the assembly of the head of bacteriophage T4. Nature 227: 680-685.

Lamarche, B., Tchernof, A., Moorjani, S., Cantin, B., Dagenais, G. R., Lupien, P. J., & Despres, J. P. (1997) Small, dense low-density lipoprotein particles as a predictor of the risk of ischemic heart disease in men. Prospective results from the Quebec Cardiovascular Study. Circulation 94: 69-75.

Lang, C. A., & Davis, R. A. (1990) Fish oil fatty acids impair VLDL assembly and/or secretion by cultured rat hepatocytes. J. Lipid Res. 31: 2079-2086.

Leighton, J. K., Joyner, J., Zamarripa, J., Deines, M., & Davis, R. A. (1990) Fasting decreases apolipoprotein B mRNA editing and the secretion of small molecular weight apoB by rat hepatocytes: evidence that the total amount of apoB secreted is regulated post-transcriptionally. J. Lipid Res. 31: 1663-1668.

Lewis, G. F., Uffelman, K. D., Szeto, L. W., Weller, B., & Steiner, G. (1995) Interaction between free fatty acids and insulin in the acute control of very low density lipoprotein production in humans. J. Clin. Invest. 95: 158-166.

Li, X., Gatalina, F., Grundy, S., & Patel, S. (1996) Method to measure apolipoproteinB-48 and B-100 secretion rates in an individual mouse: evidence for a very rapid turnover of VLDL and preferential removal of B-48-relative to B-100-containinglipoproteins. J. Lipid Res. 37: 210-220.

Lichtenstein, A. H., Ausman, L. M., Carrasco, W., Jenner, J. L., Ordovas, J. M., & Schaefer, E. J. (1994) Short-term consumption of a low-fat diet beneficially affects plasma lipid concentrations only when accompanied by weight loss. Hypercholesterolemia, low-fat diet, and plasma lipids. Arterioscler. Thromb. 14: 1751-1760.

Lin, M. C., Arbeeny, C., Bergquist, K., Kienzle, B., Gordon, D. A., & Wetterau, J. R. (1994) Cloning and regulation of hamster microsomal triglyceride transfer protein. The regulation is independent from that of other hepatic and intestinal proteins which participate in the transport of fatty acids and triglycerides. J. Biol. Chem. 269: 29138-29145.

Lowry, O. H., Rosenbrough, N. J., Farr, A. L., & Randall, R. J. (1951) Protein with the folin phenol reagent. J. Biol. Chem. 193: 265-275.

Mack, K. D., Walzem, R., & Zeldis, J. B. (1994) Cationic lipid enhances in vitro receptor-mediated transfection. Am. J. Med. Sci. 307: 138-143.

Mackness, M. I., Arrol, S., Abbott, C., & Durrington, P. N. (1993) Protection of low-density lipoprotein against oxidative modification by high-density lipoprotein associated paraoxonase. Atherosclerosis 104: 129-135.

Manninen, V., Elo, M. O., Frick, M. H., Haapa, K., Heinonen, O. P., Heinsalmi, P., Helo, P., Huttunen, J. K., Kaitaniemi, P., & Koskinen, P. (1988) Lipid alterations and decline in the incidence of coronary heart disease in the Helsinki Heart Study. JAMA 260: 641-651.

Matsui, H., Okumura, K., Kawakami, K., Hibino, M., Toki, Y., & Ito, T. (1997) Improved insulin sensitivity by bezafibrate in rats: relationship to fatty acid composition of skeletal-muscle triglycerides. Diabetes 46: 348-353.

Mayes, P. A. (2000) Lipid Transport and Storage. In: Harper's Biochemistry (Murray, R.K., Granner, D.K., Mayes, P.A. & Rodwell, V.W. eds.), pp. 268-283, Appleton & Lange, Stamford, CT.

McCormick, S. P., & Nielsen, L. B. (1998) Expression of large genomic clones in transgenic mice: new insights into apolipoprotein B structure, function and regulation. Curr. Opin. Lipidol. 9: 103-111.

McNeish, J., Aiello, R. J., Guyot, D., Turi, T., Gabel, C., Aldinger, C., Hoppe, K. L., Roach, M. L., Royer, L. J., de Wet, J., Broccardo, C., Chimini, G., & Francone, O. L. (2000) High density lipoprotein deficiency and foam cell accumulation in mice with targeted disruption of ATP-binding cassette transporter-1. Proc. Natl. Acad. Sci. U. S. A. 97: 4245-4250.

Meigs, J. B., Mittleman, M. A., Nathan, D. M., Tofler, G. H., Singer, D. E., Murphy-Sheehy, P. M., Lipinska, I., D'Agostino, R. B., & Wilson, P. W. (2000) Hyperinsulinemia, hyperglycemia, and impaired hemostasis: the Framingham Offspring Study. JAMA 283: 221-228.

Melish, J., Le, N. A., Ginsberg, H., Steinberg, D., & Brown, W. V. (1980) Dissociation of apoprotein B and triglyceride production in very-low- density lipoproteins. Am. J. Physiol. 239: E354-362.

Moberly, J. B., Cole, T. G., Alpers, D. H., & Schonfeld, G. (1990) Oleic acid stimulation of apolipoprotein B secretion from HepG2 and Caco-2 cells occurs post-transcriptionally. Biochim. Biophys. Acta 1042: 70-80.

Mooradian, A. D., Wong, N. C., & Shah, G. N. (1997) Apolipoprotein A1 expression in young and aged rats is modulated by dietary carbohydrates. Metabolism. 46: 1132-1136.

Nakamura, N., Lowe, M., Levine, T. P., Rabouille, C., & Warren, G. (1997) The vesicle docking protein p115 binds GM130, a cis-Golgi matrix protein, in a mitotically regulated manner. Cell 89: 445-455.

NCEP (2001) Executive Summary of the Third Report of the National Cholesterol Education Program (NCEP) Expert Panel on Detection, Evaluation, and Treatment of High Blood Cholesterol in Adults (Adult Treatment Panel III). JAMA 285: 2486-2497.

Newby, A. C. (2000) An overview of the vascular response to injury: a tribute to the late Russell Ross. Toxicol. Lett. 112-113: 519-529.

Newby, A. C., & Zaltsman, A. B. (2000) Molecular mechanisms in intimal hyperplasia. J. Pathol. 190: 300-309.

Nichols, A. V., Krauss, R. M., & Musliner, T. A. (1986) Nondenaturing polyacrylamide gradient gel electrophoresis. Methods Enzymol. 128: 417-431.

Nielsen, L. B., Stender, S., Jauhiainen, M., & Nordestgaard, B. G. (1996) Preferential influx and decreased fractional loss of lipoprotein(a) in atherosclerotic compared with nonlesioned rabbit aorta. Atherosclerosis 123: 1-15.

Nielsen, L. B., Veniant, M., Boren, J., Raabe, M., Wong, J. S., Tam, C., Flynn, L., Vanni-Reyes, T., Gunn, M. D., Goldberg, I. J., Hamilton, R. L., & Young, S. G. (1998) Genes for apolipoprotein B and microsomal triglyceride transfer protein are expressed in the heart: evidence that the heart has the capacity to synthesize and secrete lipoproteins. Circulation 98: 13-16.

Nigon, F., Lesnik, P., Rouis, M., & Chapman, M. J. (1991) Discrete subspecies of human low density lipoproteins are heterogeneous in their interaction with the cellular LDL receptor. J. Lipid Res. 32: 1741-1753.

Nilsson-Ehle, P., Garfinkel, A. S., & Schotz, M. C. (1980) Lipolytic enzymes and plasma lipoprotein metabolism. Annu. Rev. Biochem. 49: 667-693.

Nordestgaard, B. G., & Nielsen, L. B. (1994) Atherosclerosis and arterial influx of lipoproteins. Curr. Opin. Lipidol. 5: 252-257.

Ntambi, J. M., Buhrow, S. A., Kaestner, K. H., Christy, R. J., Sibley, E., Kelly, T. J., Jr., & Lane, M. D. (1988) Differentiation-induced gene expression in 3T3-L1 preadipocytes. Characterization of a differentially expressed gene encoding stearoyl-CoA desaturase. J. Biol. Chem. 263: 17291-17300.

Olofsson, S. O., Asp, L., & Boren, J. (1999) The assembly and secretion of apolipoprotein B-containing lipoproteins. Curr. Opin. Lipidol. 10: 341-346.

Olofsson, S. O., Stillemark-Billton, P., & Asp, L. (2000) Intracellular assembly of VLDL: two major steps in separate cell compartments. Trends Cardiovasc. Med. 10: 338-345.

Ornish, D. (1998) Low-fat diets. N. Engl. J. Med. 338: 127; author reply 128-129.

Otway, S., & Robinson, D. S. (1967) The use of a non-ionic detergent (Triton WR-1339) to determine rates of triglyceride entry into the circulation of the rt under different physiological conditions. J. Physiol. 190: 321-332.

Ozasa, S., Kempner, E. S., & Erickson, S. K. (1989) Functional size of acyl coenzyme A:diacylglycerol acyltransferase by radiation inactivation. J. Lipid Res. 30: 1759-1762.

Packard, C. J., Munro, A., Lorimer, A. R., Gotto, A. M., & Shepherd, J. (1984) Metabolism of apolipoprotein B in large triglyceride-rich very low density lipoproteins of normal and hypertriglyceridemic subjects. J. Clin. Invest. 74: 2178-2192.

Packard, C. J., & Shepherd, J. (1997) Lipoprotein heterogeneity and apolipoprotein B metabolism. Arterioscler. Thromb. Vasc. Biol. 17: 3542-3556.

Parks, E. J., Krauss, R. M., Christiansen, M. P., Neese, R. A., & Hellerstein, M. K. (1999) Effects of a low-fat, high-carbohydrate diet on VLDL-triglyceride assembly, production, and clearance. J. Clin. Invest. 104: 1087-1096.

Pennington, R. J. (1961) Biochemistry of dystrophic muscle. Mitochondrial succinate-tetrazolium reductase and adenosine triphosphatase. Biochem. J. 80: 649-654.

Phung, T. L., Roncone, A., Jensen, K. L., Sparks, C. E., & Sparks, J. D. (1997) Phosphoinositide 3-kinase activity is necessary for insulin-dependent inhibition of apolipoprotein B secretion by rat hepatocytes and localizes to the endoplasmic reticulum. J. Biol. Chem. 272: 30693-30702.

Piedrahita, J. A., Zhang, S. H., Hagaman, J. R., Oliver, P. M., & Maeda, N. (1992) Generation of mice carrying a mutant apolipoprotein E gene inactivated by gene targeting in embryonic stem cells. Proc. Natl. Acad. Sci. U. S. A. 89: 4471-4475.

Plump, A. S., Smith, J. D., Hayek, T., Aalto-Setala, K., Walsh, A., Verstuyft, J. G., Rubin, E. M., & Breslow, J. L. (1992) Severe hypercholesterolemia and atherosclerosis in apolipoprotein E- deficient mice created by homologous recombination in ES cells. Cell 71: 343-353.

Pullinger, C. R., North, J. D., Teng, B. B., Rifici, V. A., Ronhild de Brito, A. E., & Scott, J. (1989) The apolipoprotein B gene is constitutively expressed in HepG2 cells: regulation of secretion by oleic acid, albumin, and insulin, and measurement of the mRNA half-life. J. Lipid Res. 30: 1065-1077.

Raabe, M., Flynn, L. M., Zlot, C. H., Wong, J. S., Veniant, M. M., Hamilton, R. L., & Young, S. G. (1998) Knockout of the abetalipoproteinemia gene in mice: reduced lipoprotein secretion in heterozygotes and embryonic lethality in homozygotes. Proc. Natl. Acad. Sci. U. S. A. 95: 8686-8691.

Raabe, M., Veniant, M. M., Sullivan, M. A., Zlot, C. H., Bjorkegren, J., Nielsen, L. B., Wong, J. S., Hamilton, R. L., & Young, S. G. (1999) Analysis of the role of microsomal triglyceride transfer protein in the liver of tissue-specific knockout mice. J. Clin. Invest. 103: 1287-1298.

Rader, D. J. (2002) High-density lipoproteins and atherosclerosis. Am. J. Cardiol. 90: 62i-70i.

Reaven, G. M. (1997) Do high carbohydrate diets prevent the development or attenuate the manifestations (or both) of syndrome X? A viewpoint strongly against. Curr. Opin. Lipidol. 8: 23-27.

Reaven, G. M., Hill, D. B., Gross, R. C., & Farquhar, J. W. (1965) Kinetics of triglyceride turnover of very low density lipoproteins of human plasma. J. Clin. Invest. 44: 1826-1833.

Remillard, P., Shen, G., Milne, R., & Maheux, P. (2001) Induction of cholesterol ester transfer protein in adipose tissue and plasma of the fructose-fed hamster. Life Science 69: 677-687.

Reusch, J. E. (2002) Current concepts in insulin resistance, type 2 diabetes mellitus, and the metabolic syndrome. Am. J. Cardiol. 90: 19G-26G.

Richmond, W. (1973) Preparation and properties of a cholesterol oxidase from *Nocardia sp.* and its application to the enzymatic assay of total cholesterol in serum. Clin. Chem. 19: 1350-1356.

Rigotti, A., Trigatti, B., Babitt, J., Penman, M., Xu, S., & Krieger, M. (1997) Scavenger receptor BI--a cell surface receptor for high density lipoprotein. Curr. Opin. Lipidol. 8: 181-188.

Rizzo, M., Barbagallo, C. M., Severino, M., Polizzi, F., Onorato, F., Noto, D., Cefalu, A. B., Pace, A., Marino, G., Notarbartolo, A., & Averna, R. M. (2003) Low-density-lipoprotein peak particle size in a Mediterranean population. Eur. J. Clin. Invest. 33: 126-133.

Robertson, T. L., Kato, H., Gordon, T., Kagan, A., Rhoads, G. G., Land, C. E., Worth, R. M., Belsky, J. L., Dock, D. S., Miyanishi, M., & Kawamoto, S. (1977) Epidemiologic studies of coronary heart disease and stroke in Japanese men living in

Japan, Hawaii and California. Coronary heart disease risk factors in Japan and Hawaii. Am. J. Cardiol. 39: 244-249.

Ross, R. (1993) The pathogenesis of atherosclerosis: a perspective for the 1990s. Nature 362: 801-809.

Ross, R. (1999) Atherosclerosis--an inflammatory disease. N. Engl. J. Med. 340: 115-126.

Rudel, L. L. (1998) Low-fat diets. N. Engl. J. Med. 338: 128; author reply 128-129.

Rudel, L. L., Kelley, K., Sawyer, J. K., Shah, R., & Wilson, M. D. (1998) Dietary monounsaturated fatty acids promote aortic atherosclerosis in LDL receptor-null, human ApoB100-overexpressing transgenic mice. Arterioscler. Thromb. Vasc. Biol. 18: 1818-1827.

Rusinol, A., Verkade, H., & Vance, J. E. (1993) Assembly of rat hepatic very low density lipoproteins in the endoplasmic reticulum. J. Biol. Chem. 268: 3555-3562.

Rustaeus, S., Lindberg, K., Boren, J., & Olofsson, S. O. (1995) Brefeldin A reversibly inhibits the assembly of apoB containing lipoproteins in McA-RH7777 cells. J. Biol. Chem. 270: 28879-28886.

Rustaeus, S., Lindberg, K., Stillemark, P., Claesson, C., Asp, L., Larsson, T., Boren, J., & Olofsson, S. O. (1999) Assembly of very low density lipoprotein: a two-step process of apolipoprotein B core lipidation. J. Nutr. 129: 463S-466S.

Rustaeus, S., Stillemark, P., Lindberg, K., Gordon, D., & Olofsson, S. O. (1998) The microsomal triglyceride transfer protein catalyzes the post- translational assembly of apolipoprotein B-100 very low density lipoprotein in McA-RH7777 cells. J. Biol. Chem. 273: 5196-5203.

Sacks, F. M. (2002) The role of high-density lipoprotein (HDL) cholesterol in the prevention and treatment of coronary heart disease: expert group recommendations. Am. J. Cardiol. 90: 139-143.

Sakata, N., Wu, X., Dixon, J. L., & Ginsberg, H. N. (1993) Proteolysis and lipid-facilitated translocation are distinct but competitive processes that regulate secretion of apolipoprotein B in Hep G2 cells. J. Biol. Chem. 268: 22967-22970.

Santamarina-Fojo, S., Lambert, G., Hoeg, J. M., & Brewer, H. B., Jr. (2000) Lecithin-cholesterol acyltransferase: role in lipoprotein metabolism, reverse cholesterol transport and atherosclerosis. Curr. Opin. Lipidol. 11: 267-275.

Schonfeld, G. (1970) Changes in the composition of very low density lipoprotein during carbohydrate induction in man. J. Lab. Clin. Med. 75: 206-211.

Shaikh, M., Wootton, R., Nordestgaard, B. G., Baskerville, P., Lumley, J. S., La Ville, A. E., Quiney, J., & Lewis, B. (1991) Quantitative studies of transfer in vivo of low density, Sf 12-60, and Sf 60-400 lipoproteins between plasma and arterial intima in humans. Arteriosclerosis Thromb. 11: 569-577.

Sharp, D., Blinderman, L., Combs, K. A., Kienzle, B., Ricci, B., Wager-Smith, K., Gil, C. M., Turck, C. W., Bouma, M. E., & Rader, D. J. (1993) Cloning and gene defects in microsomal triglyceride transfer protein associated with abetalipoproteinaemia Goddess lanced through the heart. Nature 365: 65-69.

Shimano, H., Horton, J. D., Hammer, R. E., Shimomura, I., Brown, M. S., & Goldstein, J. L. (1996) Overproduction of cholesterol and fatty acids causes massive liver enlargement in transgenic mice expressing truncated SREBP-1a. J. Clin. Invest. 98: 1575-1584.

Shimano, H., Shimomura, I., Hammer, R. E., Herz, J., Goldstein, J. L., Brown, M. S., & Horton, J. D. (1997) Elevated levels of SREBP-2 and cholesterol synthesis in livers of mice homozygous for a targeted disruption of the SREBP-1 gene. J. Clin. Invest. 100: 2115-2124.

Shimano, H., Yahagi, N., Amemiya-Kudo, M., Hasty, A. H., Osuga, J., Tamura, Y., Shionoiri, F., Iizuka, Y., Ohashi, K., Harada, K., Gotoda, T., Ishibashi, S., & Yamada, N. (1999) Sterol regulatory element-binding protein-1 as a key

transcription factor for nutritional induction of lipogenic enzyme genes. J. Biol. Chem. 274: 35832-35839.

Shimomura, I., Bashmakov, Y., & Horton, J. D. (1999) Increased levels of nuclear SREBP-1c associated with fatty livers in two mouse models of diabetes mellitus. J. Biol. Chem. 274: 30028-30032.

Shimomura, I., Shimano, H., Korn, B. S., Bashmakov, Y., & Horton, J. D. (1998) Nuclear sterol regulatory element-binding proteins activate genes responsible for the entire program of unsaturated fatty acid biosynthesis in transgenic mouse liver. J. Biol. Chem. 273: 35299-35306.

Shore, V. G. (1991) Nondenaturing Electrophoresis of Lipoproteins in Agarose and Polyacrylamide Gradient Gels. In: Analysis of Fats, Oils and Lipoproteins (Perkins,E.G. ed.), pp. 573-588. American Oil Chemists' Society, Champaign, IL.

Siri, P., Candela, N., Zhang, Y. L., Ko, C., Eusufzai, S., Ginsberg, H. N., & Huang, L. S. (2001) Post-transcriptional stimulation of the assembly and secretion of triglyceride-rich apolipoprotein B lipoproteins in a mouse with selective deficiency of brown adipose tissue, obesity, and insulin resistance. J. Biol. Chem. 276: 46064-46072.

Sniderman, A. D. (2000) Postprandial hypertriglyceridemia(s): time to enlarge our pathophysiologic perspective. Eur. J. Clin. Invest. 30: 935-937.

Sniderman, A. D., Scantlebury, T., & Cianflone, K. (2001) Hypertriglyceridemic hyperapob: the unappreciated atherogenic dyslipoproteinemia in type 2 diabetes mellitus. Ann. Intern. Med. 135: 447-459.

Spady, D. K., & Dietschy, J. M. (1985) Dietary saturated triacylglycerols suppress hepatic low density lipoprotein receptor activity in the hamster. Proc. Natl. Acad. Sci. U. S. A. 82: 4526-4530.

Spector, A. A., Mathur, S. N., & Kaduce, T. L. (1979) Role of acylcoenzyme A: cholesterol o-acyltransferase in cholesterol metabolism. Prog. Lipid Res. 18: 31-53.

Spillane, D., Missler, M., Herz, J., Selig, D. K., Wolff, J. R., Hammer, R. E., Malenka, R. C., & Sudhof, T. C. (1995) Lipoprotein and receptor interactions in vivo. Nature 375: 488-493.

Spring, D. J., Chen-Liu, L. W., Chatterton, J. E., Elovson, J., & Schumaker, V. N. (1992) Lipoprotein assembly. Apolipoprotein B size determines lipoprotein core circumference. J. Biol. Chem. 267: 14839-14845.

Stalenhoef, A. F., Malloy, M. J., Kane, J. P., & Havel, R. J. (1984) Metabolism of apolipoproteins B-48 and B-100 of triglyceride-rich lipoproteins in normal and lipoprotein lipase-deficient humans. Proc. Natl. Acad. Sci. U. S. A. 81: 1839-1843.

Stein, Y., Dabach, Y., Hollander, G., & Stein, O. (1990) Cholesteryl ester transfer activity in hamster plasma: increase by fat and cholesterol rich diets. Biochim. Biophys. Acta 1042: 138-141.

Steinberg, D., Carew, T. E., Fielding, C., Fogelman, A. M., Mahley, R. W., Sniderman, A. D., & Zilversmit, D. B. (1989a) Lipoproteins and the pathogenesis of atherosclerosis. Circulation 80: 719-723.

Steinberg, D., Parthasarathy, S., Carew, T. E., Khoo, J. C., & Witztum, J. L. (1989b) Beyond cholesterol. Modifications of low-density lipoprotein that increase its atherogenicity. N. Engl. J. Med. 320: 915-924.

Steinberg, D., & Witztum, J. L. (1999) Lipoproteins, Lipoprotein Oxidation, and Atherogenesis. In: Molecular Basis of Cardiovascular Disease (Chien, K.R. ed.), pp. 428-457. WB Saunders Company, Philadelphia, PA.

Steiner, G., Haynes, F. J., Yoshino, G., & Vranic, M. (1984) Hyperinsulinemia and in vivo very-low-density lipoprotein-triglyceride kinetics. Am. J. Physiol. 246: E187-192.

Stewart, M. W., Laker, M. F., Dyer, R. G., Game, F., Mitcheson, J., Winocour, P. H., & Alberti, K. G. (1993) Lipoprotein compositional abnormalities and insulin

resistance in type II diabetic patients with mild hyperlipidemia. Arterioscler. Thromb. 13: 1046-1052.

Stillemark, P., Boren, J., Andersson, M., Larsson, T., Rustaeus, S., Karlsson, K. A., & Olofsson, S. O. (2000) The assembly and secretion of apolipoprotein B-48-containing very low density lipoproteins in McA-RH7777 cells. J. Biol. Chem. 275: 10506-10513.

Sul, H. S., & Wang, D. (1998) Nutritional and hormonal regulation of enzymes in fat synthesis: studies of fatty acid synthase and mitochondrial glycerol-3-phosphate acyltransferase gene transcription. Ann. Rev. Nutr. 18: 331-351.

Tabas, I., & Krieger, M. (1999) Lipoprotein Receptors and Cellular Cholesterol Metabolism in Health and Disease. In: Molecular Basis of Cardiovascular Disease (Chien, K.R. ed.), pp. 458-476. WB Saunders Company, Philadelphia, PA.

Taghibiglou, C., Carpentier, A., Van Iderstine, S. C., Chen, B., Rudy, D., Aiton, A., Lewis, G. F., & Adeli, K. (2000a) Mechanisms of hepatic very low density lipoprotein overproduction in insulin resistance. Evidence for enhanced lipoprotein assembly, reduced intracellular ApoB degradation, and increased microsomal triglyceride transfer protein in a fructose-fed hamster model. J. Biol. Chem. 275: 8416-8425.

Taghibiglou, C., Rudy, D., Van Iderstine, S. C., Aiton, A., Cavallo, D., Cheung, R., & Adeli, K. (2000b) Intracellular mechanisms regulating apoB-containing lipoprotein assembly and secretion in primary hamster hepatocytes. J. Lipid Res. 41: 499-513.

Takayama, M., Itoh, S., Nagasaki, T., & Tanimizu, I. (1977) A new enzymatic method for determination of serum choline-containing phospholipids. Clin. Chim. Acta 79: 93-98.

Tall, A. R. (1990) Plasma high density lipoproteins. Metabolism and relationship to atherogenesis. J. Clin. Invest. 86: 379-384.

Tangirala, R. K., Rubin, E. M., & Palinski, W. (1995) Quantitation of atherosclerosis in murine models: correlation between lesions in the aortic origin and in the entire aorta, and differences in the extent of lesions between sexes in LDL receptor-deficient and apolipoprotein E-deficient mice. J. Lipid Res. 36: 2320-2328.

Theriault, A., Ogbonna, G., & Adeli, K. (1992) Thyroid hormone modulates apolipoprotein B gene expression in HepG2 cells. Biochem. Biophys. Res. Commun. 186: 617-623.

Tobey, T. A., Mondon, C. E., Zavaroni, I., & Reaven, G. M. (1982) Mechanism of insulin resistance in fructose-fed rats. Metabolism. 31: 608-612.

Tribble, D. L., Holl, L. G., Wood, P. D., & Krauss, R. M. (1992) Variations in oxidative susceptibility among six low density lipoprotein subfractions of differing density and particle size. Atherosclerosis 93: 189-199.

Tribble, D. L., Rizzo, M., Chait, A., Lewis, D. M., Blanche, P. J., & Krauss, R. M. (2001) Enhanced oxidative susceptibility and reduced antioxidant content of metabolic precursors of small, dense low-density lipoproteins. Am. J. Med. 110: 103-110.

Truswell, A. S. (1994) Food carbohydrates and plasma lipids--an update. Am. J. Clin. Nutr. 59: 710S-718S.

Turley, M. L., Skeaff, C. M., Mann, J. I., & Cox, B. (1998) The effect of a low-fat, high-carbohydrate diet on serum high density lipoprotein cholesterol and triglyceride. Eur. J. Clin. Nutr. 52: 728-732.

Vaisman, B. L., Klein, H. G., Rouis, M., Berard, A. M., Kindt, M. R., Talley, G. D., Meyn, S. M., Hoyt, R. F., Jr., Marcovina, S. M., & Albers, J. J. (1995) Overexpression of human lecithin cholesterol acyltransferase leads to hyperalphalipoproteinemia in transgenic mice. J. Biol. Chem. 270: 12269-12275.

Van Golde, L. M., Fleischer, B., & Fleischer, S. (1971) Some studies on the metabolism of phospholipids in Golgi complex from bovine and rat liver in comparison to other subcellular fractions. Biochim. Biophys. Acta 249: 318-330.

Veniant, M. M., Pierotti, V., Newland, D., Cham, C. M., Sanan, D. A., Walzem, R. L., & Young, S. G. (1997) Susceptibility to atherosclerosis in mice expressing exclusively apolipoprotein B48 or apolipoprotein B100. J. Clin. Invest. 100: 180-188.

Veniant, M. M., Sullivan, M. A., Kim, S. K., Ambroziak, P., Chu, A., Wilson, M. D., Hellerstein, M. K., Rudel, L. L., Walzem, R. L., & Young, S. G. (2000) Defining the atherogenicity of large and small lipoproteins containing apolipoprotein B100. J. Clin. Invest. 106: 1501-1510.

Veniant, M. M., Zlot, C. H., Walzem, R. L., Pierotti, V., Driscoll, R., Dichek, D., Herz, J., & Young, S. G. (1998) Lipoprotein clearance mechanisms in LDL receptor-deficient "Apo-B48- only" and "Apo-B100-only" mice. J. Clin. Invest. 102: 1559-1568.

Verkade, H. J., Fast, D. G., Rusinol, A. E., Scraba, D. G., & Vance, D. E. (1993) Impaired biosynthesis of phosphatidylcholine causes a decrease in the number of very low density lipoprotein particles in the Golgi but not in the endoplasmic reticulum of rat liver. J. Biol. Chem. 268: 24990-24996.

Voet, D., Voet, J. G., & Pratt, C. W. (1999) Fundamentals of Biochemistry. John Wiley & Sons, Inc., New York, NY.

Vrana, A., Fabry, P., Slabochova, Z., & Kazdova, L. (1974) Effect of dietary fructose on free fatty acid release from adipose tissue and serum free fatty acid concentration in the rat. Nutr. Metab. 17: 74-83.

Walsh, B. W., Schiff, I., Rosner, B., Greenberg, L., Ravnikar, V., & Sacks, F. M. (1991) Effects of postmenopausal estrogen replacement on the concentrations and metabolism of plasma lipoproteins. N. Engl. J. Med. 325: 1196-1204.

Walzem, R. L. (1996) Lipoproteins and the laying hen: form follows function. Poult. Avian Biol. Rev. 7: 31-64.

Walzem, R. L., Davis, P. A., & Hansen, R. J. (1994) Overfeeding increases very low density lipoprotein diameter and causes the appearance of a unique lipoprotein particle in association with failed yolk deposition. J. Lipid Res. 35: 1354-1366.

Walzem, R. L., Watkins, S., Frankel, E. N., Hansen, R. J., & German, J. B. (1995) Older plasma lipoproteins are more susceptible to oxidation: a linking mechanism for the lipid and oxidation theories of atherosclerotic cardiovascular disease. Proc. Natl. Acad. Sci. U. S. A. 92: 7460-7464.

Wang, C. S., Hartsuck, J., & McConathy, W. J. (1992) Structure and functional properties of lipoprotein lipase. Biochim. Biophys. Acta 1123: 1-17.

Wang, H., Yao, Z., & Fisher, E. A. (1994) The effects of n-3 fatty acids on the secretion of carboxyl-terminally truncated forms of human apoprotein B. J. Biol. Chem. 269: 18514-18520.

Wang, S. R., Pessah, M., Infante, J., Catala, D., Salvat, C., & Infante, R. (1988) Lipid and lipoprotein metabolism in Hep G2 cells. Biochim. Biophys. Acta 961: 351-363.

Wang, Y., Tran, K., & Yao, Z. (1999) The activity of microsomal triglyceride transfer protein is essential for accumulation of triglyceride within microsomes in McA-RH7777 cells. A unified model for the assembly of very low density lipoproteins. J. Biol. Chem. 274: 27793-27800.

Watkin, D. M., Froeb, H. F., Hatch, F. T., & Gutman, A. B. (1950) Effects of diet in essential hypertension. II. Results with unmodified Kempner rice diet in fifty hospitalized patients. Am. J. Med. 9: 491-493.

Wetterau, J. R., Aggerbeck, L. P., Bouma, M. E., Eisenberg, C., Munck, A., Hermier, M., Schmitz, J., Gay, G., Rader, D. J., & Gregg, R. E. (1992) Absence of

microsomal triglyceride transfer protein in individuals with abetalipoproteinemia. Science 258: 999-1001.

Williams, K. J., Brocia, R. W., & Fisher, E. A. (1990) The unstirred water layer as a site of control of apolipoprotein B secretion. J. Biol. Chem. 265: 16741-16744.

Williams, K. J., & Fisher, E. A. (2001) Atherosclerosis: cell biology and lipoproteins--three distinct processes that control apolipoprotein-B secretion. Curr. Opin. Lipidol. 12: 235-237.

Williams, K. J., Fless, G. M., Petrie, K. A., Snyder, M. L., Brocia, R. W., & Swenson, T. L. (1992) Mechanisms by which lipoprotein lipase alters cellular metabolism of lipoprotein(a), low density lipoprotein, and nascent lipoproteins. Roles for low density lipoprotein receptors and heparan sulfate proteoglycans. J. Biol. Chem. 267: 13284-13292.

Williams, K. J., & Tabas, I. (1995) The response-to-retention hypothesis of early atherogenesis. Arterioscler. Thromb. Vasc. Biol. 15: 551-561.

Williams, K. J., & Tabas, I. (1998) The response-to-retention hypothesis of atherogenesis reinforced. Curr. Opin. Lipidol. 9: 471-474.

Williams, P. T., Superko, H. R., Haskell, W. L., Alderman, E. L., Blanche, P. J., Holl, L. G., & Krauss, R. M. (2003) Smallest LDL particles are most strongly related to coronary disease progression in men. Arterioscler. Thromb. Vasc. Biol. 23: 314-321.

Williams, S. B., Cusco, J. A., Roddy, M. A., Johnstone, M. T., & Creager, M. A. (1996) Impaired nitric oxide-mediated vasodilation in patients with non-insulin-dependent diabetes mellitus. J. Am. Coll. Cardiol. 27: 567-574.

Wood, D., De Backer, G., Faergeman, O., Graham, I., Mancia, G., & Pyorala, K. (1998) Prevention of coronary heart disease in clinical practice. Summary of recommendations of the Second Joint Task Force of European and other Societies on Coronary Prevention. Blood Press. 7: 262-269.

Wu, X., Sakata, N., Lui, E., & Ginsberg, H. N. (1994) Evidence for a lack of regulation of the assembly and secretion of apolipoprotein B-containing lipoprotein from HepG2 cells by cholesteryl ester. J. Biol. Chem. 269: 12375-12382.

Wu, X., Shang, A., Jiang, H., & Ginsberg, H. N. (1996) Low rates of apoB secretion from HepG2 cells result from reduced delivery of newly synthesized triglyceride to a "secretion-coupled" pool. J. Lipid Res. 37: 1198-1206.

Yao, Z., Tran, K., & McLeod, R. S. (1997) Intracellular degradation of newly synthesized apolipoprotein B. J. Lipid Res. 38: 1937-1953.

Young, S. G. (1990) Recent progress in understanding apolipoprotein B. Circulation 82: 1574-1594.

Young, S. G., Cham, C. M., Pitas, R. E., Burri, B. J., Connolly, A., Flynn, L., Pappu, A. S., Wong, J. S., Hamilton, R. L., & Farese, R. V., Jr. (1995) A genetic model for absent chylomicron formation: mice producing apolipoprotein B in the liver, but not in the intestine. J. Clin. Invest. 96: 2932-2946.

Zammit, V. A., Waterman, I. J., Topping, D., & McKay, G. (2001) Insulin stimulation of hepatic triacylglycerol secretion and the etiology of insulin resistance. J. Nutr. 131: 2074-2077.

Zannis, V. I., & Breslow, J. L. (1982) Apolipoprotein E. Molecular & Cellular Biochemistry 42: 3-20.

Zhou, M., Wu, X., Huang, L. S., & Ginsberg, H. N. (1995) Apoprotein B100, an inefficiently translocated secretory protein, is bound to the cytosolic chaperone, heat shock protein 70. J. Biol. Chem. 270: 25220-25224.

Zilversmit, D. B. (1979) Atherogenesis: a postprandial phenomenon. Circulation 60: 473-485.

APPENDIX

Model	Variables in Model	Adjusted R-Square	Unadjusted R-Square
1	HDL cholesterol (HDLc)	0.392	0.392
1	apoB	0.308	0.153
1	Cholesterol (Chol)	0.180	0.180
1	Moderate Diameter Particle (PV2)	0.038	0.038
1	Body wight (BW)	0.038	0.038
1	Small Diameter Particles (PV1)	-0.008	-0.008
1	Triacylglycerols (TG)	-0.014	-0.014
2	apoB + HDLc	0.522	0.473
2	PV2 + Chol	0.458	0.458
2	Chol + HDLc	0.437	0.437
2	PV2 + HDLc	0.433	0.433
2	BW + HDLc	0.412	0.412
2	PV1 + HDLc	0.408	0.408
2	TG + HDLc	0.389	0.389
2	apoB + PV2	0.349	0.189
2	apoB + BW	0.309	0.166
2	apoB + Chol	0.308	0.212
2	apoB + TG	0.302	0.145
2	apoB +PV1	0.297	0.139
2	PV1 +Chol	0.252	0.252
2	BW + Chol	0.176	0.176
2	TG + Chol	0.169	0.169
2	PV2 + BW	0.113	0.113
2	PV1 + PV2	0.086	0.086
2	PV1 + BW	0.040	0.040
2	PV2 + TG	0.038	0.038
2	BW + TG	0.022	0.022
2	PV1 + TG	-0.015	-0.015
3	PV2+ Chol + HDLc	0.612	0.612
3	PV1+ PV2+ Chol	0.577	0.577
3	apoB+ PV2 + HDLc	0.566	0.512
3	apoB+ PV1 + HDLc	0.525	0.475
3	apoB+ BW + HDLc	0.525	0.481
3	apoB+ TG + HDLc	0.523	0.474
3	apoB+ Chol + HDLc	0.515	0.473
3	PV1+ Chol + HDLc	0.502	0.502
3	apoB+ PV1 + PV2	0.490	0.335
3	PV2+ BW + HDLc	0.482	0.482
3	PV2+ Chol + Chol	0.474	0.474

(Continued)

Model	Variables in Model	Adjusted R-Square	Unadjusted R-Square
3	apoB+ PV2 + Chol	0.464	0.448
3	PV2+ TG + Chol	0.454	0.454
3	PV2+ TG + HDLc	0.450	0.450
3	PV1+ BW + HDLc	0.441	0.441
3	BW + Chol + HDLc	0.439	0.439
3	PV1+ PV2+ HDLc	0.432	0.432
3	PV1+ TG + HDLc	0.423	0.423
3	TG + Chol + HDLc	0.423	0.423
3	BW+ TG + HDLc	0.404	0.404
3	apoB+ PV2 + BW	0.369	0.229
3	apoB+ PV2 + TG	0.361	0.198
3	apoB+ PV1 + Chol	0.311	0.246
3	apoB+ BW + Chol	0.304	0.208
3	apoB+ PV1 + BW	0.300	0.156
3	apoB+ BW + TG	0.299	0.153
3	apoB+ PV1 + TG	0.295	0.134
3	PV1+ BW + Chol	0.253	0.253
3	PV1+ TG + Chol	0.243	0.243
3	PV1 + PV2 + BW	0.177	0.177
3	BW+ TG + Chol	0.168	0.168
3	PV2 + BW + TG	0.103	0.103
3	PV1 + PV2 + TG	0.072	0.072
3	PV1+ BW + TG	0.026	0.026
4	PV1 + PV2 + Chol + HDLc	0.659	0.659
4	PV2 + BW+ Chol + HDLc	0.630	0.630
4	PV2 + TG + Chol + HDLc	0.618	0.618
4	apoB + PV2 + Chol + HDLc	0.616	0.607
4	apoB + PV1 +PV2 + HDLc	0.613	0.552
4	apoB + PV1 +PV2 + Chol	0.605	0.580
4	PV1 + PV2 + BW + Chol	0.603	0.603
4	apoB+ PV2 + TG + HDLc	0.588	0.535
4	apoB+ PV2 + BW + HDLc	0.586	0.542
4	PV1 + PV2 + TG + Chol	0.574	0.574
4	apoB+ PV1 + TG + HDLc	0.542	0.493
4	apoB+ PV1 + BW + HDLc	0.534	0.491
4	apoB+ PV1 + Chol + HDLc	0.528	0.503
4	apoB+ BW + TG + HDLc	0.521	0.476
4	apoB+ PV1 +PV2 + BW	0.517	0.384
4	apoB + BW + Chol + HDLc	0.516	0.476

(Continued)

Model	Variables in Model	Adjusted R-Square	Unadjusted R-Square
4	apoB + TG + Chol + HDLc	0.515	0.469
4	PV1 + TG + Chol + HDLc	0.513	0.513
4	PV1 + PV2 +BW + HDLc	0.487	0.487
4	PV2 + BW + TG +HDLc	0.486	0.486
4	apoB + PV1 + PV2 + TG	0.481	0.324
4	apoB + PV2 + BW + Chol	0.477	0.465
4	PV2 + BW + TG + Chol	0.467	0.467
4	apoB + PV2 + TG + Chol	0.464	0.444
4	PV1 + BW+ TG + HDLc	0.449	0.449
4	PV1 + PV2 + TG + HDLc	0.441	0.441
4	BW + TG + Chol + HDLc	0.429	0.429
4	apoB + PV1 + BW + Chol	0.309	0.247
4	apoB + PV1 + TG + Chol	0.306	0.238
4	apoB + PV1 + BW + TG	0.293	0.145
4	aPoB + BW + TG + Chol	0.293	0.195
4	PV1 + BW+ TG + Chol	0.242	0.242
4	PV1 + PV2 +BW + TG	0.165	0.165
5	PV1 + PV2 +BW + Chol + HDLc	0.683	0.683
5	apoB + PV1 + PV2 + Chol + HDLc	0.676	0.664
5	PV1 + PV2 +TG +Chol + HDLc	0.653	0.653
5	apoB + PV1 + PV2 + BW + HDLc	0.638	0.588
5	apoB + PV2 + BW + Chol + HDLc	0.632	0.625
5	PV2 + BW + TG + Chol + HDLc	0.631	0.631
5	apoB + PV2 + TG + Chol + HDLc	0.626	0.625
5	apoB + PV1 + PV2 + BW + Chol	0.625	0.604
5	apoB + PV1 + PV2 + TG + HDLc	0.614	0.554
5	PV1 + PV2 +BW + TG + Chol	0.608	0.608
5	apoB + PV1 + PV2 + TG + Chol	0.600	0.577
5	apoB + PV2 + BW + TG + HDLc	0.598	0.553
5	apoB + PV1 + BW + TG + HDLc	0.543	0.483
5	apoB + PV1 + TG + Chol + HDLc	0.541	0.515
5	apoB + PV1 + BW + Chol + HDLc	0.533	0.511
5	PV1 + BW+ TG + Chol + HDLc	0.515	0.515
5	apoB + BW + TG + Chol + HDLc	0.513	0469
5	apoB + PV1 + PV2 + BW + TG	0.510	0.376
5	PV1 + PV2 +BW + TG + HDLc	0.483	0.483
5	apoB + PV2 + BW + TG + Chol	0.472	0.457
5	apoB + PV1 + BW + TG + Chol	0.301	0.236
6	apoB + PV1 + PV2 + BW + Chol + HDLc	0.696	0.687

(Continued)

Model	Variables in Model	Adjusted R-Square	Unadjusted R-Square
6	PV1 + PV2 +BW + TG + Chol + HDLc	0.678	0.678
6	apoB + PV1 + PV2 + TG + Chol + HDLc	0.671	0.658
6	apoB + PV1 + PV2 + BW + TG + HDLc	0.633	0.582
6	apoB + PV1 + PV2 + BW + TG + Chol	0.626	0.608
6	apoB + PV1 + BW + TG + Chol + HDLc	0.541	0.516
7	apoB + PV1 + PV2 + BW + TG + Chol + HDLc	0.691	0.682

VITA

LIMIN WANG

Permanent Address
TAMU 2472
College Station, TX 77843-2472
(979)-845-7537

Education

Ph.D in Nutrition, August 2003
Texas A&M University, College Station, Texas, USA

M.S. in Nuclear Medicine, July 1997
Shanghai Medical University, Shanghai, China

M.D., July 1992
Taishan Medical College, Shandong, China